



US Army Corps
of Engineers

AD-A199 450



FILE COPY

2

TECHNICAL REPORT GL-87-14

SEISMIC STABILITY EVALUATION OF FOLSOM DAM AND RESERVOIR PROJECT

Report 7
UPSTREAM RETAINING WALL

by

Harold J. Leeman, Jr., Mary E. Hynes
Wipawi Vanadit-Ellis, Takashi Tsuchida

Geotechnical Laboratory

DEPARTMENT OF THE ARMY
Waterways Experiment Station, Corps of Engineers
PO Box 631, Vicksburg, Mississippi 39180-0631



DTIC
ELECTE
SEP 27 1988
S E D

July 1988

Report 7 of a Series

Approved For Public Release. Distribution Unlimited

Original contains color
plates: All DTIC reproductions
will be in black and
white

88 9 26 066

Prepared for US Army Engineer District, Sacramento
Sacramento, California 95814-4794

**Destroy this report when no longer needed. Do not return
it to the originator.**

**The findings in this report are not to be construed as an official
Department of the Army position unless so designated
by other authorized documents.**

**The contents of this report are not to be used for
advertising, publication, or promotional purposes.
Citation of trade names does not constitute an
official endorsement or approval of the use of
such commercial products.**

Unclassified
SECURITY CLASSIFICATION OF THIS PAGE

REPORT DOCUMENTATION PAGE				Form Approved OMB No. 0704-0188	
1a. REPORT SECURITY CLASSIFICATION Unclassified		1b. RESTRICTIVE MARKINGS Unclassified			
2a. SECURITY CLASSIFICATION AUTHORITY		3. DISTRIBUTION / AVAILABILITY OF REPORT Approved for public release; distribution unlimited			
2b. DECLASSIFICATION / DOWNGRADING SCHEDULE					
4. PERFORMING ORGANIZATION REPORT NUMBER(S) Technical Report GL-87-14		5. MONITORING ORGANIZATION REPORT NUMBER(S)			
6a. NAME OF PERFORMING ORGANIZATION USAEWES Geotechnical Laboratory	6b. OFFICE SYMBOL (If applicable) CEWES-GH	7a. NAME OF MONITORING ORGANIZATION			
6c. ADDRESS (City, State, and ZIP Code) PO Box 631 Vicksburg, MS 39180-0631		7b. ADDRESS (City, State, and ZIP Code)			
8a. NAME OF FUNDING / SPONSORING ORGANIZATION US Army Engineer District, Sacramento	8b. OFFICE SYMBOL (If applicable) CESPK-ED	9. PROCUREMENT INSTRUMENT IDENTIFICATION NUMBER			
8c. ADDRESS (City, State, and ZIP Code) 650 Capitol Mall Sacramento, CA 95814-4794		10. SOURCE OF FUNDING NUMBERS			
		PROGRAM ELEMENT NO.	PROJECT NO.	TASK NO.	WORK UNIT ACCESSION NO.
11. TITLE (Include Security Classification) Seismic Stability Evaluation of Folsom Dam and Reservoir Project; Report 7: Upstream Retaining Wall					
12. PERSONAL AUTHOR(S) Leeman, Harold J., Jr., Hynes, Mary E., Vanadit-Ellis, Wipawi, and Tsuchida, Takashi					
13a. TYPE OF REPORT Report 7 of a series	13b. TIME COVERED FROM 1982 TO 1988	14. DATE OF REPORT (Year, Month, Day) July 1988		15. PAGE COUNT 103	
16. SUPPLEMENTARY NOTATION Available from National Technical Information Service, 5285 Port Royal Road, Springfield, VA 22161.					
17. COSATI CODES			18. SUBJECT TERMS (Continue on reverse if necessary and identify by block number) Dam safety Earthquakes and hydraulic structures Folsom Dam (Calif.)		
FIELD	GROUP	SUB-GROUP			
19. ABSTRACT (Continue on reverse if necessary and identify by block number) The man-made water retaining structures at the Folsom Dam and Reservoir Project, located on the American River about 20 miles upstream of the City of Sacramento, Calif., have been evaluated for their seismic safety in the event of a Magnitude 6.5 earthquake occurring on the East Branch of the Bear Mountains Fault Zone at a distance of about 15 km. The evaluation process involved extensive review of construction records, field and laboratory investigations, and analytical studies. This report documents studies of Retaining Wall B, a submerged retaining wall at the base of the Right Wing Dam upstream envelopment fill. It has been concluded that Retaining Wall B will perform satisfactorily during the design earthquake.					
20. DISTRIBUTION / AVAILABILITY OF ABSTRACT <input checked="" type="checkbox"/> UNCLASSIFIED/UNLIMITED <input type="checkbox"/> SAME AS RPT <input type="checkbox"/> DTIC USERS			21. ABSTRACT SECURITY CLASSIFICATION Unclassified		
22a. NAME OF RESPONSIBLE INDIVIDUAL			22b. TELEPHONE (Include Area Code)		22c. OFFICE SYMBOL

DD Form 1473, JUN 86

Previous editions are obsolete.

SECURITY CLASSIFICATION OF THIS PAGE

Unclassified

PREFACE

The US Army Engineer Waterways Experiment Station (WES) was authorized to conduct this study by the US Army Engineer District, Sacramento (SPK), by Intra-Army Order for Reimbursable Services Nos. SPKED-F-82-2, SPKED-F-82-11, SPKED-F-82-34, SPKED-F-83-15, SPKED-F-83-17, SPKED-F-84-14, and SPKED-D-85-12. This report is one in a series of reports which document the seismic stability evaluations of the man-made water retaining structures of the Folsom Dam and Reservoir Project, located on the American River in California. The Reports in this series are as follows:

- Report 1: Summary
- Report 2: Interface Zone
- Report 3: Concrete Gravity Dam
- Report 4: Mormon Island Auxiliary Dam - Phase I
- Report 5: Dike 5
- Report 6: Right and Left Wing Dams
- Report 7: Upstream Retaining Wall
- Report 8: Mormon Island Auxiliary Dam - Phase II

The work on these reports is a joint endeavor between SPK and WES. Messrs. John W. White and John S. Nickell, of Civil Design Section 'A', Civil Design Branch, Engineering Division (SPKED-D) at SPK were the overall SPK project coordinators. Messrs. Gil Avila and Matthew G. Allen, of the Soil Design Section, Geotechnical Branch, Engineering Division (SPKED-F) at SPK, made critical geotechnical contributions to field and laboratory investigations. Support was also provided by the South Pacific Division Laboratory. The WES Principal Investigator and Research Team Leader was Dr. Mary Ellen Hynes, of the Earthquake Engineering and Geophysics Division (EEGD), Geotechnical Laboratory (GL), WES. Primary Engineers on the WES team for the portion of the study documented in this report were MAJ Harold J. Leeman, Jr., on temporary assignment to WES from the US Military Academy, West Point, New York, Ms. Wipawi Vanadit-Ellis of the Soil Mechanics Division (SMD), GL, WES, and Mr. Takashi Tsuchida, on temporary assignment to WES from the Port and Harbour Research Institute, Yokosuka, Japan. Geophysical support was provided by Mr. Jose Llopis, EEGD. Additional engineering support was provided by Mr. David S. Sykora, EEGD, Mr. Ronald E. Wahl, EEGD, and

Mr. Richard S. Olsen, EEGD. Large-scale laboratory investigations were conducted by Mr. Robert T. Donaghe, SMD. Laboratory instrumentation services were provided by Mr. Thomas V. McEwen, of the Data Acquisition Section, Instrumentation Services Division, WES. Mr. W. L. Hanks, SMD, Mr. C. Schneider, SMD, Mr. B. L. Washington of the Engineering Geology and Rock Mechanics Division, EGRMD, GL, WES, Mr. M. H. Seid, EEGD, Mr. J. D. Myers, EEGD, Mr. H. Alderson, EEGD, and Mr. T. Cho, EEGD, assisted in preparation of figures. Key contributions also were made by Dr. Leslie F. Harder, Jr., of Sacramento, California; Professor Shobha Bhatia, Syracuse University; Professor Tarik Hadj-Hamou, Tulane University; and Professor David Elton, Auburn University.

Professors H. Bolton Seed, Anil K. Chopra and Bruce A. Bolt of the University of California, Berkeley; Professor Clarence R. Allen of the California Institute of Technology; and Professor Ralph B. Peck, Professor Emeritus of the University of Illinois, Urbana, served as Technical Specialists and provided valuable guidance during the course of the investigation.

Overall direction at WES was provided by Dr. A. G. Franklin, Chief, EEGD, and Dr. W. F. Marcuson III, Chief, GL.

COL Dwayne G. Lee, CE, is Commander and Director of WES. Dr. Robert W. Whalin is Technical Director.

Accession For	
NTIS GRA&I	<input checked="" type="checkbox"/>
DTIC TAB	<input type="checkbox"/>
Unannounced	<input type="checkbox"/>
Justification	
By _____	
Distribution/	
Availability Codes	
Dist	Avail and/or Special
A-1	



"Original contains color plates: All DTIC reproductions will be in black and white"

CONTENTS

	<u>Page</u>
PREFACE.....	1
PART I: INTRODUCTION.....	5
General.....	5
Project History.....	6
Hydrology and Pool Levels.....	6
Site Geology.....	7
Seismic Hazard Assessment.....	8
Seismological and geological investigations.....	8
Selection of design ground motions.....	9
PART II: REVIEW OF CONSTRUCTION RECORDS.....	11
General.....	11
Description of Retaining Wall B.....	11
Foundation Conditions.....	11
Backfill Materials.....	12
Construction Sequence.....	13
Retaining Walls A and E.....	13
PART III: BACKFILL MATERIALS.....	15
General.....	15
Field and Laboratory Investigations Performed for this Study.....	15
Liquefaction Susceptibility.....	17
Residual Strength.....	20
PART IV: STABILITY EVALUATION OF RETAINING WALL B.....	21
General.....	21
Yield Acceleration Analyses.....	22
Mononobe-Okabe.....	22
UTEXAS2 approach.....	25
Summary of yield acceleration computations.....	26
Permanent Deformation Estimates.....	27
Makdisi-Seed calculations.....	27
Sarma-Ambraseys calculations.....	29
Modified Richards-Elms calculations.....	30
Post-Earthquake Stability Studies for Worst Case Scenarios.....	31
Stability Evaluation.....	32
PART V: SUMMARY AND CONCLUSIONS.....	33
REFERENCES.....	35
TABLES 1-4	
FIGURES 1-46	
APPENDIX A: COMPUTER PROGRAM LISTINGS AND OUTPUT FOR YIELD ACCELERATION COMPUTATIONS WITH THE MONONOBE-OKABE PROCEDURE.....	A1

SEISMIC STABILITY EVALUATION OF FOLSOM DAM AND RESERVOIR PROJECT

Report 7: Upstream Retaining Wall

PART I: INTRODUCTION

General

1. This report is one of a series of reports that document the investigations and results of a seismic stability evaluation of the man-made water retaining structures at the Folsom Dam and Reservoir Project, located on the American River in Sacramento, Placer and El Dorado Counties, California, about 20 airline miles northeast of the City of Sacramento. This seismic safety evaluation was performed as a cooperative effort between the US Army Engineer Waterways Experiment Station (WES) and the US Army Engineer District, Sacramento (SPK). Professors H. Bolton Seed, Anil K. Chopra, and Bruce A. Bolt of the University of California, Berkeley, Professor Clarence R. Allen of the California Institute of Technology, and Professor Ralph B. Peck, Professor Emeritus of the University of Illinois, Urbana, served as Technical Specialists for the study. This report documents seismic stability studies of Retaining Wall B, a submerged retaining wall located at the base of the Right Wing Dam envelopment fill, at the contact between the Right Wing Dam and the Concrete Gravity Dam. A location map and plan of the project are shown in Figures 1 and 2.

2. Three retaining walls were constructed in the vicinity of the main dam in the wrap-around area parallel to the river. Downstream retaining walls were constructed on both the Right and Left wrap-around areas. Upstream, only the Right wrap-around area required a retaining wall, denoted Retaining Wall B in Figure 3. Failure of the downstream walls would not result in catastrophic loss of the reservoir. The upstream wall is of concern since the embankment shell is saturated and the intake ports for the powerhouse are located riverward of the wall, and could be blocked if the wall and embankment slid due to the design earthquake. The investigation was aimed at determining what movements the wall might experience during the design earthquake and whether such movements would threaten the integrity of the embankment. If excessive

sliding were to occur, the freeboard could be lost and the reservoir contents could escape, leading to catastrophic failure of the dam.

3. Conservative estimates of earthquake-induced permanent displacements were made with Makdisi-Seed, Sarma-Ambraseys and modified Richards-Elms approaches. Yield accelerations were determined with Mononobe-Okabe and UTEXAS2 techniques. The estimates of earthquake-induced permanent displacement in Retaining Wall B and Right Wing envelopment fill are less than 10 ft. These Newmark sliding-block analyses indicate that some damage to the wall is expected but the deformations will be limited, and there will be no catastrophic loss of the reservoir.

Project History

4. The Folsom project was designed and built by the Corps of Engineers in the period 1948 to 1956, as authorized by the Flood Control Act of 1944 and the American River Basin Development Act of 1949. Upon completion of the project in May 1956, ownership of the Folsom Dam and Reservoir was transferred to the US Bureau of Reclamation for operation and maintenance. As an integral part of the Central Valley Project, the Folsom Project provides water supplies for irrigation, domestic, municipal, industrial and power production purposes as well as flood protection for the Sacramento Metropolitan area and extensive water related recreational facilities. Releases from the Folsom Reservoir are also used to provide water quality control for project diversions from the Sacramento-San Joaquin Delta, to maintain fish-runs in the American River below the dam, and to help maintain navigation along the lower reaches of the Sacramento River.

Hydrology and Pool Levels

5. Folsom Lake impounds the runoff from 1,875 square miles of rugged mountainous terrain. The reservoir has a storage capacity of 1 million acre-ft at gross pool and is contained by approximately 4.8 miles of man-made water-retaining structures that have a crest Elevation of 480.5 ft above sea level. These structures are the Right and Left Wing Dams, the Concrete

Gravity Dam, Mormon Island Auxiliary Dam, and 8 Saddle Dikes. At gross pool, Elevation 466 ft, there is 14.5 ft of freeboard. This pool level was selected for the safety evaluation, based on a review of current operational procedures and hydrologic records (obtained for a 29-year period, from 1956 to 1984) for the reservoir which shows that the pool typically reaches Elevation 466 ft about 10 percent of the time during the month of June, and considerably less than 10 percent of the time during the other months of the year. Under normal operating conditions, the pool is not allowed to exceed Elevation 466 ft. Hydrologic records show that emergency situations which would cause the pool to exceed Elevation 466 ft are rare events.

Site Geology

6. At the time of construction, the geology and engineering geology concerns at the site were carefully detailed by Kiersch and Treasher (1955). Their observations and the foundation reports from construction records are the sources for the summary of site geology provided in this section.

7. The Folsom Dam and Reservoir Project is located in the low, western-most foothills of the Sierra Nevada in central California, at the confluence of the North and South Forks of the American River. Relief ranges from a maximum of 1242 ft near Flagstaff Hill located between the upper arms of the reservoir, to 150 ft near the town of Folsom just downstream of the Concrete Gravity Dam. The North and South Forks entered the confluence in mature valleys up to 3 miles wide, but further downcutting resulted in a V-shaped inner valley 30 to 185 ft deep. Below the confluence, the inner canyon was flanked by a gently sloping mature valley approximately 1.5 miles wide bounded on the west and southeast by a series of low hills. The upper arms of the reservoir, the North and South Forks, are bounded on the north and east by low foothills.

8. A late Pliocene-Pleistocene course of the American River flowed through the Blue Ravine and joined the present American River channel downstream of the town of Folsom. The Blue Ravine was filled with late Pliocene-Pleistocene gravels, but with subsequent downcutting and headward erosion, the Blue Ravine was eventually isolated and drainage was diverted to the present American River Channel.

9. The important formations at the dam site are: a quartz diorite granite which forms the foundation at the Concrete Gravity Dam, Wing Dams, and Saddle Dikes 1 through 7; metamorphic rocks of the Amador group which underlie Saddle Dike 8 and the foundation at Mormon Island Auxiliary Dam; the Mehrten formation, a deposit of cobbles and gravels in a somewhat cemented clay matrix which caps the low hills that separate the saddle dikes and is part of the foundation at Dike 5; and the alluvium that fills the Blue Ravine at Mormon Island Auxiliary Dam.

10. Weathered granitic or metamorphic rock is present throughout the area. Figure 4 shows a geologic map of the project area. The Concrete Gravity Dam, the Wing Dams, the retaining walls, and Dikes 1 through 7 are founded on weathered quartz diorite granite. Between Dikes 7 and 8 there is a change in the bedrock. Dike 8 and Mormon Island Auxiliary Dam are underlain by metamorphic rocks of the Amador group. The Amador group consists of predominantly schists with numerous dioritic and diobasic dikes.

Seismic Hazard Assessment

Seismological and geological investigations

11. Detailed geological and seismological investigations in the immediate vicinity of Folsom Reservoir were performed by Tierra Engineering, Incorporated to assess the potential for earthquakes in the vicinity, to estimate the magnitudes these earthquakes might have, and to assess the potential for ground rupture at any of the water-retaining structures (see Tierra Engineering, Inc., 1983, for comprehensive report). A 12-mile wide by 35-mile long study area centered on the Folsom Reservoir was extensively investigated using techniques such as areal imagery analysis, ground reconnaissance, geologic mapping, and detailed fault capability assessment. In addition, studies by others relevant to the geology and seismicity of the area around Folsom were also compiled. These additional literature sources include numerous geologic and seismologic studies published through the years, beginning with the "Gold Folios" published by the US Geological Survey in the 1890's, the engineering geology investigations for New Melones and the proposed Marysville and Auburn Dams, studies performed for the Rancho Seco Nuclear Power Plant as well as unpublished student theses and county planning studies.

12. It was determined that no capable faults underlie any of the water-retaining structures or the main body of the reservoir at the Folsom Project. The tectonic and seismicity studies also indicated that it is unlikely that Folsom Lake can induce major seismicity. Since the faults that underlie the water retaining structures at the Folsom Project were found to be noncapable, seismic fault displacement in the foundations of the water retaining structures is judged to be highly unlikely.

13. The closest capable fault is the East Branch of the Bear Mountains fault zone which has been found to be capable of generating a maximum magnitude $M = 6.5$ earthquake. The return period for this maximum earthquake is estimated to exceed 400 yrs (Tierra Eng. Inc., 1983). Determination that the East Branch of the Bear Mountains fault zone is a capable fault came from the Auburn Dam earthquake evaluation studies. The minimum distance between the East Branch of the Bear Mountains fault zone and Mormon Island Auxiliary Dam is 8 miles, and the minimum distance between this fault zone and the Concrete Gravity Dam is 9.5 miles. The focal depth of the earthquake is estimated to be 6 miles. This hypothetical maximum magnitude earthquake would cause more severe shaking at the project than earthquakes originating from other known potential sources.

Selection of design ground motions

14. The seismological and geological investigations summarized in the Tierra report were provided to Professors Bruce A. Bolt and H. B. Seed to determine appropriate ground motions for the seismic safety evaluation of the Folsom Dam Project. The fault zone of concern is the East Branch of the Bear Mountains fault zone located at a distance of about 15 kilometers from the site. This fault zone has an extensional tectonic setting and a seismic source mechanism that is normal dip-slip. The slip rate from historic geomorphic and geological evidence is very small, less than 10^{-3} centimeters per year with the most recent known displacement occurring between 10,000 and 500,000 years ago in the Pleistocene period.

15. Based on their studies of the horizontal ground accelerations recorded on an array of accelerometers normal to the Imperial Valley fault during the Imperial Valley earthquake of 1979, as well as recent studies of a large body of additional strong ground motion recordings, Bolt and Seed (1983) recommend the following design ground motions:

Peak horizontal ground acceleration = 0.35 g

Peak horizontal ground velocity = 20 cm/sec

Bracketed Duration (≥ 0.05 g) ≈ 16 sec

Because of the presence of granitic plutons at the site, it is expected that the earthquake accelerations might be relatively rich in high frequencies. Bolt and Seed (1983) provided 2 accelerograms that are representative of the design ground motions expected at the site as a result of a maximum magnitude $M = 6.5$ occurring on the East Branch of the Bear Mountains fault zone. The accelerograms are designated as follows (Bolt and Seed 1983):

M6.5 - 15K - 83A. This accelerogram is representative of the 84-percentile level of ground motions that could be expected to occur at a rock outcrop as a result of a Magnitude 6-1/2 earthquake occurring 15 kms from the site. It has the following characteristics:

Peak acceleration = 0.35g

Peak velocity ≈ 25 cm/sec

Duration ≈ 16 sec.

M6.5 - 15K - 83B. This accelerogram is representative of the 84-percentile level of ground motions that could be expected to occur at a rock outcrop as a result of a Magnitude 6-1/2 earthquake occurring 15 kms from the site. It has the following characteristics:

Peak acceleration = 0.35g

Peak velocity ≈ 19.5 cm/sec

Duration ≈ 15 sec

Figure 5 shows plots of acceleration as a function of time for the two design accelerograms and Figure 6 shows response spectra of the motions for damping ratios of 0, 2, 5, 10, and 20 percent damping.

PART II: REVIEW OF CONSTRUCTION RECORDS

General

16. Detailed construction records were kept to document the initial site reconnaissance, selection of borrow areas, foundation preparation and construction sequence for the dam. Pertinent information from these construction records are summarized in this chapter.

Description of Retaining Wall B

17. Retaining Wall B prevents the earthfill of the Right Wing Dam envelopment section from blocking the penstock and powerhouse inlets. During construction, Retaining Wall B also protected the diversion tunnel inlet channel. Plans and sections of the wall are shown in Figures 7, 8, and 9. The wall is 406 ft long and consists of 12 monoliths. The crest elevation varies between Elevation 310 and 350 ft and is controlled by the intersection of the wall with the designed slope of the earthfill envelopment. The elevation of the base of the wall varies between Elevation 270 and 290 ft. The elevation of the base of individual monoliths was adjusted according to the existing topography and the quality of the foundation rock. The maximum height of the wall is 82 ft, near wall axis Station 0+29, at the juncture of the wall with Monoliths 6 and 7 of the Concrete Gravity Dam. The minimum height of the wall is 27 ft at wall axis Station 4+35. The riverward face of the wall is battered at 1 (vertical) on 0.1 (horizontal). Monoliths shorter than 50 ft (Wall Monoliths 5, 6, 11, and 12) are battered at 1 (vertical) on 0.58 (horizontal) on the earthfill face. Monoliths taller than 50 ft have a backfill facing slope battered at 1 (vertical) on 0.65 (horizontal). A two-lane construction road exists at the base of the riverward face of the wall.

Foundation Conditions

18. The foundation rock is quartz diorite with varying degrees of weathering. Figures 10a and 10b show geologic plans and sections of the foundation. The degree of weathering is indicated in these figures. Several faults and shears were encountered in the foundation. The most significant

are two parallel faults that strike northeast (roughly N 45-1/2 E) and dip northwest (roughly 45-1/2 NW), near wall axis Stations 1+65 and 2+17 (see Section A-A in Figure 10b). The fault near wall axis Station 1+65 contains a 0.3- to 8.0-ft wide zone of weathered, brecciated rock, and was exposed in the foundation for Wall Monoliths 1 through 4. The second fault, near wall axis Station 2+17, was exposed in the foundation for Wall Monoliths 5 and 6. No brecciated zone is present where the fault near wall axis Station 2+17 passes beneath the retaining wall. After excavation and cleanup was completed, the foundation rock exposure consisted of sharp, irregularly blasted surfaces, terminating at joint planes. Where the two northwest dipping faults crossed the foundation, V-shaped excavations were used to remove the soft, brecciated, and weathered rock. Between the heel of the Concrete Gravity Dam and wall axis Station 1+20, the brecciated fault zone is at maximum width. Loose material was hand-excavated and the breccia zone was cut vertically to minimize its adverse effect on the foundation. No springs or seeps were present in the mapped area. Eight inch diameter vitrified-clay pipe drains were installed normal to the wall axis and connected to vitrified clay pipe drains installed at the heel (rear face) of Retaining Wall B. The foundation was leveled with 1,811 cubic yards of grout and concrete to facilitate forming and placement of subsequent lifts.

Backfill Materials

19. The backfill behind Retaining Wall B is the Right Wing Dam envelopment fill. Sections of the Right Wing envelopment fill are shown in Figures 7, 8, and 11. The embankment consists of three zones: Zone A, a loose rockfill with considerable fines from excavation in the American River channel, Zone B, a gravel transition zone also from excavation in the American River channel, and Zone C, a well-compacted decomposed granite core from Borrow Area No. 2 shown in Figure 2. Gradations for Zones B and C are shown in Figures 12 and 13. The gradation of Zone A is only qualitatively described in construction records. Zone A was dumped in 12-ft lifts with no compaction required. Zone B was placed in 24-in. lifts, compacted with one complete coverage* of a D-8 Caterpillar tractor. Zone C was compacted in 12-in. lifts

* It was estimated that one complete coverage is equivalent to three or four passes of the compaction equipment.

with 12 passes of a sheepsfoot roller or in 18-in. lifts with 6 passes of a pneumatic-tired roller. Construction photographs indicate that some compaction of the core in the envelopment area was also accomplished with fully-loaded dump trucks. Report 2 of this series provides more details of the construction of the envelopment areas.

20. The unit weight and shear strength characteristics of the embankment materials that were used in the original design are shown in Table 1. The Zone A rockfill was conservatively assumed to have the same characteristics as the Zone B gravel fill.

Construction Sequence

21. To better visualize the geometry of Retaining Wall B relative to the Concrete Gravity Dam, a series of construction photographs is provided. Figure 14 is a photograph of the completed wall (dated 16 April 1954) with Zone A backfill in place. Figures 15 through 23 show the chronological construction sequence of the wall and backfill placement operations. A key observation from the construction photographs is that a two-lane road exists along the base of the riverward face of the wall, as shown in Figures 14, 19, and 21. Therefore, it is apparent that the wall can displace at least 20 ft riverward without falling into the river channel. Displacements on the order of 10 to 20 ft are sufficient to block the 84-in. intake pipe in Monolith 7 of the Concrete Gravity Dam, but the penstocks would be only slightly obstructed (see Figure 9).

Retaining Walls A and E

22. Retaining Walls A and E provide support to the Right Wing and Left Wing envelopment areas, respectively. Retaining Wall A is 173 ft long and about 54 ft tall at maximum section. This is a combination gravity and cantilever structure connected to the Concrete Gravity Dam at Monolith 7. Retaining Wall E is 239 ft long and 60 ft tall at maximum section. This is a gravity type wall and adjoins the left edge of the flip bucket in Monolith 20. The surface of the backfill behind both walls, the downstream Right and Left envelopment shells, is sloped at 1 vertical to 2 horizontal at the contact with the Concrete Gravity Dam. Foundation conditions and preparation for both walls were similar to those for Retaining Wall B.

PART III: BACKFILL MATERIALS

General

23. The backfill materials at Retaining Wall B are the upstream portion of the Right Wing Dam envelopment fill. The geometries of the backfill zones are shown in Figures 7 and 8, and a typical Right Wing Dam section in the envelopment area is shown in Figure 11. There are three material zones: Zone A, a loose, dumped rockfill with a considerable fines content, Zone B, a gravel transition zone, and Zone C, a compacted decomposed granite core. The material properties of the backfill and the behavior of the backfill during and after earthquake loading were determined in order to assess the adequacy of the wall and the seismic stability of the submerged envelopment fill. This part contains a summary of the results of field investigations and complementary laboratory tests (conducted as part of the seismic stability study) performed on the embankment materials to quantitatively determine material properties under static and cyclic loading conditions. Reports 4 and 6 of this series contain more detailed descriptions of the field and laboratory investigations conducted for this study and the analytical studies to determine dynamic response, liquefaction susceptibility, and seismically-induced residual excess pore pressures. The results of the analytical studies are briefly summarized in this part since they provide the basis for several parameter values selected to determine sliding resistance and permanent displacements.

Field and Laboratory Investigations Performed for this Study

24. Undisturbed sampling with a Denison sampler and SPT borings with trip hammer equipment were performed at 5-ft intervals at the centerline to sample core material, and near the downstream edge of the crest to sample filter and core material at two locations on the Right Wing Dam, near Stations 235 and 275. Figure 3 shows the locations of the field investigations. SPT borings are denoted SS and undisturbed borings are denoted US. Steel cased borings, shown as SCB in Figure 3, were drilled with Odex equipment in the downstream gravel shells. The Odex system consists of a downhole pneumatic hammer with an expanding bit that pulls a steel casing behind the bit.

When the casing is in place, the bit can be retracted and withdrawn through the casing. The steel casing used in these investigations had an inside diameter (ID) of 5 in. The Odex system was selected for installation of cased holes for subsurface geophysical testing because it did not require grouting of the gravels, the disturbance to the gravels was relatively minor, and several holes could be installed within a single work day. Unfortunately, this system does not provide satisfactory samples of the subsurface materials.

25. The US, SS, and SCB borings were drilled in pairs for geophysical crosshole testing. Test pits, shown as TP in Figure 3, were excavated in the downstream gravel shells at these locations to determine in situ densities and obtain disturbed samples for laboratory testing. Pairs of undisturbed and SPT borings were also drilled in core material at the interface area near Station 285, as shown in Figure 3.

26. Typically, the SPT blowcounts in the core material exceeded 40 blows per ft near Stations 235 and 275, and 30 blows per ft in the immediate vicinity of the end monolith of the Concrete Gravity Dam. The fines content averaged about 20 percent non-plastic fines near Station 235 and 275, and about 25 percent slightly plastic fines in the interface area. The core materials generally classified as a silty or clayey sand (SM, SC, SC-SM) according to the Unified Soils Classification System (USCS). Gradations from these recent field investigations are compared with record samples in Figure 24 for Stations 235 and 275, and Figure 25 for the interface area. The peak effective friction angle of the core material ranged from 35° to 45° ($c' = 0$), and the peak consolidated-undrained shear strength typically exceeded 6 TSF, based on the results of S and \bar{R} triaxial tests conducted over the stress range of interest. For the analyses in this study, peak effective stress strength parameters of $\phi' = 37^\circ$ and $c' = 0$, and peak consolidated-undrained strength parameters of $\phi = 30^\circ$ and $c = 4$ tsf were selected for the core material. Shear wave velocities in the core ranged from about 900 to 1,000 fps in the top 20 ft, to about 1,100 to 1,600 fps at depth. The average dry density from record samples of core material was 127 pcf, and the total unit weight was estimated to be 142 pcf.

27. Shear wave velocities in the shell ranged from 850 fps near the surface of the slope, to 1,350 fps at depth. Large-scale in situ density tests from 3 test pits in the gravel transition material showed an average dry density of 136 pcf. The buoyant unit weight is estimated to be 90 pcf. The

gravel transition material generally classified as a sandy, silty gravel, with an average fines content of 4 percent non-plastic fines and an average D_{50} of 1 in. Maximum particle sizes were typically less than 6 in. The range of gradations observed in these test pit samples is shown in Figure 26. The in situ relative density, D_r , of the Zone B gravel is estimated to be 60 to 70 percent. The average observed in the test pits was 63 percent.

28. The Zone B gravel was compacted according to the same specifications as the gravel shell in Zone 1 of Mormon Island Auxiliary Dam. Comparison of the range of gradations observed in test pits in both dams shows the materials are very similar. Becker Hammer blowcounts in the Mormon Island Auxiliary Dam shell were translated into equivalent SPT blowcounts (Harder 1986) and the average energy and overburden corrected blowcount, $(N_1)_{60}$, is estimated to be about 25 blows per ft. Based on large-scale triaxial tests on gravel specimens from Mormon Island Auxiliary Dam, the Zone B gravel in the Right Wing Dam is estimated to have an effective friction angle of 43° ($c' = 0$).

29. As part of the field work to assess the current conditions in the interface areas, the downstream Retaining Walls A and E were inspected in June, 1985. It was observed that some (but not all) weep holes in these walls were plugged. One or two holes in each wall were producing a minute amount of water. Mosses and algae at the base of the retaining walls below these moist weep holes indicated continuous moist conditions. The pool elevation at the time of the field visit was at or above Elevation 466 ft and it was observed that the seepage through the weepholes in the downstream retaining walls was minimal. In the line of reasoning that leads to the conclusion that Retaining Walls A and E are not critical to the satisfactory seismic performance of the interface areas, it is assumed that the downstream wrap-around shell materials are unsaturated and well-drained.

Liquefaction Susceptibility

30. The seismically-induced residual excess pore pressures developed in the envelopment fill behind the retaining wall were assumed to be similar to those developed in the upstream slope of the Right Wing Dam outside the envelopment area. As described in Report 6 of this series, the section selected for analysis to represent both the Right and Left Wing Dams was the tallest

upstream section which occurs at Station 283 in the Right Wing embankment. The analysis section is shown in Figure 27. The elevation of the base of this upstream slope is 290 ft. The elevation of the base of the retaining wall varies between 270 ft and 290 ft. The slope of the envelopment fill varies between 1 (vertical) on 2 (horizontal) at the intersection with the Concrete Gravity Dam, to 1 (vertical) on 2.25 (horizontal) where the envelopment fill blends into the upstream slope of the Right Wing Dam.

31. The cyclic strengths of the shell and core materials were estimated with Seed's empirical approach (Seed et al. 1983, and Seed et al. 1984). The Zone A rockfill was assumed to have the same characteristics as the Zone B gravel transition. The average $(N_1)_{60}$ values of these materials were estimated to be 25 for the shell, Zones A and B, and 30 (plus) for the Zone C core. The fines contents average about 4 percent for the shell and 20 to 25 percent for the core.

32. Cyclic strengths were estimated from Seed's empirical chart shown in Figure 28 which shows a plot of cyclic strength versus corrected blowcount, $(N_1)_{60}$, for silty sands with different fines contents. The cyclic strength in Figure 28 is expressed as the cyclic stress ratio causing liquefaction (based on observations of liquefaction in the field), for a confining pressure of about 1 tsf and for earthquakes with $M = 7.5$. The blowcounts in this chart are corrected to an overburden pressure of 1 tsf and a 60 percent energy level, $(N_1)_{60}$. The cyclic stress ratios from this chart are interpreted to correspond to development of 100 percent residual excess pore pressure. Seed et al. (1983) has shown that for $M = 6.5$ events, the cyclic loading resistance is about 20 percent higher, for any value of $(N_1)_{60}$, than for $M = 7.5$ earthquakes.

33. The cyclic strength for the embankment shell was determined by entering the chart in Figure 28 at $(N_1)_{60} = 25$ and selecting the corresponding cyclic stress ratio from the curve for fines less than or equal to 5 percent, to obtain a cyclic stress ratio of 0.29. This chart value was then adjusted to correspond to a $M = 6.5$ event by the factor $K_M = 1.2$, to obtain a cyclic stress ratio of 0.35. The core materials have a value of $(N_1)_{60} = 30$ which exceeds the limits of the cyclic strength chart for silty sand with fines contents of about 20 to 25 percent. The asymptotic limit for this curve is $(N_1)_{60} \cong 23$. Consequently, the core materials are clearly not susceptible to liquefaction.

34. The ϵ bankment shells were further analyzed with finite element techniques. Initial static stresses in the analysis section were determined in static finite element analyses with the program FEADAM. The finite element mesh is shown in Figure 29, and the input properties are listed in Table 2. For each element, the vertical effective stress and initial horizontal shear stress were computed. The cyclic strength for each element is the cyclic stress ratio 0.35 adjusted by the factors K_{σ} , to account for the non-linear relationship between cyclic strength and overburden stress, and K_{α} , to account for the increase in cyclic strength with α defined as the ratio of initial horizontal shear stress to vertical effective stress. The factor K_{σ} is plotted in Figure 30 versus vertical effective stress. The factor K_{α} is plotted in Figure 31 versus initial shear stress ratio, α . The curves in Figures 30 and 31 were developed from large-scale cyclic triaxial tests on compacted specimens of gravel from test pits at Mormon Island Auxiliary Dam.

35. Dynamic shear stresses developed in the analysis section were computed with FLUSH, a two-dimensional, total stress, dynamic response finite element program, which solves the equations of motion in the frequency domain and accounts for non-linear soil behavior with an equivalent linear model. Of the two accelerograms provided for the analyses, Accelerogram B (denoted M6.5 - 15K - 83B in Part I) was selected for input to FLUSH since it resulted in slightly higher dynamic shear stresses in preliminary SHAKE analyses than Accelerogram A (denoted M6.5 - 15K - 83A in Part I). The accelerogram was input to the problem at the rock surface of an outcropping bedrock layer. The finite element mesh used in the FLUSH computations was the same as that used in the FEADAM computations. An average sand modulus degradation curve was used in the equivalent linear solution. Shear moduli for the section were estimated from the field geophysical measurements and the static stress analyses. Peak accelerations computed for several points in the section are shown in Figure 32.

36. The maximum horizontal dynamic shear stresses computed with FLUSH were multiplied by 0.65 to determine the average cyclic shear stress for each element. The available cyclic strength was compared to the earthquake-induced cyclic shear stress, and safety factors against liquefaction were computed for each element. Typically, the safety factors against liquefaction in the upstream shell exceeded 1.5. In the core, the safety factors were higher. Residual excess pore pressures of about 20 to 25 percent are expected to

develop in the upstream shell based on the relationship between residual excess pore pressure and factor of safety against liquefaction shown in Figure 33. This figure was developed from large-scale triaxial tests on gravels from Mormon Island Auxiliary Dam, as well as data on gravels from Evans (1987). No significant residual excess pore pressures are expected to develop in the core.

Residual Strength

37. To estimate stability of the retaining wall and backfill in worst-case scenarios, residual strength of the embankment shell material was estimated with Seed's empirical procedure (Seed 1986) which relates $(N_1)_{60}$ to residual (post-liquefaction) shear strength, S_{ur} . This relationship is shown in Figure 34. Since the average $(N_1)_{60}$ of the core exceeds a reasonable extrapolation of Seed's chart, worst-case post-earthquake strengths of the core were estimated from reduced laboratory strength values.

General

38. Because failure of the downstream walls ("A" and "E") would not result in catastrophic loss of the reservoir, detailed study of these walls was not performed. The upstream wall, Retaining Wall B, is of concern since the embankment shell is saturated and the intake ports for the powerhouse are located riverward of the wall, and could be blocked if the wall and embankment slid due to the design earthquake. The investigation was aimed at determining what movements the wall might experience during the design earthquake and whether such movements would threaten the integrity of the embankment.

39. The construction photograph dated 16 April 1954, Figure 14, shows the completed wall with Zone A backfill in place. It is evident that a two-lane construction road exists at the base of the riverward face of the wall. Thus, the wall can undergo at least 20 ft of horizontal displacement without falling into the river channel.

40. However, horizontal displacements on the order of 20 ft or more, along with a deep-seated sliding failure surface through the embankment fill would seriously threaten the integrity of the envelopment area and reduce the crest elevation to the pool level. It is estimated that 10 ft of horizontal displacement could safely be tolerated since this corresponds roughly to a 5 ft reduction in crest height, leaving a freeboard of about 10 ft, and since a large volume of cohesionless material, Zone A and Zone B fills, are involved in the slide and would be available to fill cracks that developed.

41. A Newmark sliding block approach (Newmark 1965) was adopted to estimate the earthquake-induced permanent displacement of the wall and backfill. The Newmark approach for estimation of earthquake-induced permanent displacements involves determination of yield accelerations, estimation of embankment response and calculation of displacements. Yield acceleration is defined as the horizontal acceleration applied to the center of gravity of a sliding mass that results in a factor of safety against sliding of unity in a pseudo-static stability analysis. Two methods of stability analysis, Mononobe-Okabe (Seed and Whitman 1970) and UTEXAS2 (Wright 1985), and a range of material strengths were used to determine yield accelerations for Retaining Wall B. Vertical acceleration and possible hydrodynamic effects were expected

to be minimal, and with the concurrence of the Technical Specialists, were not included in the analyses.

42. The dynamic response of the embankment calculated with SEISCOE (a shear beam approach by Sarma 1979) and with FLUSH and the dynamic response of the Concrete Gravity Dam calculated with EADHI-84 were used to determine the earthquake-induced accelerations (loads) to be compared with the yield accelerations (available strength) in the backfill and retaining wall system. The earthquake-induced permanent displacements were then calculated with three different techniques, Makdisi-Seed (Makdisi and Seed 1979), Sarma-Ambraseys (Hynes-Griffin 1979, and Hynes-Griffin and Franklin 1984), and modified Richards-Elms (Whitman and Liao 1985). In addition to these analyses, an assessment of the post-earthquake stability of the wrap around was made with UTEXAS2 for a range of material strengths and geometries. A worst case scenario including a complete loss of Retaining Wall B and the Zone A material was included in these investigations.

Yield Acceleration Analyses

43. Yield accelerations, k_y (the pseudo-static acceleration applied at the center of gravity of a sliding mass which will reduce the safety factor against sliding to one), were computed for two locations, Section A-A which represents the wall and backfill geometry at the contact with the Concrete Gravity Dam (the tallest wall section), and Section C-C, in the vicinity of Wall Station 2+00. These sections and locations are shown in Figure 7. For the two-dimensional stability analyses, Sections A-A and C-C were idealized as simple gravity retaining walls resting on a level rock surface. The idealized sections are shown in Figures 35 and 36. The friction angle at the base of the wall was conservatively estimated as 30 degrees.

Mononobe-Okabe

44. Classically, seismically induced lateral earth pressures in dry granular media have been calculated with the Mononobe-Okabe approach. The complete form of the equation for the combined active and seismic force on the wall is:

$$P_{AE} = \frac{1}{2} \gamma H^2 (1 - k_v) K_{AE} \quad (1)$$

Conventionally, k_v is ignored. Therefore, Equation 1 is simplified to the following form:

$$P_{AE} = \frac{1}{2} \gamma H^2 K_{AE} \quad (2)$$

where

$$K_{AE} = \frac{\cos^2 (\phi - \psi - \beta)}{\cos \psi \cos^2 \beta \cos (\psi + \beta + \delta) \left[1 + \sqrt{\frac{\sin (\phi + \delta) \sin (\phi - \psi - i)}{\cos (i - \beta) \cos (\psi + \beta + \delta)}} \right]^2} \quad (3)$$

The force P_{AE} is the combined static and dynamic force due to the earth wedge defined by the assumptions made in deriving the equation for K_{AE} . The equation for K_{AE} is subject to all of the limitations applicable to a Coulomb formulation. Definitions of terms are as follows:

k_h = horizontal seismic coefficient

k_v = vertical seismic coefficient

γ = effective unit weight of backfill

H = backfill height

ϕ = internal friction angle, backfill

β = wall inclination angle (with respect to vertical)

i = inclination of backfill surface

$\psi = \tan^{-1}(k_h / 1 - k_v)$

(conventionally, k_v can be ignored and ψ equals $\tan^{-1}(k_h)$)

ϕ_b = wall friction angle, it was assumed to be $\phi/2$

Because k_v can be ignored, from this point on the subscript, v or h , will be dropped, and the seismic coefficient will just be called k . (See Figure 37 for a visual representation of the variables).

45. Retaining Wall B is completely submerged and this fact was accounted for in the analysis. A homogeneous backfill with a total unit weight of 152 pcf was used in the Mononobe-Okabe calculations. The problem was solved as if the wall and backfill were not submerged. The procedure to compute the equivalent seismic coefficient, k_y^* , is discussed in the following paragraphs. Finally, k_y^* , was determined using the computer programs in Appendix A. Then the resulting yield acceleration, k_y^* , was multiplied by

the ratio of buoyant unit weight to total unit weight to determine k_y , the yield acceleration that accounts for the effect of submergence. In this way, horizontal loads are computed with the total unit weight of the backfill but effective or buoyant unit weight controls the vertical stresses and hence shear strength along the critical sliding surface. The ratio of buoyant unit weight to total unit weight is 0.6 for the rockfill and gravel transition backfill.

46. In the Mononobe-Okabe procedure, there is a condition that ψ , the arctan of the horizontal seismic coefficient, must be less than or equal to the friction angle, ϕ , minus the slope angle, i . Values larger than this correspond to a non-equilibrium condition, and backfill material would fail by raveling and sliding until the slope angle i was reduced to the limiting value of $\phi - \psi$. Over the range of backfill strengths investigated, the condition that ψ be less than or equal to $\phi - i$ was maintained for all computed yield accelerations without changing the slope angle i .

47. Because of the uncertainties in dealing with a submerged retaining wall in a seismic environment (there have been no documented cases to verify the theoretical approach), two parameters were varied in the analyses and conservative conclusions were drawn from the results. The parameters varied were the pore pressure coefficient, reflected in the angle of internal friction utilized for the backfill, ϕ , and the wall inclination angle, β .

48. The backfill strengths were selected to correspond to excess pore pressure levels uniformly distributed throughout the backfill. With no excess pore pressure, $r_u = 0$, the effective friction angle of the Zone B gravel and that assumed for the Zone A rockfill is 43° , as presented earlier in Part III. It was estimated in the Wing Dam studies that the upstream shell of the Right Wing Dam may develop an average r_u about equal to or slightly less than 25 percent. The simple p-q diagram construction shown in Figure 38 was used to determine backfill friction angles of 43° , 37.9° , 33.1° , and 29.9° to correspond to excess pore pressure levels of 0 percent, 10 percent, 20 percent, and 25 percent, respectively. Yield accelerations were computed for these four excess pore pressure levels. The friction angle at the base of the wall, ϕ_b , was assumed to be 30 degrees. As mentioned in paragraph 18, the foundation rock exposure consisted of sharp, irregularly blasted surfaces. This foundation feature makes the selection of a 30 degree sliding friction angle

conservative. Two wall inclination angles were studied, the actual as-built value of 33 degrees and 0 degrees.

49. Short computer programs were developed to determine the values of k_y for the various parameter values presented above. See Appendix A for a listing of the programs and detailed output. The computed yield accelerations are summarized in Figure 39 and Table 3. As expected, as excess pore pressures increase, the yield acceleration decreases. The most critical seismic coefficient leading to a safety factor of 1.0 against sliding was $k = 0.025$ for Section A-A with a wall inclination angle of β equal to 33 degrees and an excess pore pressure of 25 percent ($\phi = 29.9^\circ$). The corresponding failure surface is inclined at an angle of 34° which intercepts the core as shown in Figure 40a. The minimum yield acceleration computed for Section C-C was 0.034 for the excess pore pressure field of 25 percent. This failure surface is inclined at 34.5° and also intercepts the core, as shown in Figure 40b. The failure surface angle α is defined in Figure 35. Eccentricities of loads were also computed, and it was found that the resultants fell within the base of the wall. These calculations imply that sliding is more critical than overturning, however, it is recognized that the assumed friction at the base of the wall is quite conservative.

UTEXAS2 approach

50. As a check on the Mononobe-Okabe assumptions and calculations, the yield accelerations were also computed using UTEXAS2. The program has the capability to search for the most critical non-circular sliding surface, and was expected to provide a better estimate of the involvement of the core in the slide.

51. The UTEXAS2 program uses Spencer's procedure which satisfies all requirements for static equilibrium by assuming that all side forces have the same inclination. The trial and error solution involves successive assumptions for the factor of safety and side force inclination to search for the most critical shear surface.

52. For the two cross sections A-A and C-C, the seismic coefficient was varied until a factor of safety against sliding approximately equal to unity was determined. As in the Mononobe-Okabe calculations, the backfill strength parameters were $\phi = 43^\circ, 37.9^\circ, 33.1^\circ, \text{ and } 29.9^\circ$ ($c = 0$) to correspond to r_u equal to 0, 10, 20, and 25 percent, respectively. Only values of β equal to 33° were investigated with UTEXAS2 for both cross sections.

53. Core strengths of $\phi = 37^\circ$ and 31.1° ($c = 0$) were used in the calculations. The resulting yield accelerations are shown in Table 4 with the Mononobe-Okabe results, and the critical failure surfaces for Sections A-A and C-C are shown in Figure 41. The corresponding minimum yield accelerations are 0.060 and 0.065, respectively for a core strength of $\phi = 31.1^\circ$, $c = 0$. The UTEXAS2 yield accelerations are fairly close to those obtained with the Mononobe-Okabe procedure for the range of strengths investigated, and the failure surfaces are in about the same locations. At low values of r_u , the yield accelerations are almost identical, and at higher values of r_u (values greater than 20 percent), the UTEXAS2 approach gives relatively higher results. In general, Section A-A has lower yield accelerations than Section C-C.

54. The strengths assumed for the core are conservative since the core is very densely compacted and has very high strength in consolidated-undrained loading. Figure 42 shows an R-strength envelope (total stress) with $c = 4.06$ tsf and $\phi = 30.6^\circ$ determined from laboratory tests on samples from Dike 5 which are representative of the core material, Zone C. Due to this high consolidated-undrained strength, it is unlikely that the core will undergo any Newmark-type deformation due to movement of the wall. A check on this assumption was made with a reduced undrained core strength of $c = 4,000$ psf and $\phi = 0$ for Section A-A. The shell strength corresponded to $r_u = 25$ percent. In this case, the yield acceleration was 0.073 and the critical failure surface, shown in Figure 41, did not involve the core.

Summary of yield acceleration computations

55. In summary, yield accelerations were calculated for two wall locations, Sections A-A and C-C, for a range of shell and core strengths by Mononobe-Okabe and UTEXAS2 procedures. A lower-bound estimate of the yield acceleration is 0.025g, based on Mononobe-Okabe calculations for Section A-A, with a residual excess pore pressure field of 25 percent ($\phi = 29.9^\circ$, $c = 0$) in the Zone A and Zone B shell materials. This failure surface is inclined at 34° and intercepts the core. A more representative, yet conservative UTEXAS2 analysis of Section A-A with a shell strength of $\phi = 29.9^\circ$ and $c = 0$, and a core strength of $\phi = 0$ and $c = 4,000$ psf (less than half the measured

laboratory R-strength), resulted in a yield acceleration of 0.073g and a failure surface that does not intercept the core, but is confined to the upstream shell.

56. A degree of conservatism is called for in the analysis of Retaining Wall B due to a lack of well-documented case histories of submerged retaining walls subjected to seismic loading, variability in Newmark-type displacement calculations, and uncertainties in the material properties of the embankment fill, particularly Zone A, which construction records show is a rockfill with considerable fines dumped in 12-ft lifts. In view of these uncertainties, and to determine an upper bound for Newmark-type displacement of the wall and backfill, the displacement calculations were carried out with $k_y = 0.025g$, with the understanding that the actual displacements in the field should be less than the computed values.

Permanent Deformation Estimates

57. Earthquake-induced permanent displacements were estimated with three methods: Makdisi-Seed, Sarma-Ambraseys and modified Richards-Elms. The Makdisi-Seed and Sarma-Ambraseys methods explicitly include embankment amplification effects in the displacement calculations. The modified Richards-Elms approach is more approximate with regard to ground motion amplification, but due to the modifications developed by Whitman and Liao (1985) it quantitatively accounts for the many uncertainties in Newmark displacement calculations such as theoretical deficiencies in the sliding-block model, the random nature of earthquake ground motions, uncertainty in parameters characterizing the backfill, wall and foundation, and other, poorly understood deficiencies of the simple sliding block model. Each of these methods was applied to the retaining wall problem to estimate the range of earthquake-induced displacements consistent with the conservatively computed minimum yield acceleration of 0.025g. As discussed earlier, the wall and wrap-around backfill should be able to easily tolerate displacements of about 10 ft.

Makdisi-Seed calculations

58. The parameters needed for these calculations are:
- a. The yield acceleration, k_y (fixed at 0.025).
 - b. The maximum crest acceleration, \ddot{u}_{max} .

- c. The maximum earthquake seismic coefficient, k_{\max} (the maximum earthquake-induced acceleration averaged over the sliding surface boundary).
- d. The depth of the failure surface, y , relative to the total embankment height, h (only failure surfaces that extend over the full height of the embankment were considered, so $y/h = 1.0$).

The peak crest acceleration at the wrap-around is estimated to be somewhat greater than that calculated with FLUSH for the Wing Dams, but less than that calculated with EADHI-84 for the Concrete Gravity Dam. Figure 32 shows that the calculated \ddot{u}_{\max} for the Wing Dams was 0.54g, which implies an amplification factor of the base ground motion of about 1.5. A peak crest acceleration of about 2.8g was estimated for the Concrete Gravity Dam, based on a single-mode approximation from the EADHI-84 results. Peak crest accelerations that ranged from 0.54 to 1.7g (the average of the embankment and gravity dam peak values) were considered in these displacement calculations. These values of \ddot{u}_{\max} correspond to amplification factors that range from 1.5 to 5. Since the concrete dam is embedded in the embankment at the wrap-around, it is estimated that its dynamic response will be considerably reduced by the upstream and downstream fill. It is assumed that a good estimate for \ddot{u}_{\max} at the wrap-around is 1g.

59. The maximum earthquake seismic coefficient, k_{\max} , is estimated from \ddot{u}_{\max} and Figure 43, which shows a range of values for k_{\max}/\ddot{u}_{\max} (determined from numerous dynamic analyses) plotted versus y/h . For $y/h = 1.0$, the average value of k_{\max}/\ddot{u}_{\max} is 0.34 and the upper bound value is 0.47. Both of these values for k_{\max}/\ddot{u}_{\max} were used to estimate k_{\max} for the various \ddot{u}_{\max} values considered. The best estimate for k_{\max} is $0.34 \times (\ddot{u}_{\max} = 1.0g) = 0.34$. The upper bound estimate for k_{\max} is $0.47 \times (\ddot{u}_{\max} = 1.7g) = 0.80$.

60. Figure 44 shows a range of Newmark-type displacements determined for various values of k_y/k_{\max} for Magnitude 6.5 earthquakes. For the best estimate of $k_{\max} = 0.34$, the ratio k_y/k_{\max} is equal to $0.025/0.34 = 0.07$. The corresponding approximate displacement is 70 cm or 2.3 ft. For the upper-bound estimate of $k_{\max} = 0.80$, the lower-bound value of k_y/k_{\max} is equal to $0.025/0.80 = 0.03$. The corresponding upper-bound displacement is 7.2 ft. With the compounded conservatism of lower-bound yield acceleration and upper-bound seismic coefficient and displacement values, it is expected from this

application of the Makdisi-Seed procedure that movement along the failure surface will occur, but be limited to less than 7 ft.

Sarma-Ambraseys calculations

61. This procedure involves the following parameters:

- a. The yield acceleration, k_y (fixed at 0.025).
- b. The fundamental period of the system, T_o .
- c. The amplification factor a , from which the maximum earthquake seismic coefficient (A , defined as the maximum embankment acceleration averaged over the sliding mass) is determined as $A = a \times \text{peak bedrock acceleration}$.
- d. The ratio y/h as defined above. For this case, $y/h = 1.0$.

Values of amplification factor a were computed with SEISCOE for both earthquake records A and B for a range of fundamental periods, $T_o = 0.1$ to 4 sec., and are shown in Figure 45 for several values of y/h . The maximum value of a from Figure 45 is 2.25 for $y/h = 1.0$, and occurs over the range $T_o = 0.20$ to 0.25 sec. The fundamental period of the Wing Dam section computed with FLUSH was 0.83 sec. At $T_o = 0.83$ sec, the amplification factor a is 1.0. The fundamental period of the concrete gravity dam, including foundation stiffness and the presence of the reservoir, is approximately 0.3 sec, and the corresponding amplification factor is approximately 1.75. The maximum value of $a = 2.25$ was used for the displacement calculations.

62. Newmark displacement charts were calculated for earthquake records A and B for several values of k_y/A , and are shown in Figure 46. For $k_y = 0.025$ and $A = 2.25 \times 0.35 = 0.79$, $k_y/A = 0.32$. The corresponding chart displacement, U_c , is 91 cm (3 ft) for record A and 36 cm (1.2 ft) for record B. The field displacement, U_f is calculated as $\alpha \times a \times U_c$. The factor α is a term from the solution to the equations of motion for relative displacement of the sliding block (see Hynes-Griffin and Franklin, 1984), and is a function of the inclination of the sliding surface (34°) and the friction angle of the backfill (29.9°). The factor α is equal to $\cos(34^\circ - 29.9^\circ) / \cos(29.9^\circ) = 1.15$. The resulting field displacement for record A is $U_f = 1.15 \times 2.25 \times 91 \text{ cm} = 235 \text{ cm}$ (7.7 ft), and for record B, $U_f = 1.15 \times 2.25 \times 36 \text{ cm} = 93 \text{ cm}$ (3 ft). The Makdisi-Seed estimated displacements of 2.3 ft (best estimate) and 7.2 ft (maximum) are very similar to those calculated with the Sarma-Ambraseys approach.

Modified Richards-Elms calculations

63. The sliding-block method of analysis developed by Richards and Elms (1979) was modified by Whitman and Liao (1985) to quantitatively account for uncertainties in the input parameters and inadequacies in the model itself. These errors can be attributed to the uncertainty associated with ground motions, the uncertainties associated with resistance (unit weights of the backfill or the retaining wall, friction angles, or wall friction), due to model errors (assuming vertical acceleration is negligible, assuming that the slope failure angle is constant with time, or that the one-block model is accurate enough), or due to the effect of tilting (from Whitman and Liao, 1985). The Richards-Elms approach attempts to take these uncertainties into account when computing seismic induced displacements.

64. The basic equation proposed by Whitman and Liao is:

$$d_{Rw} = d_{Rv} \times R_{2/1} \times Q \times R_{\phi} \times M \quad (4)$$

where

- d_{Rw} = predicted residual displacement
- d_{Rv} = mean (expected) residual displacement for a sliding block exposed to ground motion characterized by a small number of parameters (such as peak acceleration, A, and peak velocity, V)
- $R_{2/1}$ = deterministic term accounting for a specific kinematic deficiency in the single sliding block model
- Q = term accounting for the unpredictable details in the random nature of future earthquake shaking
- R = term accounting for the uncertainty in the parameters characterizing the backfill, wall and foundation soil
- M = term accounting for other, and as yet, poorly understood deficiencies of the simple sliding block model

65. Whitman and Liao (1985) recommend values for $R_{2/1}$, Q, R, and M to simplify Equation 4. Equation 4 can be rewritten to account for the probability of a computed displacement occurring. A 95 percent probability level corresponds to a factor of safety of 4 on the computed displacement, which means that the computed displacement for a 95 percent non-exceedance reliability is 4 times the best estimate value of displacement. The formula that relates the input parameters to displacement for a 95 percent probability of non-exceedance is:

$$\frac{k_y}{A_{\max}} = 0.66 + \frac{1}{9.4} \ln \frac{V_{\max}^2}{A_{\max} g d_L} \quad (5)$$

where

$$g = 981 \text{ cm/sec}^2$$

d_L = limiting value of displacement in cm for a 95 percent probability of non-exceedance

The parameters required to substitute into the equation above are:

- a. The yield acceleration, $k_y = 0.025$ from the Mononobe-Okabe calculations.
- b. The design ground motion parameters, $A_{\max} = 0.35g$ and $V_{\max} = 20 \text{ cm/sec}$.
- c. The degree of conservatism in the displacement calculations expressed as the probability that the wall displacement will not exceed the computed value. A 95 percent probability of non-exceedance was selected.

With these values and the Richards-Elms equation, the limiting value of displacement is computed to be 9.7 ft, and the best estimate for wall displacement is computed to be 2.4 ft. These values are quite similar to those computed with the Makdisi-Seed and Sarma-Ambraseys approaches, and are within tolerable limits.

Post-Earthquake Stability Studies for Worst Case Scenarios

66. A study was made of the consequences of complete wall failure by investigating two worst-case scenarios. In one case, the wall is assumed to have toppled, and the backfill slope is still approximately 1 vertical to 2 horizontal but the shell strength is reduced to a residual value of 1,800 psf (based on a reduced $(N_1)_{60}$ value of 19 for the envelopment shell from adjusted Becker data, and a corresponding residual strength from Seed (1986) shown in Figure 34). In this extreme case, the slope has a factor of safety of 1.12 against post-earthquake sliding. In the other case, the retaining wall and all of Zone A are assumed to be lost, leaving the gravel transition Zone B exposed at a slope of 1 vertical on 1.5 horizontal, with a residual strength of 1,800 psf. In this extreme case, the factor of safety against post-earthquake sliding was 1.07. Since the safety factors against liquefaction typically exceed 1.5 in the Right Wing Dam, the post-earthquake

stability of the wrap-around slope will be greater than that for the residual conditions listed above, and the deformations associated with development of soil strength will be considerably less than those needed for residual conditions.

67. The Newmark-type displacement analyses for the Wing Dams described in Report 6 of this series concluded that earthquake-induced deformations in the downstream shells would be less than 0.5 m. If Retaining Walls A and E were to fail due to earthquake loads, the deformed slope of the envelopment fill would be approximately 35°. Since this slope is significantly less than the friction angle of the fill, the deformed slope should be stable.

Stability Evaluation

68. The Makdisi-Seed, Sarma-Ambraseys and modified Richards-Elms approaches all gave earthquake-induced permanent displacement estimates of Retaining Wall B and Right Wing envelopment fill less than or equal to 5 ft for average estimates and less than 10 ft for upper-bound estimates. These Newmark sliding-block analyses indicate that some damage to the wall is expected but the deformations will be limited. Worst-case scenario investigations show the slopes will be stable even with total failure of Retaining Wall B. Catastrophic loss of the reservoir is not expected as a result of the damage to the upstream retaining wall and envelopment fill. It is concluded that failure of Retaining Walls A and E would not threaten the integrity of the envelopment area as long as the backfill is unsaturated.

PART V: SUMMARY AND CONCLUSIONS

69. There are many uncertainties associated with computing the displacements of a retaining wall in a seismic environment. These uncertainties have been compounded for Retaining Wall B because it is submerged, and there are no case studies to allow a comparison of computed displacements with actual field performances.

70. Therefore, a very conservative approach has been used in these analyses. Two procedures, Mononobe-Okabe and UTEXAS2, were used to compute the seismic coefficient, k_y . Within each procedure, conservative estimates of parameters were used. For example, reduced backfill strengths were used in both procedures. The minimum yield acceleration was computed with a reduced backfill strength of $\phi' = 29.9^\circ$, which corresponds to a uniform excess pore pressure field in the backfill of 25 percent. Several different parameter variations were investigated, and the most conservative combination was the basis for determining k_y . The final value of k_y used for displacement calculations was 0.025g.

71. With this value of k_y , an estimate of the movement of the wall was performed using three different methods, Makdisi-Seed, Sarma-Ambraseys, and Richards-Elms. In each method an average value of displacement was computed, as well as, the worst possible displacement. The worst possible displacement, a slip of 9.7 ft along the failure angle with a vertical drop of 6.5 ft, was determined from the Richards-Elms method.

72. A vertical drop of 6.5 ft would cause a noticeable slip in the interface area, even in the core of the Right Wing Dam. However, with a free-board of 15 ft a drop of 6.5 ft is an acceptable displacement. There should not be a breach in the dam, the reservoir will not be lost, and the intakes to the penstocks will not be completely blocked.

73. A case has also been made, that even if Retaining Wall B is completely removed from the site, the integrity of the interface will remain intact. With the loss of the Zone A shell, the Zone B shell at a slope of 1.5 to 1 has a factor of safety against sliding greater than 1.0. Therefore, the core of the dam will still be safe even if Retaining Wall B has been destroyed.

74. It is concluded that failure of Retaining Walls A and E would not threaten the integrity of the envelopment area as long as the backfill is

unsaturated. Periodic inspection and maintenance of the weep holes in these walls is recommended to assure backfill drainage.

REFERENCES

- Allen, M. G. 1984. "Liquefaction Potential Investigation of Mormon Island Auxiliary Dam, Folsom Project, California", Soil Design Section, US Army Engineer District, Sacramento, CA.
- Banerjee, N. G., Seed, H. B. and Chan, C. K. 1979. "Cyclic Behavior of Dense Coarse-Grained Materials in Relation to the Seismic Stability of Dams", Report No. EERC 79-13, Earthquake Engineering Research Center, University of California, Berkeley, CA.
- Bhatia, S. 1986. "Dynamic Effective Stress Analysis, Folsom Project," WES Contract Report, Vicksburg, MS.
- Bolt, B. A., and Seed, H. B. 1983. "Accelerogram Selection Report for Folsom Dam Project, California." Contract Report DACW 05-83-Q-0205, US Army Engineer District, Sacramento, CA.
- Elms, D., and Richards, R. 1979. "Seismic Behavior of Gravity Retaining Walls." Journal of the Geotechnical Engineering Division, American Society of Engineers. Vol 105, No. GT4, pp 449-464.
- Evans, M. 1987. "Undrained Cyclic Triaxial Testing of Gravels-The Effect of Membrane Compliance," PhD Thesis in Engineering, University of California, Berkeley, CA.
- Hynes-Griffin, M. E. 1979. "Dynamic Analyses of Earth Embankments for Richard B. Russell Dam and Lake Project," Final report prepared for US Army Engineer District, Savannah, GA.
- _____. 1987. "Seismic Stability Evaluation of Folsom Dam and Reservoir Project, Vol 1, Summary Report." Draft Technical Report GL-87-14, US Army Engineer Waterways Experiment Station, CE, Vicksburg, MS.
- Hynes-Griffin, M. E., and Franklin, A. G. 1984. "Rationalizing the Seismic Coefficient Method." Miscellaneous Paper S-84-13, US Army Engineer Waterways Experiment Station, CE, Vicksburg, MS.
- JSCE. 1977. "Earthquake Resistant Design for Civil Engineering Structures, Earth Structures and Foundations in Japan," Japan Society of Civil Engineers.
- Kiersch, G. A., and Treasher, R. C. 1955. "Investigations, Areal and Engineering Geology - Folsom Dam Project, Central California," Economic Geology, Vol 50, No. 3, pp 271-310.
- Liao, S., and Whitman, R., 1984. "Seismic Design of Gravity Retaining Walls," Eighth World Conference on Earthquake Engineering, July 21-28, 1984, San Francisco, CA. Vol III, pp 533-540.
- Makdisi, F. I., and Seed, H. B. 1979. "Simplified Procedure for Estimating Dam and Embankment Earthquake-Induced Deformations." Journal of the Geotechnical Engineering Division, American Society of Civil Engineers. Vol 104, No. GT7, pp 849-867.
- Newmark, N. M. 1965. "Effects of Earthquakes on Dams and Embankments," Geotechnique, Vol 15, No. 2, pp 139-160.

- Roddy, R. Jr. 1955. "Stilling Basin and Retaining Walls, Folsom Project, Foundation Report, American River, California." US Army Corps of Engineers, Sacramento District, Sacramento, CA.
- Sarma, S. K. 1979. "Response and Stability of Earth Dam. During Strong Earthquakes." Miscellaneous Paper GL-79-13, US Army Engineer Waterways Experiment Station, CE, Vicksburg, MS.
- Seed, H. B. 1986. "Design Problems in Soil Liquefaction," UCB/EERC Report No. 86/02, University of California, Berkeley, CA.
- Seed, H. B., Idriss, I. M., and Arango, I. 1983. "Evaluation of Liquefaction Potential Using Field Performance Data," Journal of the Geotechnical Engineering Division, American Society of Civil Engineers, Vol 109, No. GT3, pp 458-482.
- Seed, H. B., Lee, K. L., Idriss, I. M., and Makdisi, F. 1973. "Analysis of the Slides in the San Fernando Dams during the Earthquake of February 9, 1971." Report No. EERC 73-2. Earthquake Engineering Research Center, University of California, Berkeley, CA.
- Seed, H. B., Tokimatsu, K., Harder, L. F., and Chung, R. M. 1984. "The Influence of SPT Procedures in Soil Liquefaction Resistance Evaluations," UCB/EERC Report No. 84/15, University of California, Berkeley, CA.
- Seed, H. B., and Whitman, R. V. 1970. "Design of Earth Retaining Structures for Dynamic Loads," ASCE Specialty Conference, Lateral Stresses in the Ground and Design of Earth Retaining Structures, pp 103-147.
- Sykora, D. W., and Hynes-Griffin, M. E. 1987. "Seismic Stability Evaluation of Folsom Dam and Reservoir Project, Vol 2, Interface Report." Draft Technical Report GL-87- , US Army Engineer Waterways Experiment Station, CE, Vicksburg, MS.
- Tierra Engineering Consultants, Inc., 1983. "Geologic and Seismologic Investigations of the Folsom, California Area." Contract Report DACW 05-82-C-0042, US Army Engineer District, Sacramento, CA.
- Tsuchida, T. 1986. "Stability Analysis of Retaining Walls," working papers.
- Whitman, R., and Liao, S. 1985. "Seismic Design of Gravity Retaining Walls," Miscellaneous Paper GL-85-1, US Army Engineer Waterways Experiment Station, CE, Vicksburg, MS.
- Wright, S. G. 1985. "UTEXAS2 (University of Texas Analysis of Slopes - Version 2), A Computer Program for Slope Stability Calculations," US Army Engineer District, Ft. Worth Contract Report.

Table 1

Summary of Design Values of Embankment Soil Properties in Wing Dams
from Construction Records

<u>Zone</u>	<u>Description</u>	<u>Dry Unit Weight (pcf)</u>	<u>Moist Unit Weight (pcf)</u>	<u>Saturated Unit Weight (pcf)</u>	<u>Effective Friction Angle (°)</u>	<u>Effective Cohesion (psf)</u>	<u>Permeability (ft/day)</u>
A	Rockfill Shell	125.0	133.0	143.8	40°	0	--
B	Gravel Transition	125.0	133.0	143.8	40°	0	--
C	Impervious Core	123.4*	134.0	140.0	35°	0	0.5

* At 95% Modified A.A.S.H.O. Density.

Table 2
Hyperbolic Parameters Input to FEADAM for Static Analysis of Wing Dams

Material Location	Effective Unit Weight (pcf)	Young's Modulus		Young's Modulus Exponent N	Failure Ratio R _f	Bulk Modulus K _b	Bulk Modulus Exponent M	Effective Cohesion Intercept C (ksf)	Effective Friction Angle φ (°)	Change in φ Per Log Cycle Change in Confining Stress Δφ	Static Stress Ratio K _o
		Loading K (ksf)	Unloading K _{ur} (ksf)								
Saturated Shell	90	1,900	1,900	.39	.9	1,287	.33	0	43	0	0.5
Dry Shell	139	1,900	1,900	.39	.9	1,267	.33	0	43	0	0.5
Saturated Core	79.4	1,175	1,175	.15	.69	979	.43	0	37	0	0.43
Dry Core	136	1,175	1,175	.15	.69	979	.43	0	37	0	0.43
Rock	150	10,000	10,000	1.0	.9	10,000	1.0	5	50	0	0.5

Table 3
Yield Accelerations Computed with Mononobe-Okabe Approach

		Yield Acceleration, K_y			
		Excess Pore Pressure, r_u (%)			
<u>Cross Section</u>		<u>0</u>	<u>10</u>	<u>20</u>	<u>25</u>
C A S E 1	A-A	0.147	0.097	0.054	0.025
	C-C	0.153	0.105	0.062	0.034
C A S E 2	A-A	0.154	0.113	0.088	0.078
	C-C	0.161	0.126	0.091	0.081

Table 4
Summary of Yield Accelerations for Retaining Wall B

Residual Excess Pore Pressure r_u (%)	Corresponding Effective Friction Angle of Backfill* ϕ (°)	Yield Acceleration, k_y (g)†			
		Section A-A		Section C-C	
		Mononobe- Okabe	UTEXAS2**	Mononobe- Okabe	UTEXAS2**
0	43.0	0.15	0.13	0.15	0.16
10	37.9	0.10	0.11	0.11	0.125
20	33.1	0.05	0.08	0.06	0.09
25	29.9	0.025	0.06	0.03	0.065

* For gravel shell, $c = 0$.

** Core strengths are $c = 0$, $\phi' = 31.1^\circ$.

† $\phi_b = 30^\circ$.

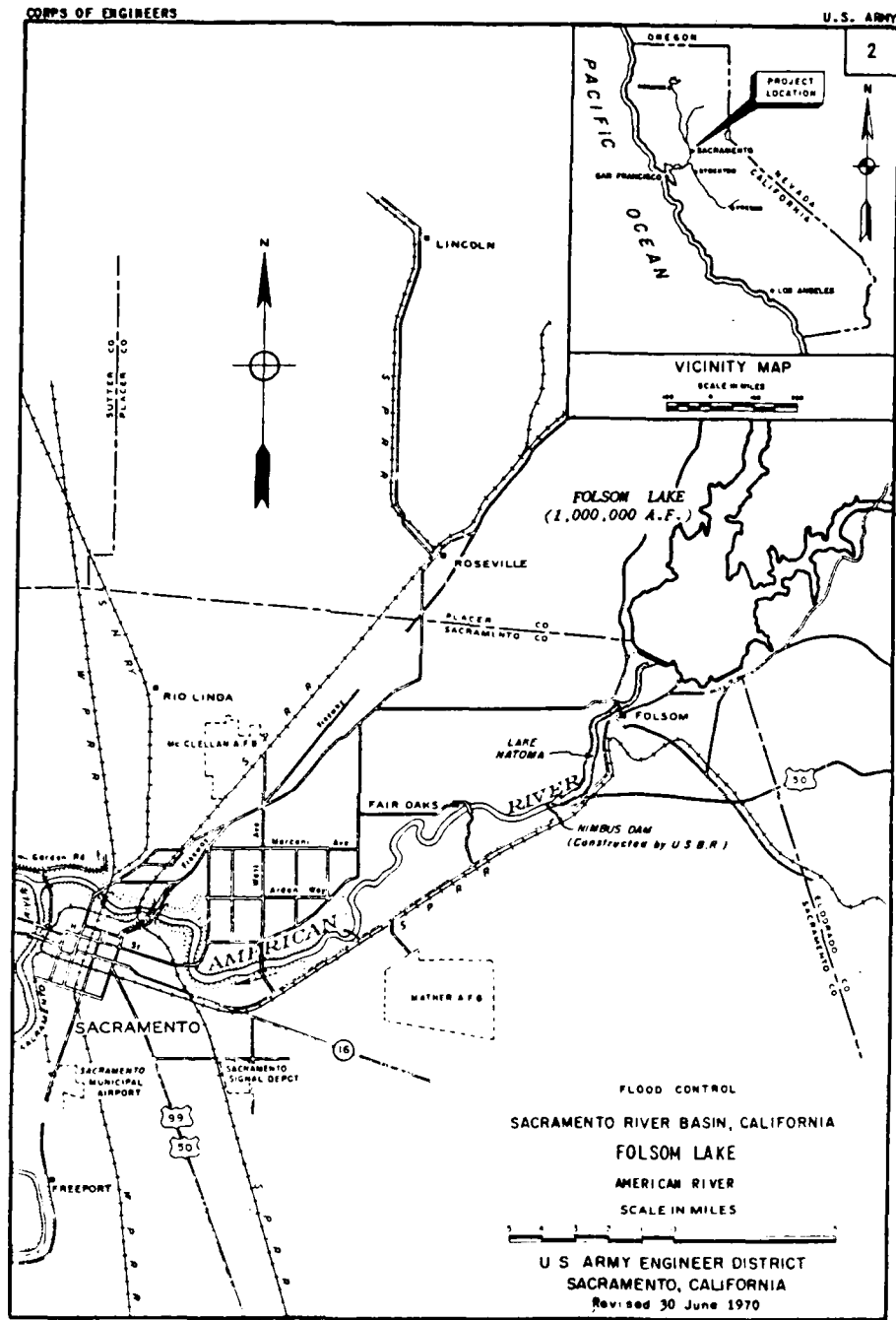


Figure 1. Location of Folsom Dam and Reservoir Project

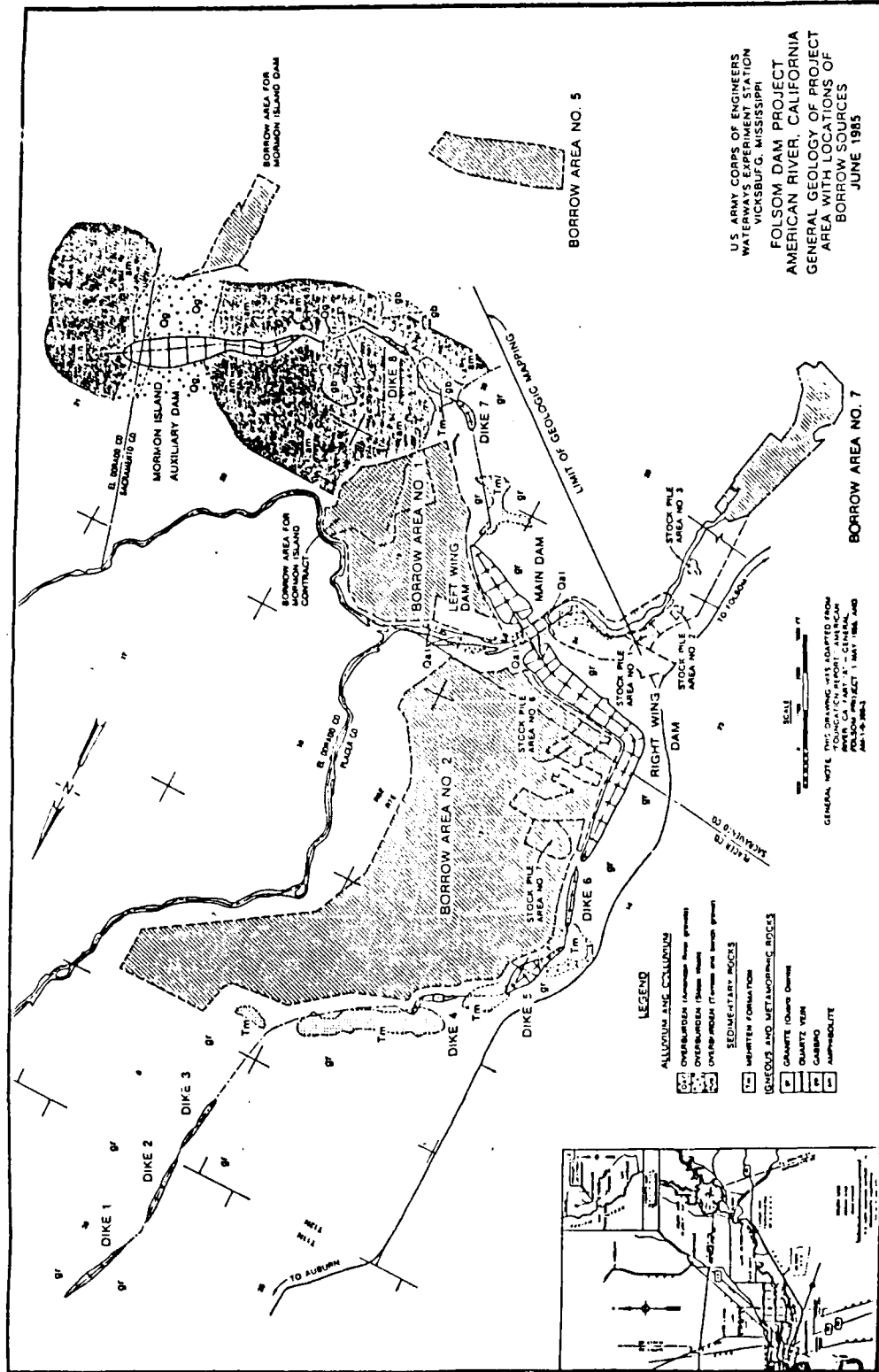


Figure 2. Plan of man-made retaining structures at Folsom Dam Project

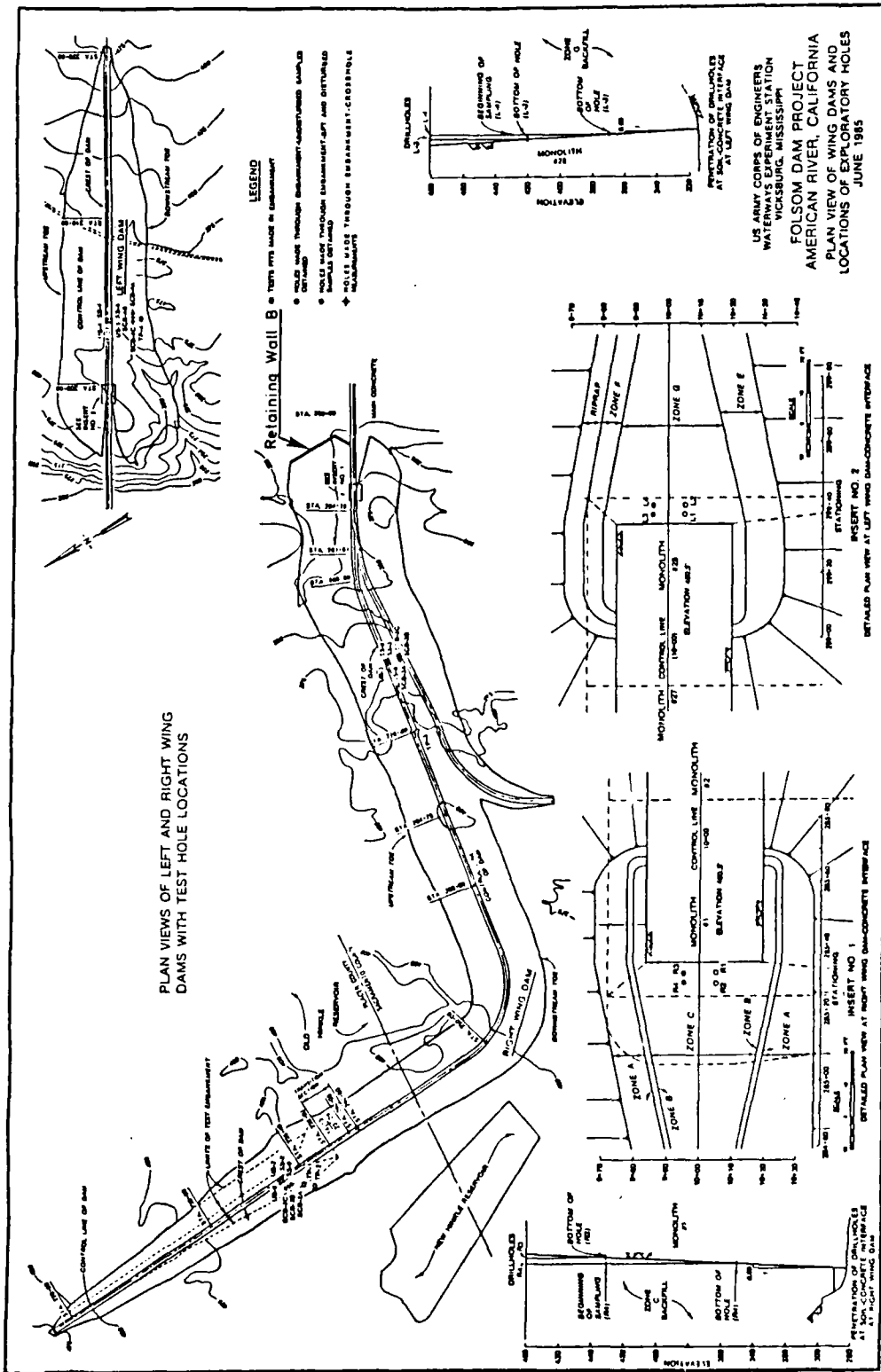


Figure 3. Plan view of Right and Left Wing Dams and detailed plan view of interface areas

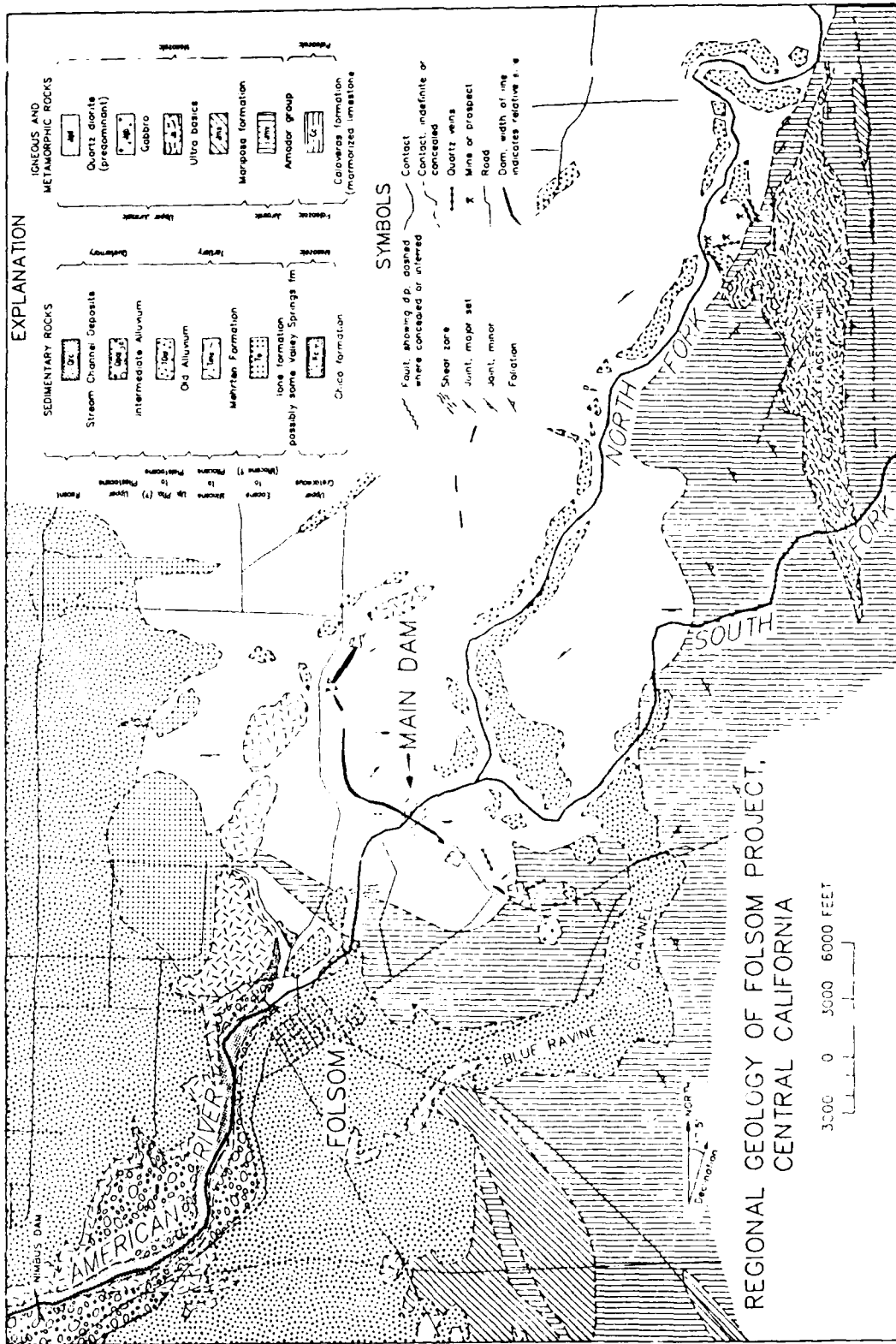
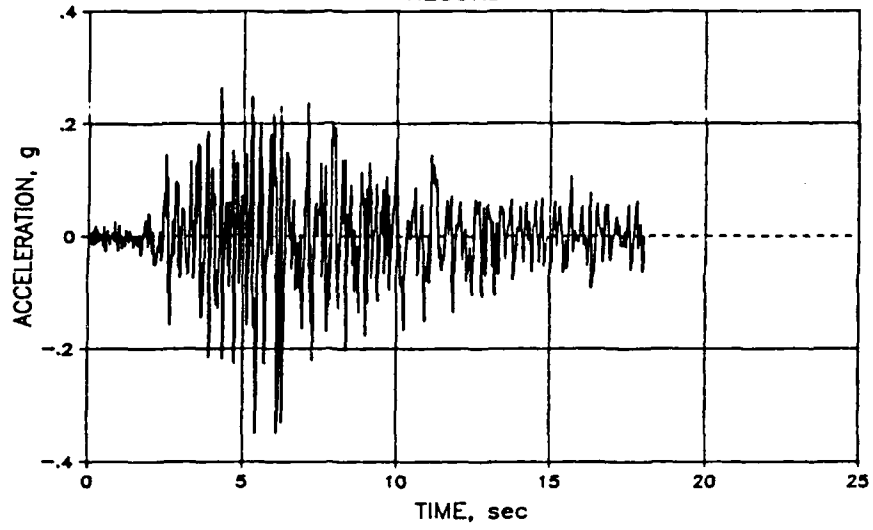


Figure 4. Geologic map, parts of the Folsom and Auburn quadrangles

FOLSOM DAM PROJECT
RECORD A



RECORD B

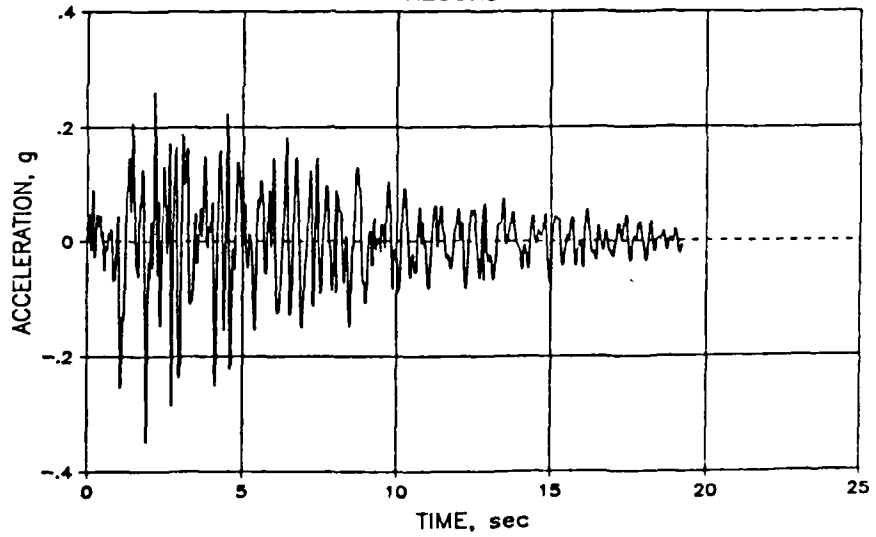


Figure 5. Acceleration histories used in the analysis

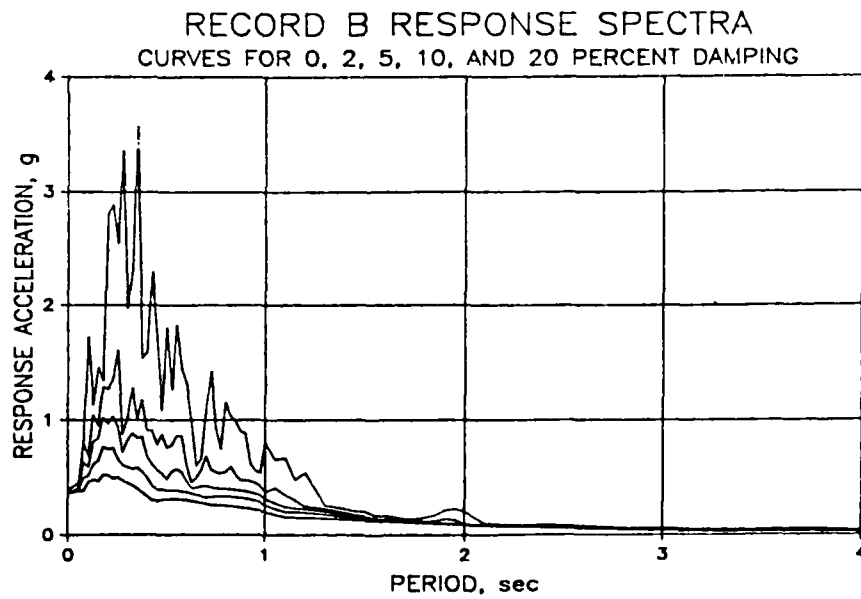
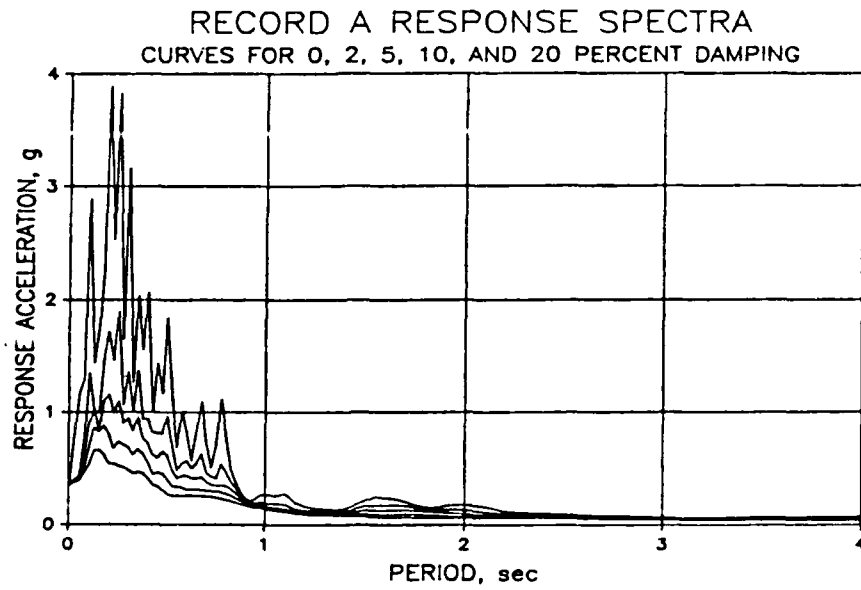


Figure 6. Response spectra of records A and B

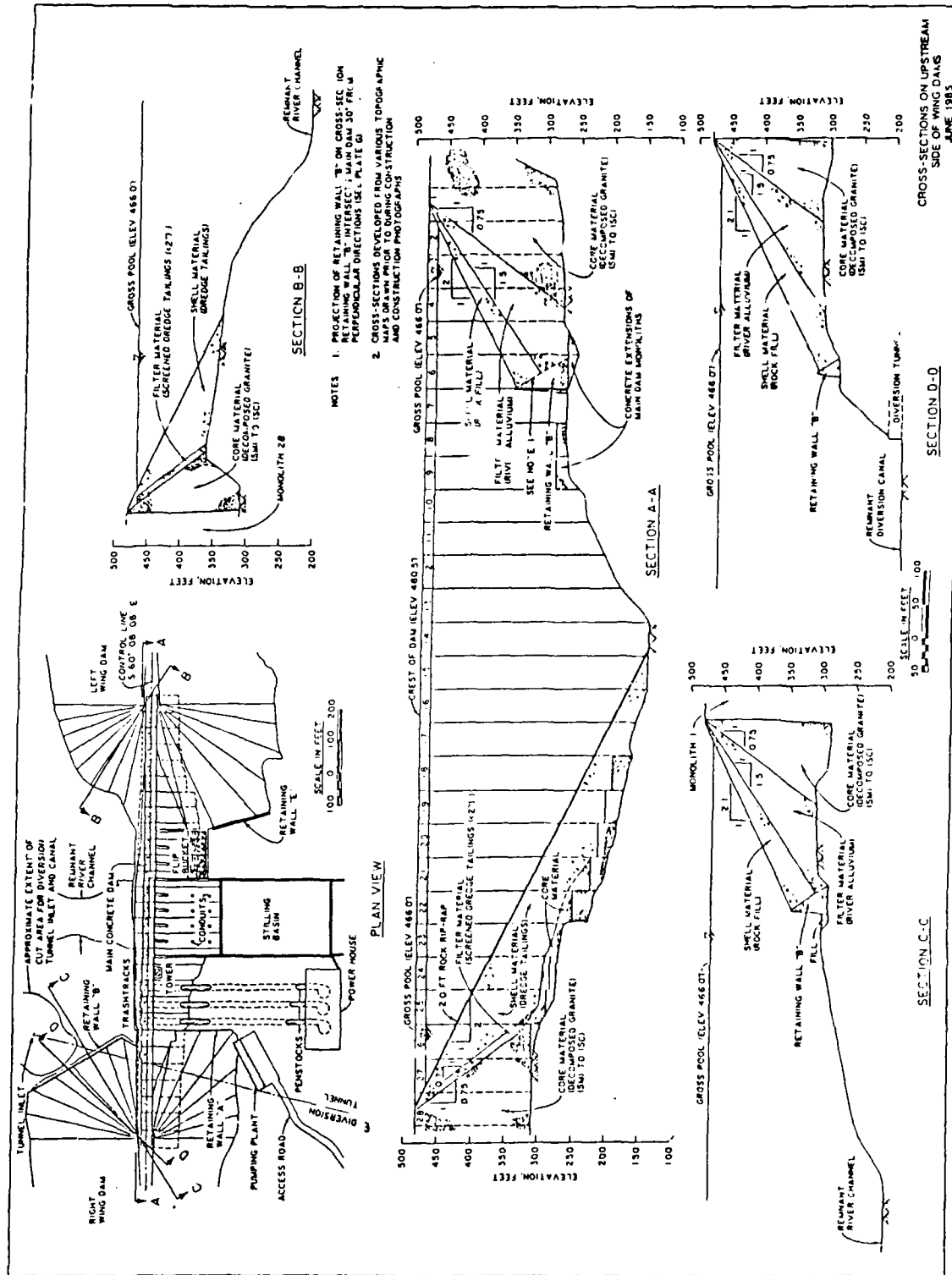


Figure 7. Plan and sections of upstream envelopment areas and Retaining Wall B

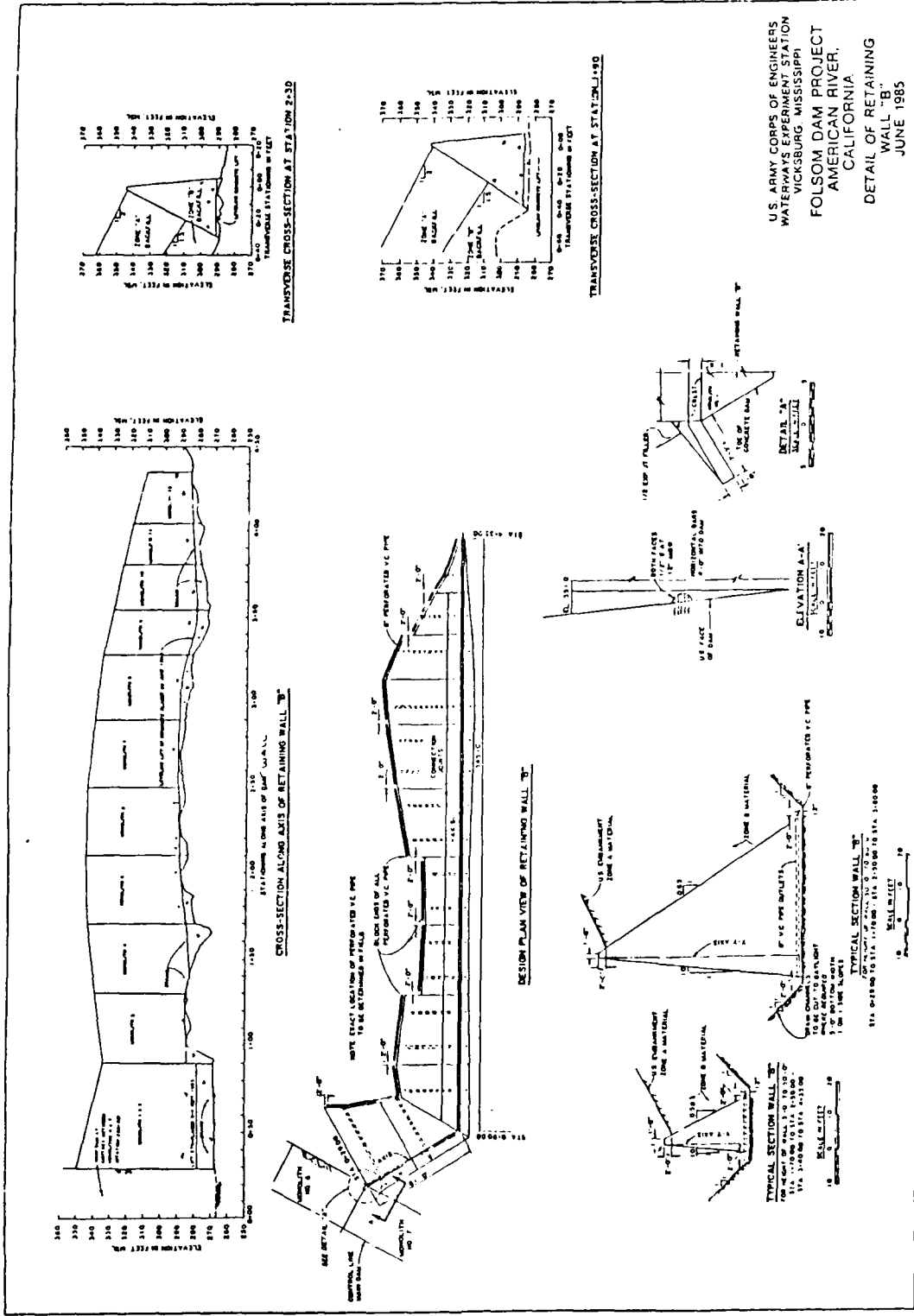


Figure 8. Plan and sections of Retaining Wall B

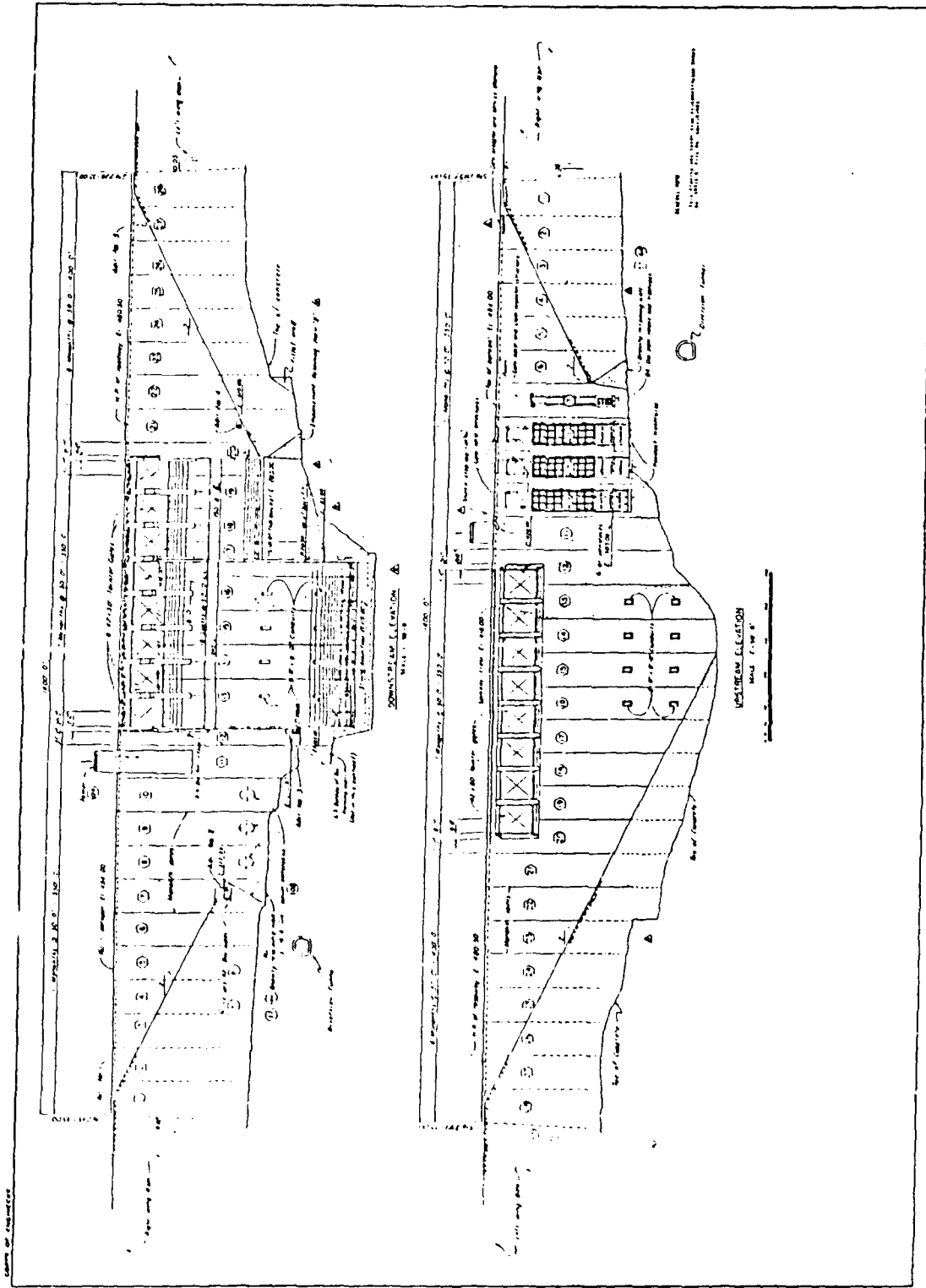
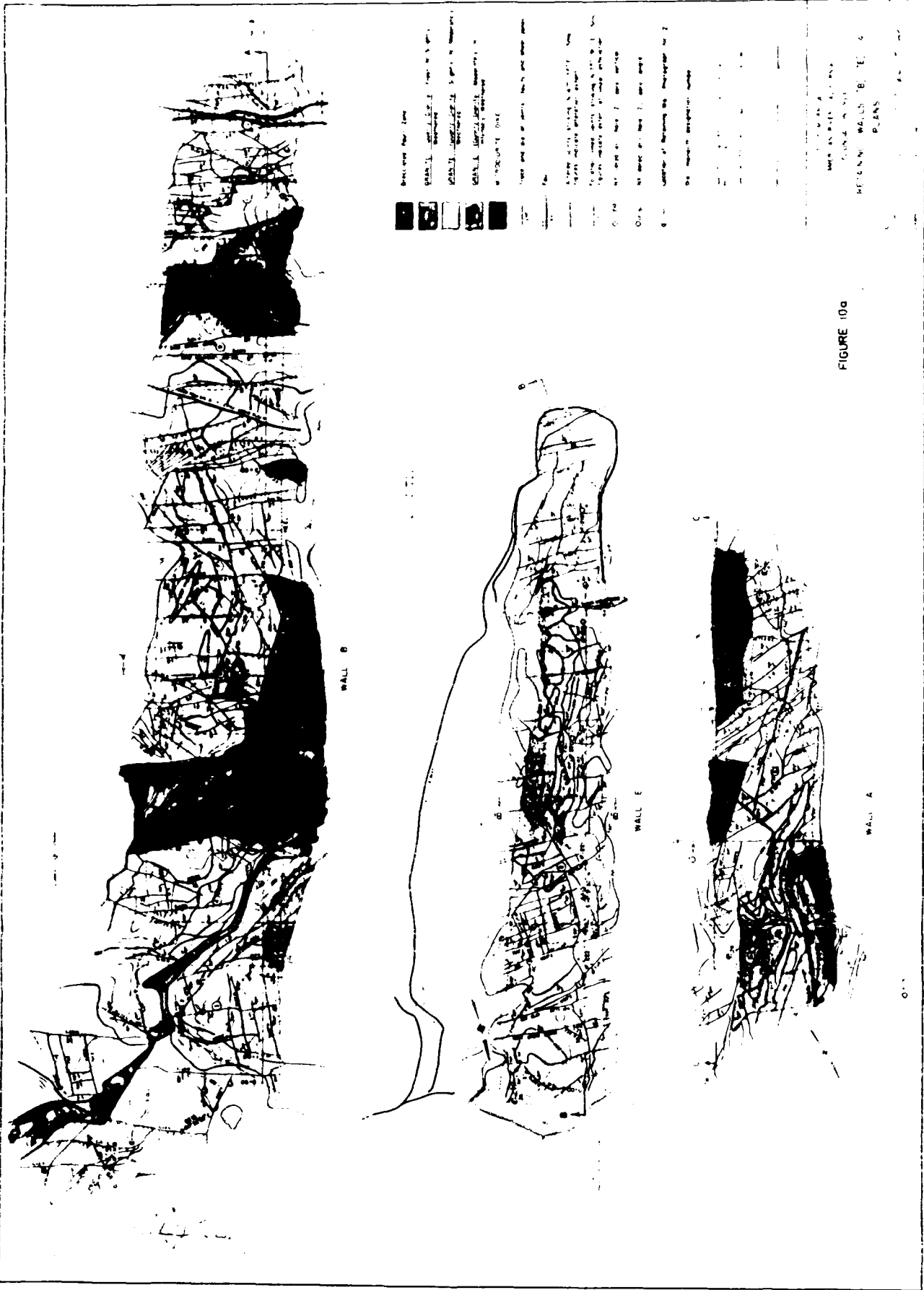
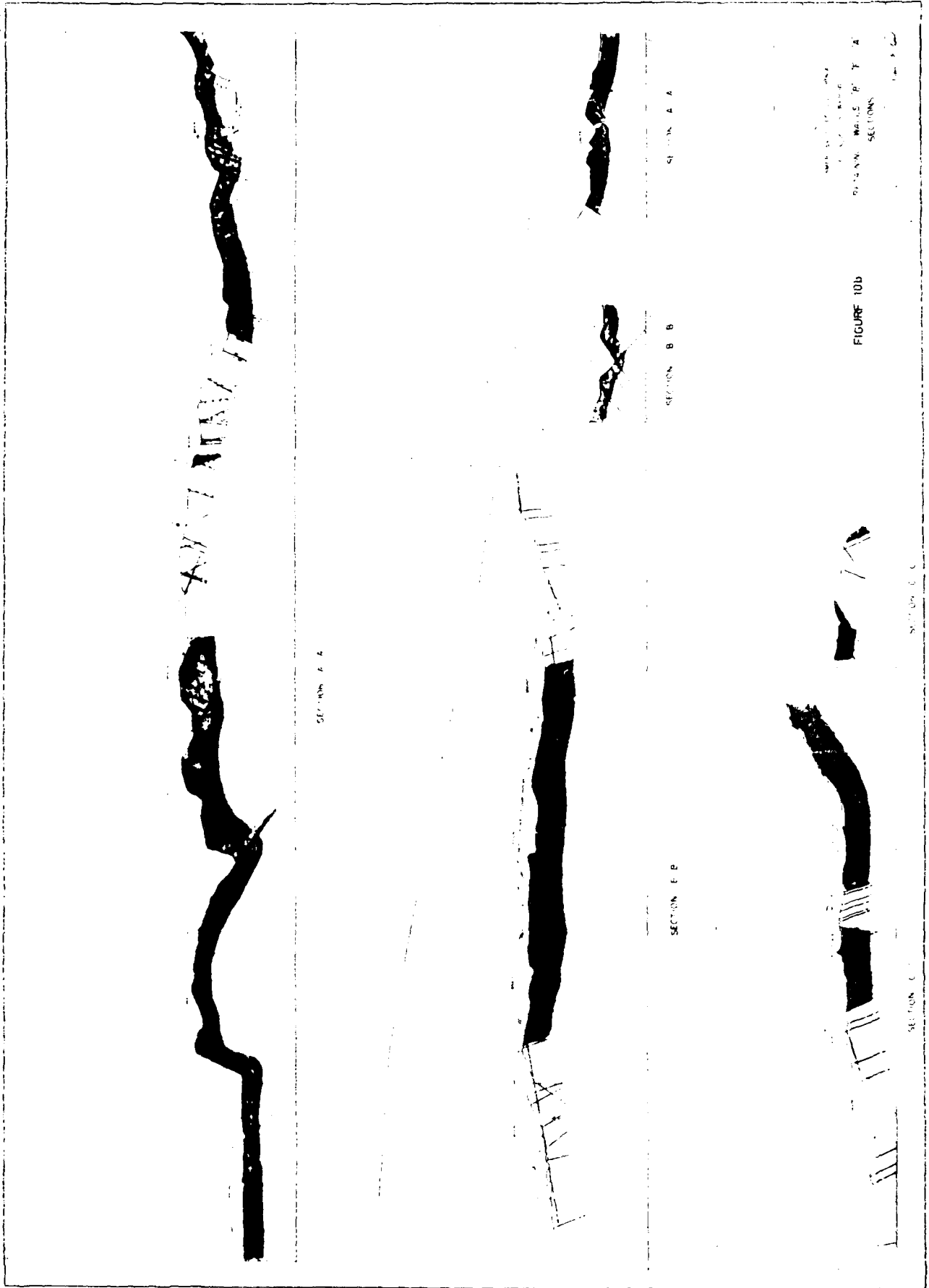


Figure 9. Concrete gravity dam elevations





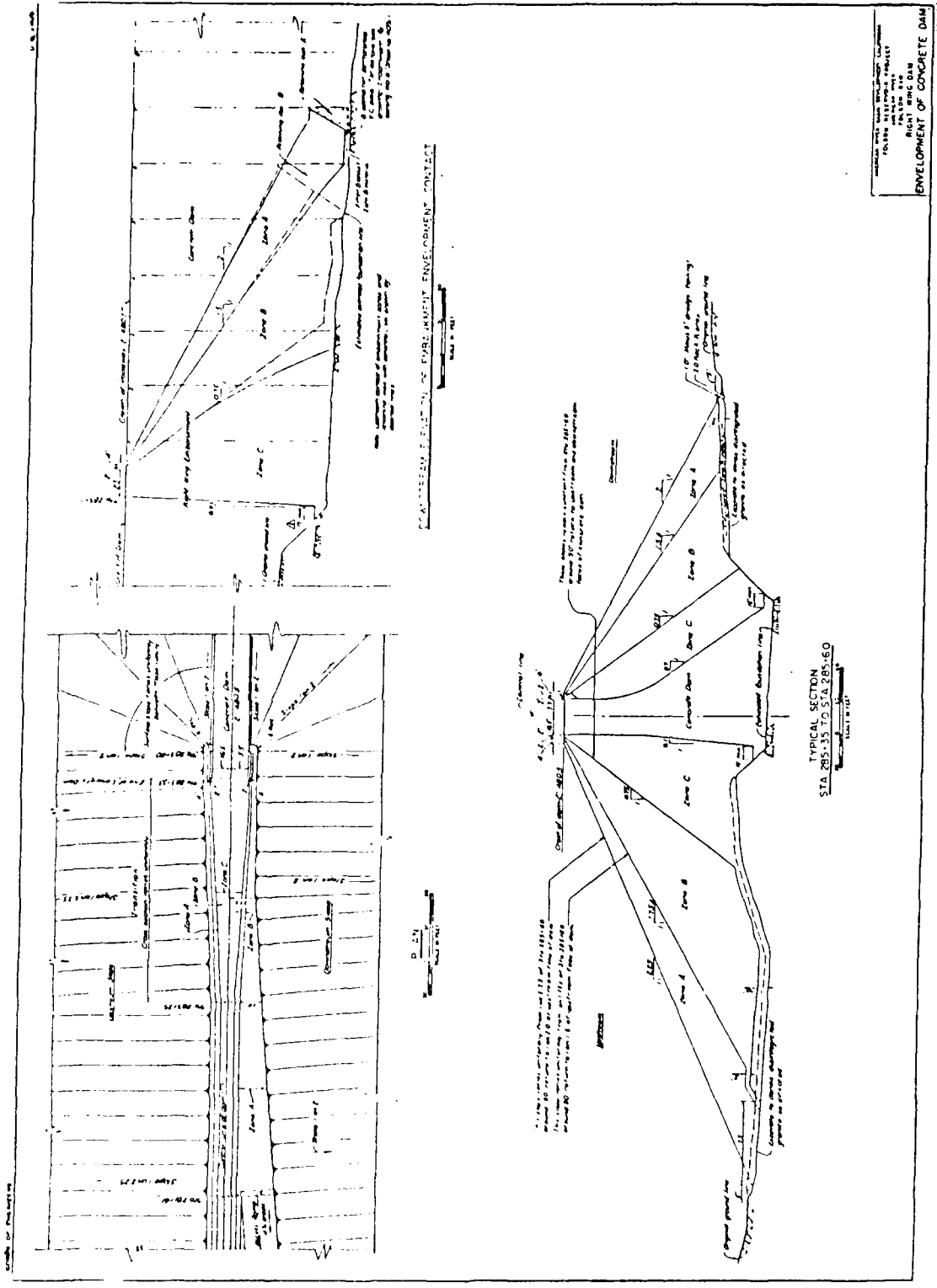


Figure 11. Plan and sections of Right Wing Dam interface area

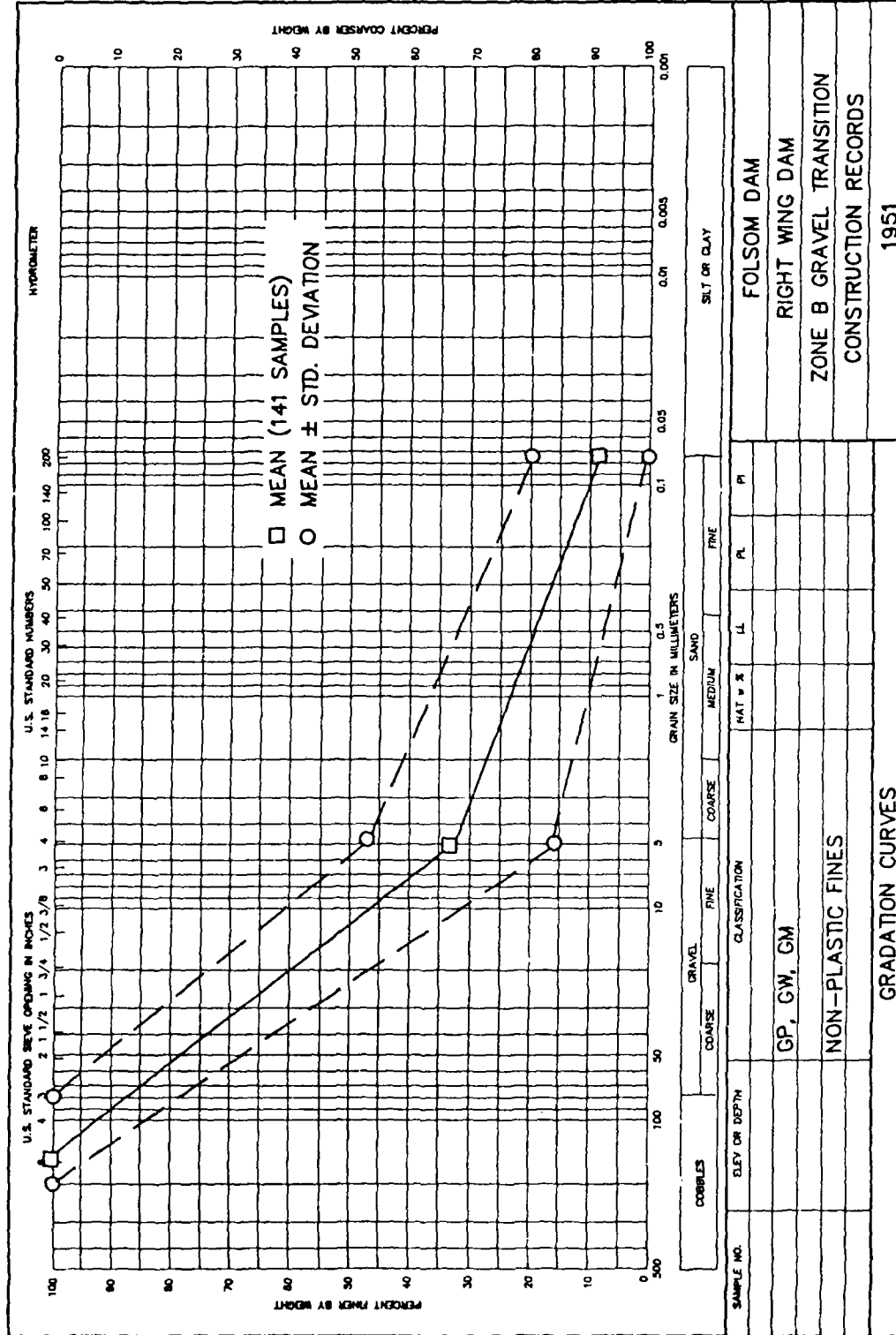


Figure 12. Gradation of Zone B gravel transition in Right Wing Dam from construction records (1951)

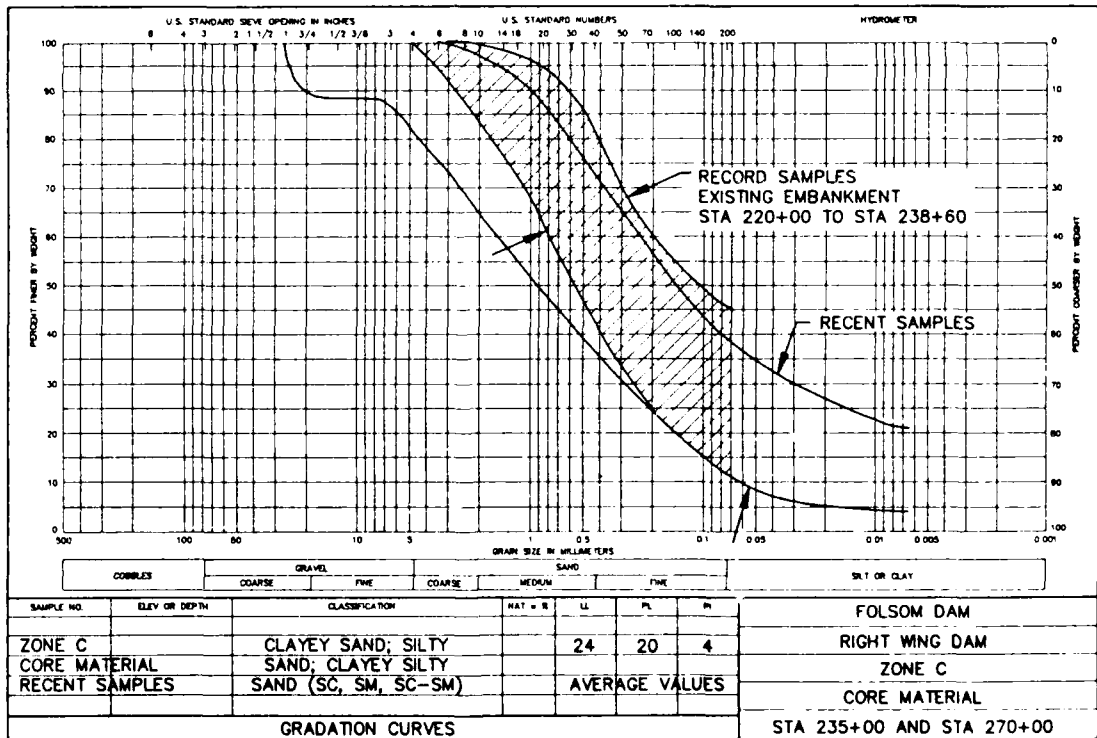
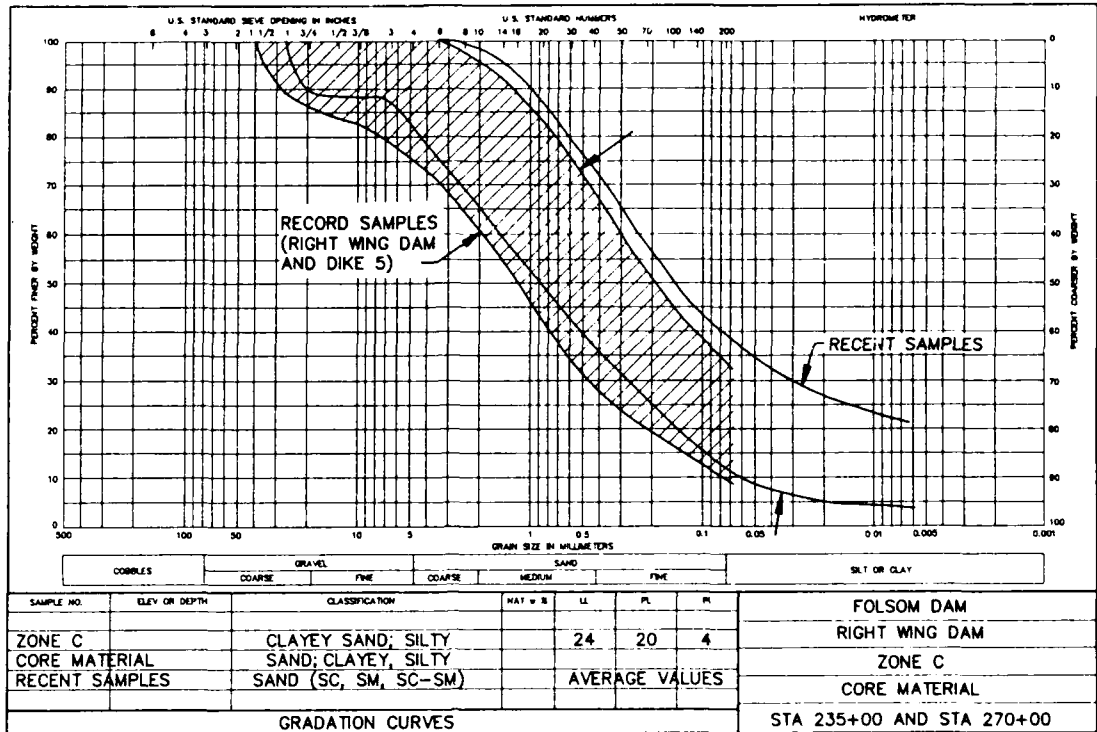


Figure 13. Grain size distribution for materials of Zone C and existing dam in Right Wing Dam (from construction records)



Figure 14. Construction photograph FOL 1818, dated 16 April 1954, showing construction of Right Wing Dam, concrete monoliths, and Retaining Wall B (completed)



Figure 15. Folsom Dam Photo FOL 1141 (25 June 1953) - excavation for Retaining Wall "B" looking downstream



Figure 16. Folsom Dam Photo FOL 1217 (29 July 1953) - Main Dam construction with the RWD
in the foreground



Figure 17. Folsom Dam Photo FOL 1282 (28 August 1953) - upstream area in right abutment



Figure 18. Folsom Dam Photo FOL 1190 (22 September 1953) - right abutment at intersection of the Main Dam and Retaining Wall "B" (looking upstream)



Figure 19. Folsom Dam Photo FOL 1364 (15 October 1953) - Main Dam and RWD construction looking from left abutment



Figure 20. Folsom Dam Photo FOL 1377 (15 October 1953) - upstream area of RWD looking downstream during placement of fill



Figure 21. Folsom Dam Photo FOL 1387 (15 October 1953) - upstream area of RWD looking upstream during placement of fill



Figure 22. Folsom Dam Photo FOL 1502 (4 December 1953) - upstream area of RWD looking upstream during placement of fill



Figure 23. Folsom Dam Photo FOL. 2065 (14 October 1954) - Left Wing Dam and MD with RWD in background shortly before completion of fill placement

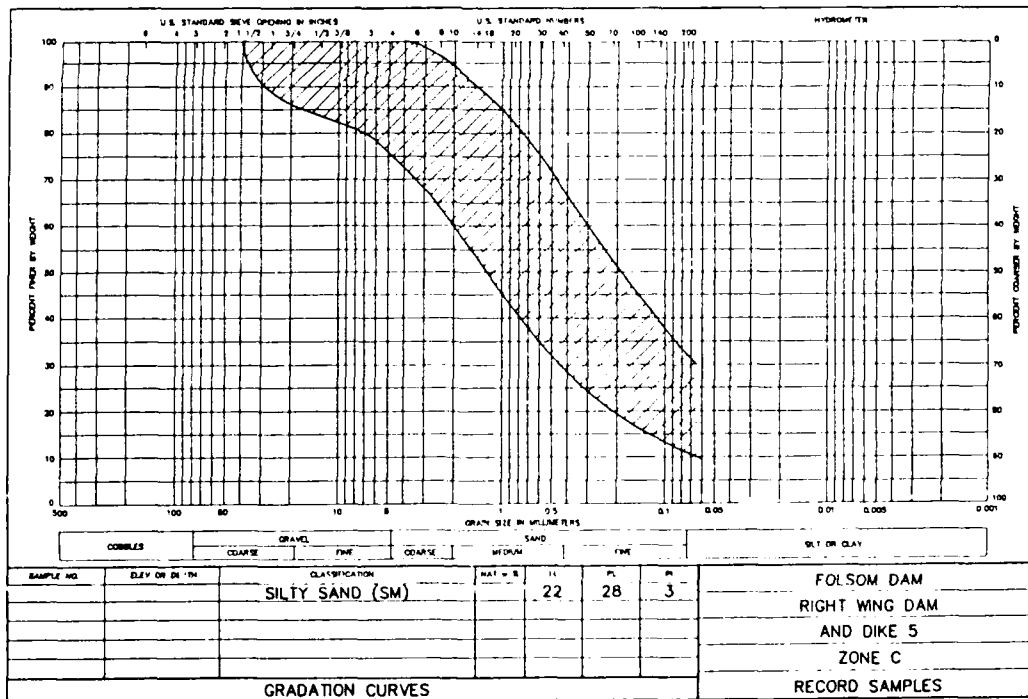
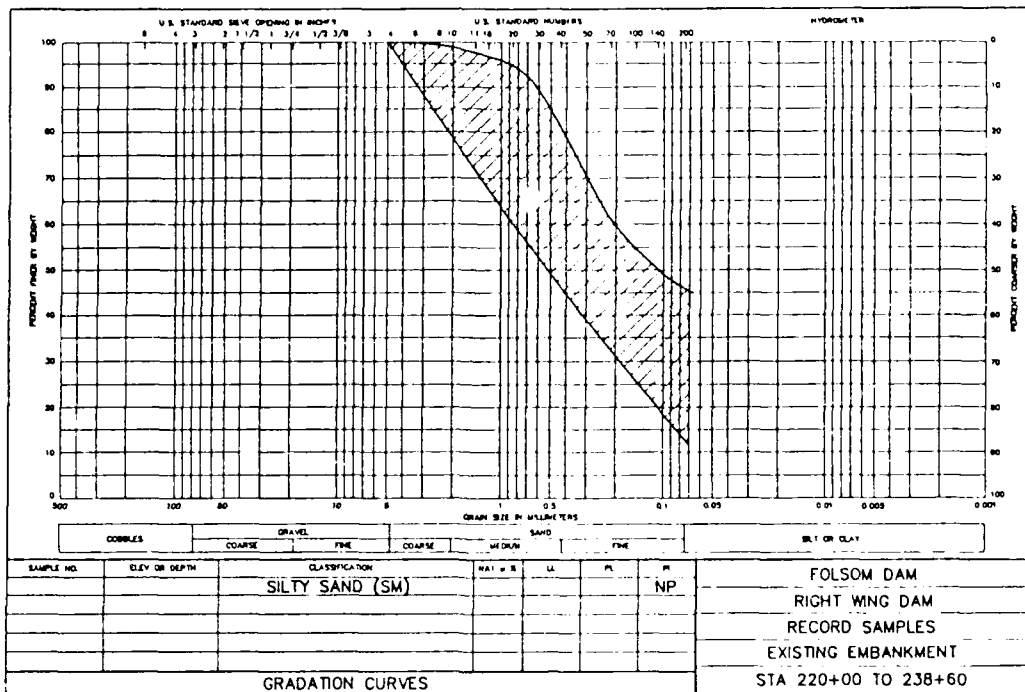


Figure 24. Comparison of ranges of gradations of Zone C core material in Right Wing Dam observed during construction (record samples) and in 1982 field investigations (recent samples)

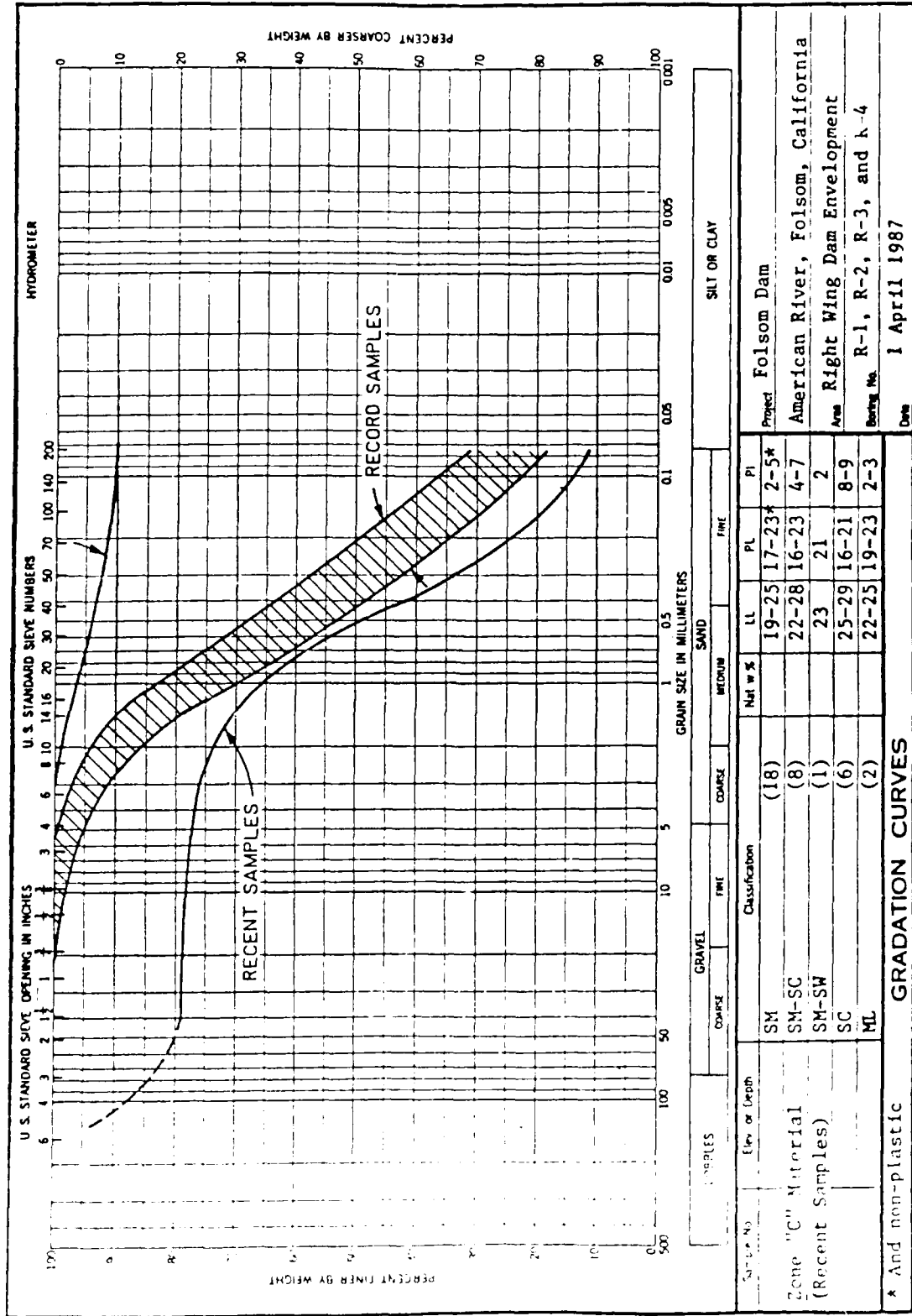


Figure 25. Comparison of gradation ranges for Zone C core material in Right Wing Dam interface area observed during construction (record samples) and in field investigations performed in 1984 (recent samples)

* And non-plastic

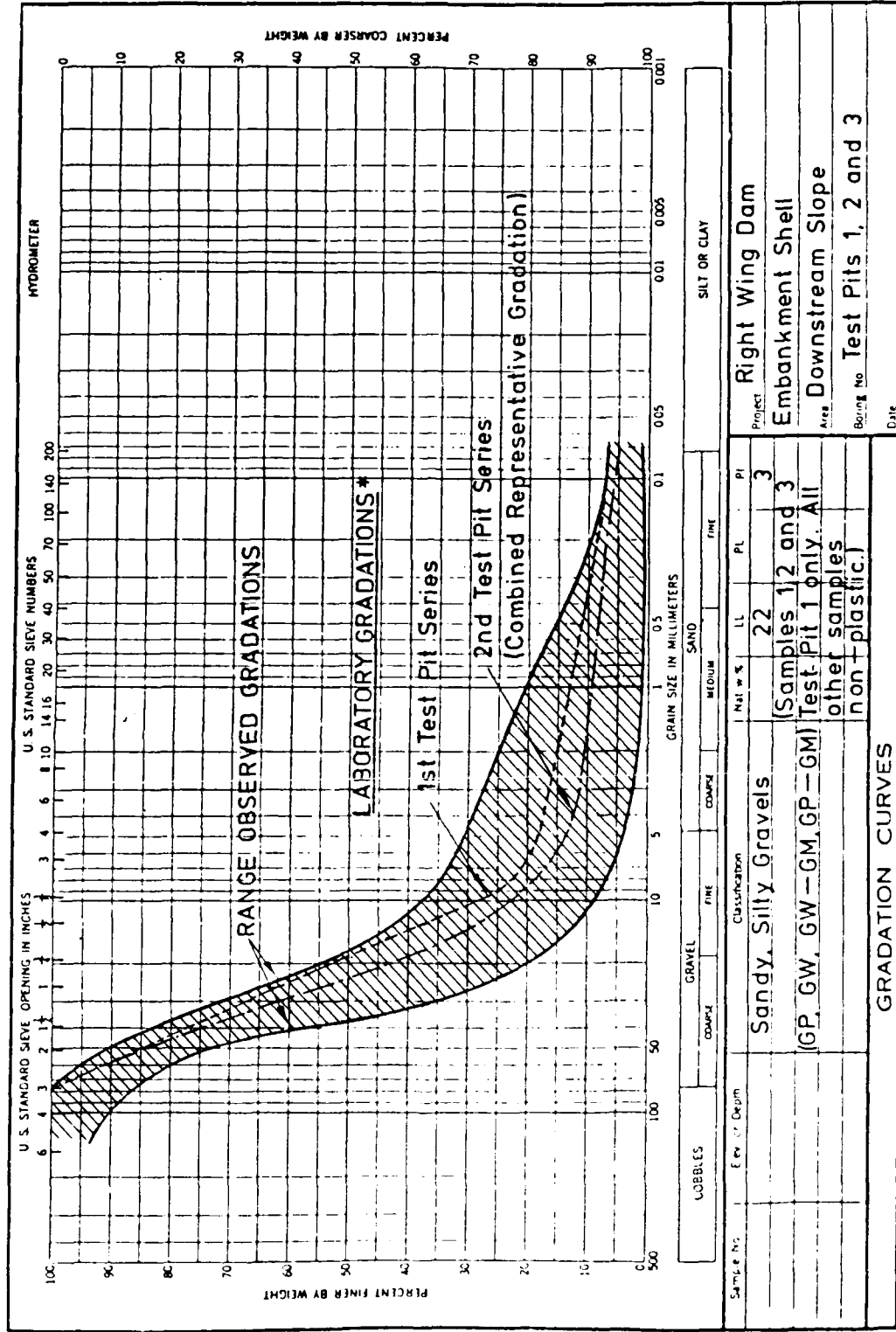


Figure 26. Range of gradations observed in test shafts excavated in downstream embankment shell gravel at Right Wing Dam, Folsom Dam Project. Range is compared with two laboratory gradations

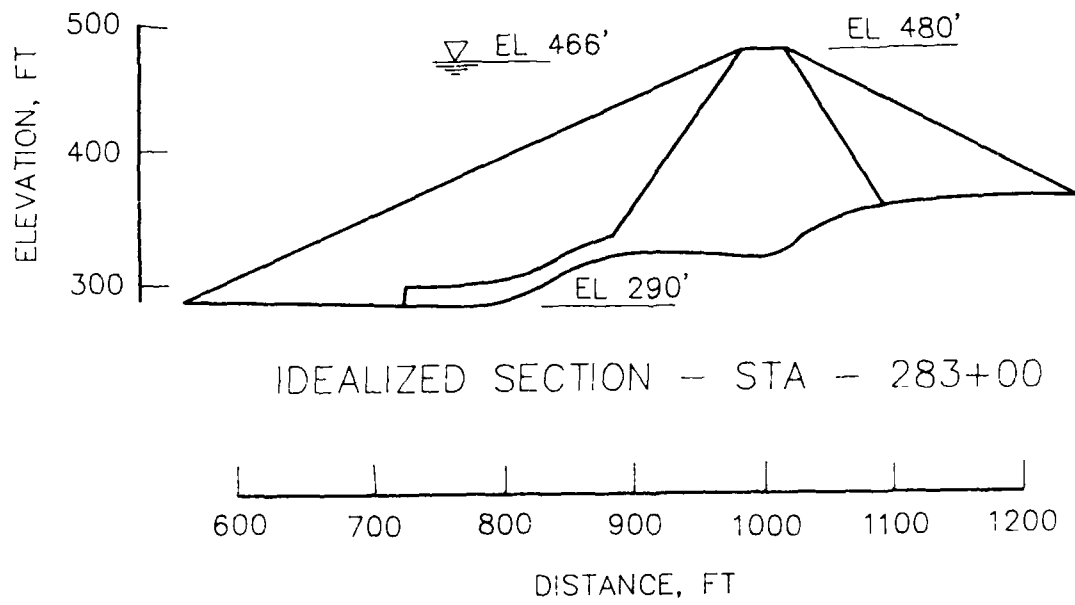
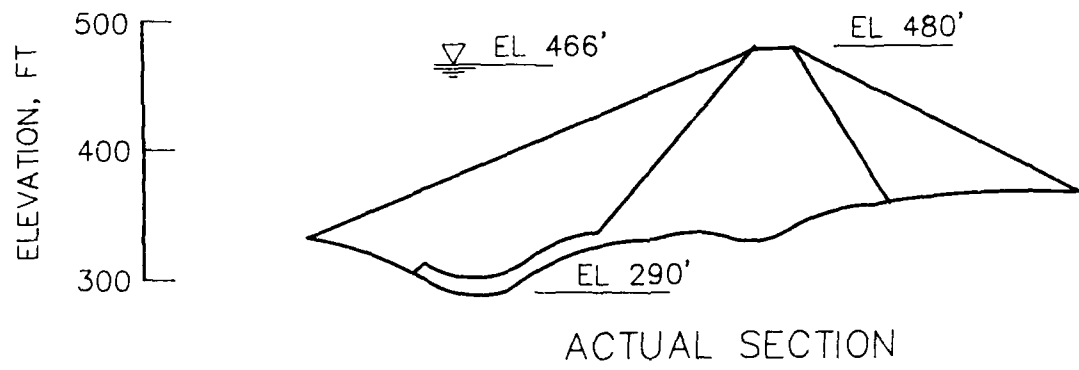


Figure 27. Cross-section views of Right Wing Dam, Sta 283

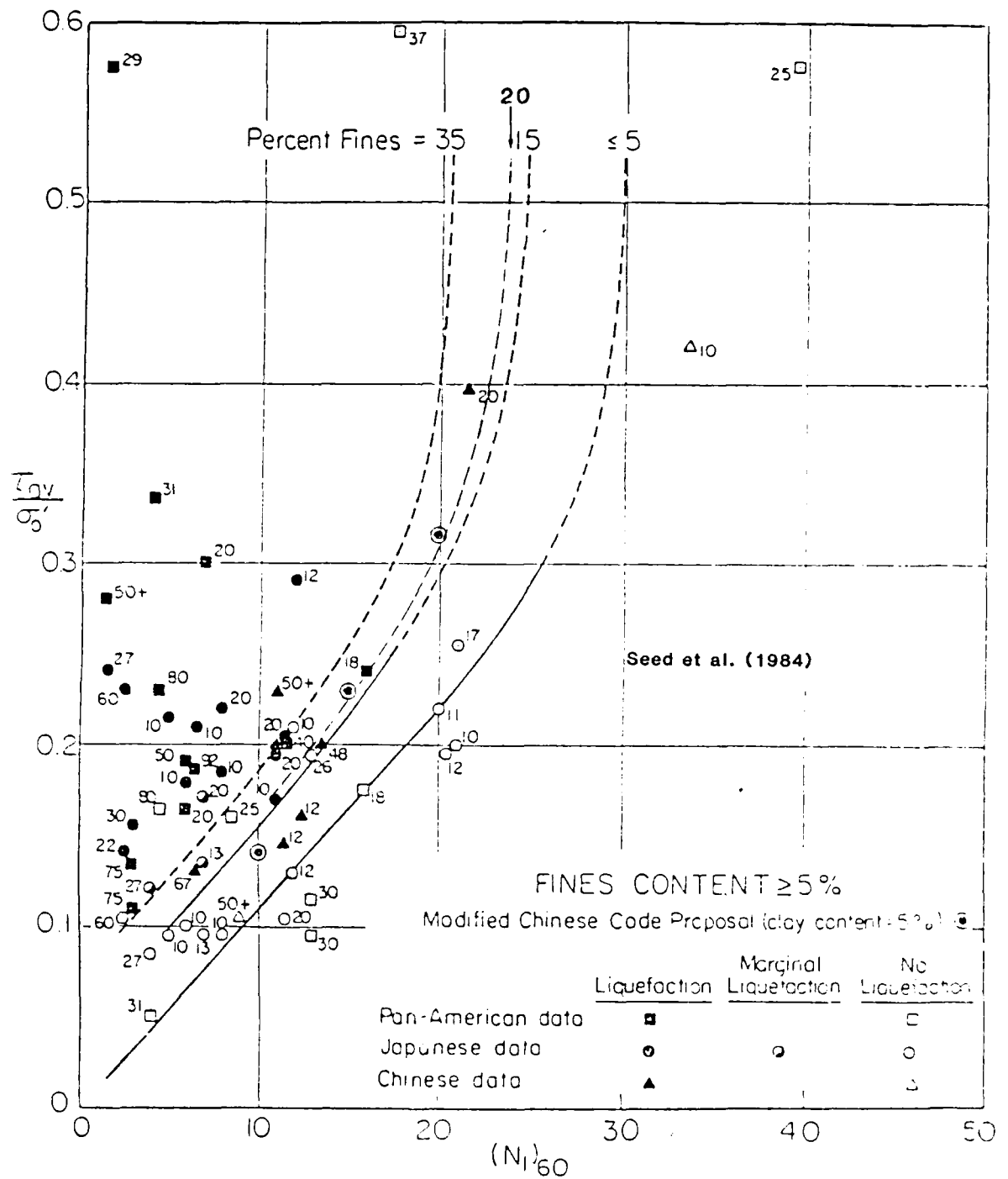


Figure 28. Relationships between stress ratio causing liquefaction and $(N_1)_{60}$ -values for silty sands and for M = 7-1/2 earthquakes (from Seed, Tokimatsu, Harder, and Chung 1984)

FINITE ELEMENT MESH FOR RIGHT WING DAM -

325 ELEMENTS
343 NODAL POINTS

NOTE: ALL ELEMENTS BELOW HEAVY LINE ARE SUBMERGED.

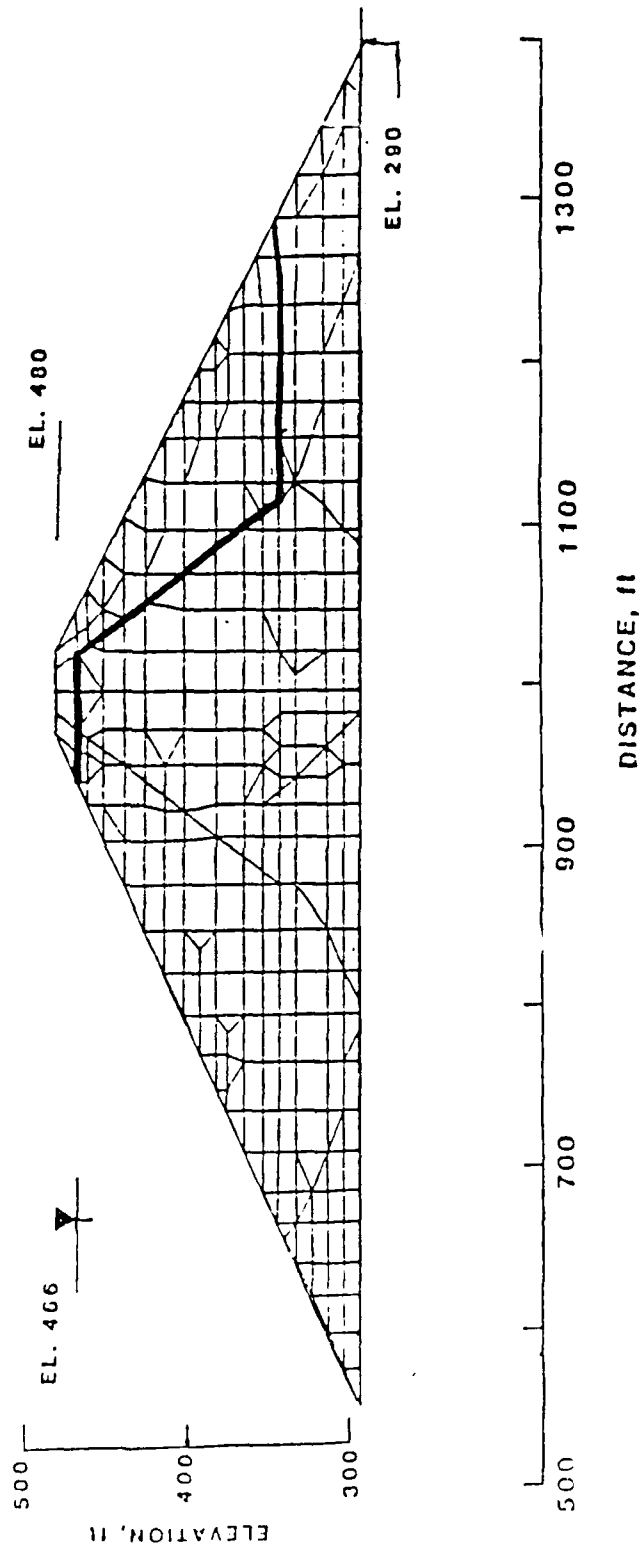


Figure 29. Finite element mesh of representative cross-section for Wing Dams

ADJUSTMENT FACTOR

K_{σ} versus Vertical Effective Stress

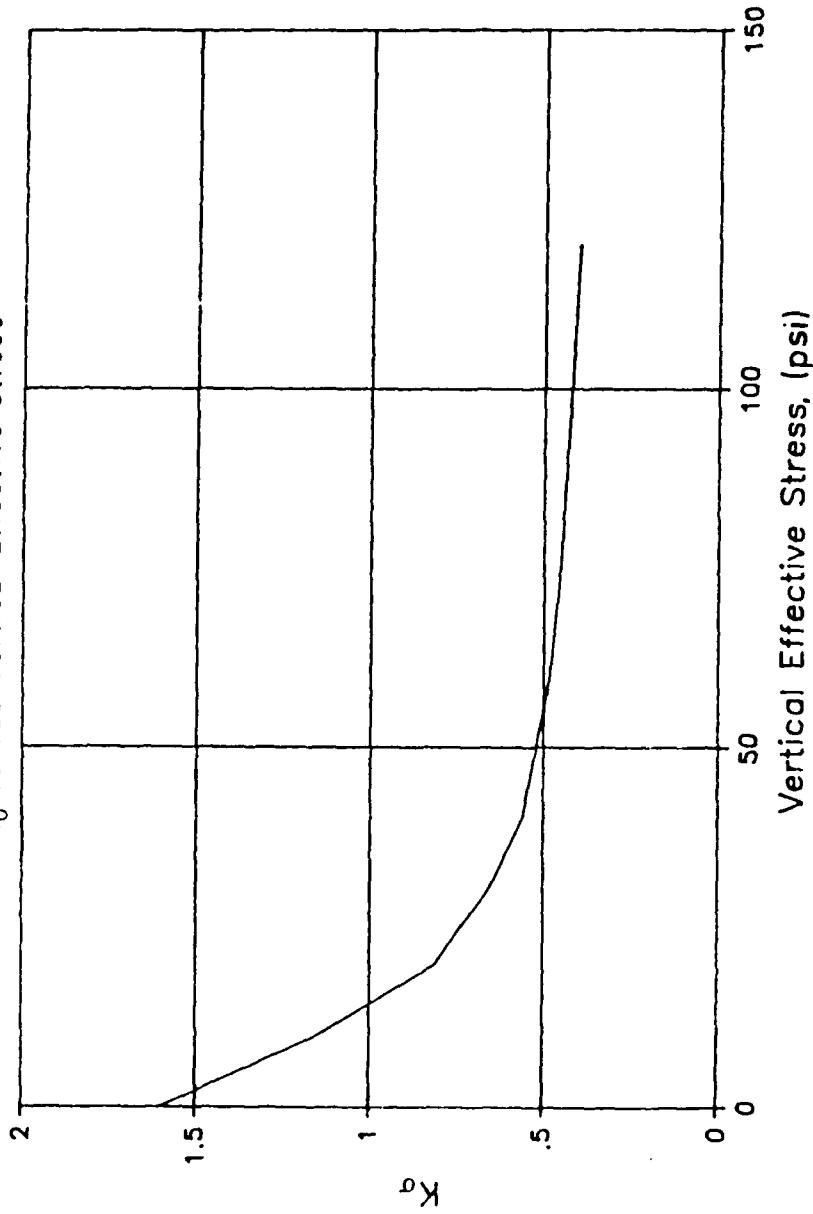


Figure 30. Adjustment factor, K_{σ} , for change in cyclic stress ratio required to cause $r_u = 100$ with change in effective normal stress, determined from laboratory tests on Folsom gravels

ADJUSTMENT FACTOR

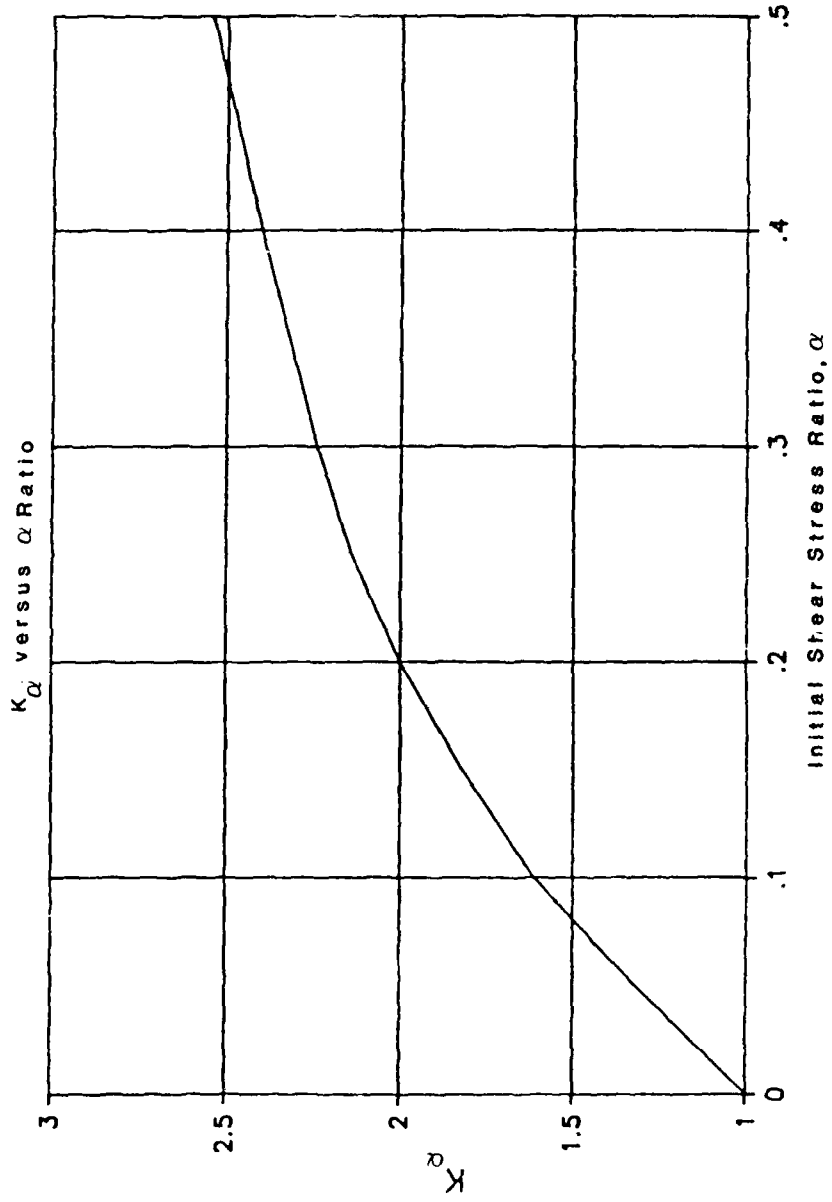


Figure 31. Adjustment factor, K_{α} , for change in cyclic stress ratio required to cause $r_u = 100$ with change in initial shear stress ratio, α , determined from laboratory tests on Folsom gravels

ACCELERATIONS COMPUTED BY FLUSH

ACCELERATIONS ARE IN g's

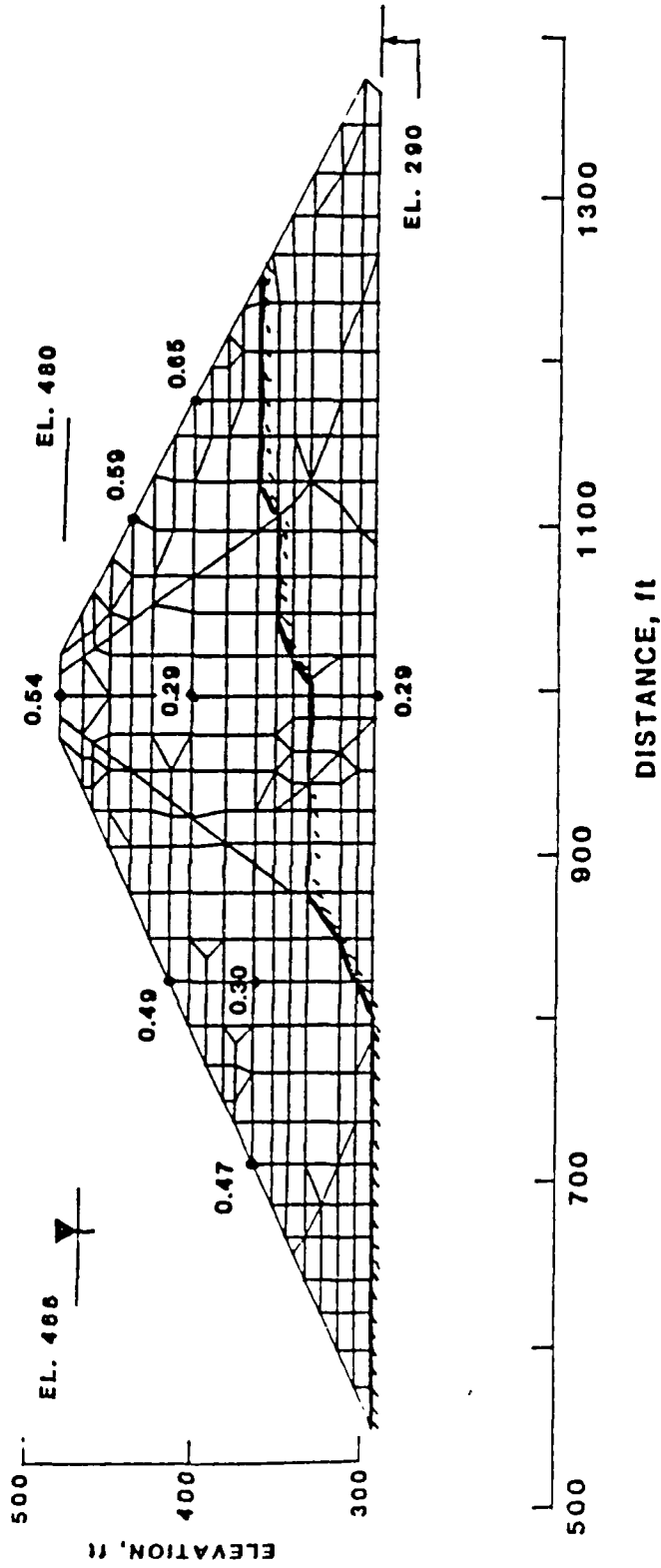


Figure 32. Peak accelerations computed by FLUSH with Accelerogram B in Wing Dam analysis section

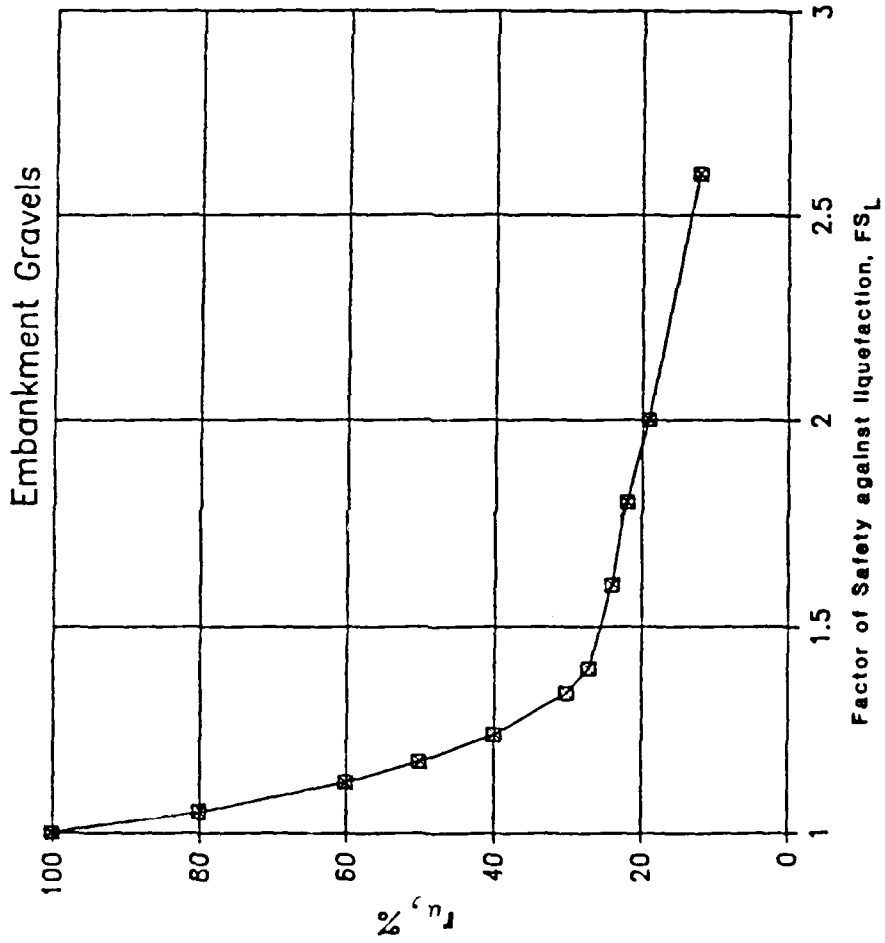


Figure 33. Residual excess pore pressure ratio, r_u , and corresponding values of factors of safety against liquefaction, FS_L , estimated from laboratory tests on Folsom gravels

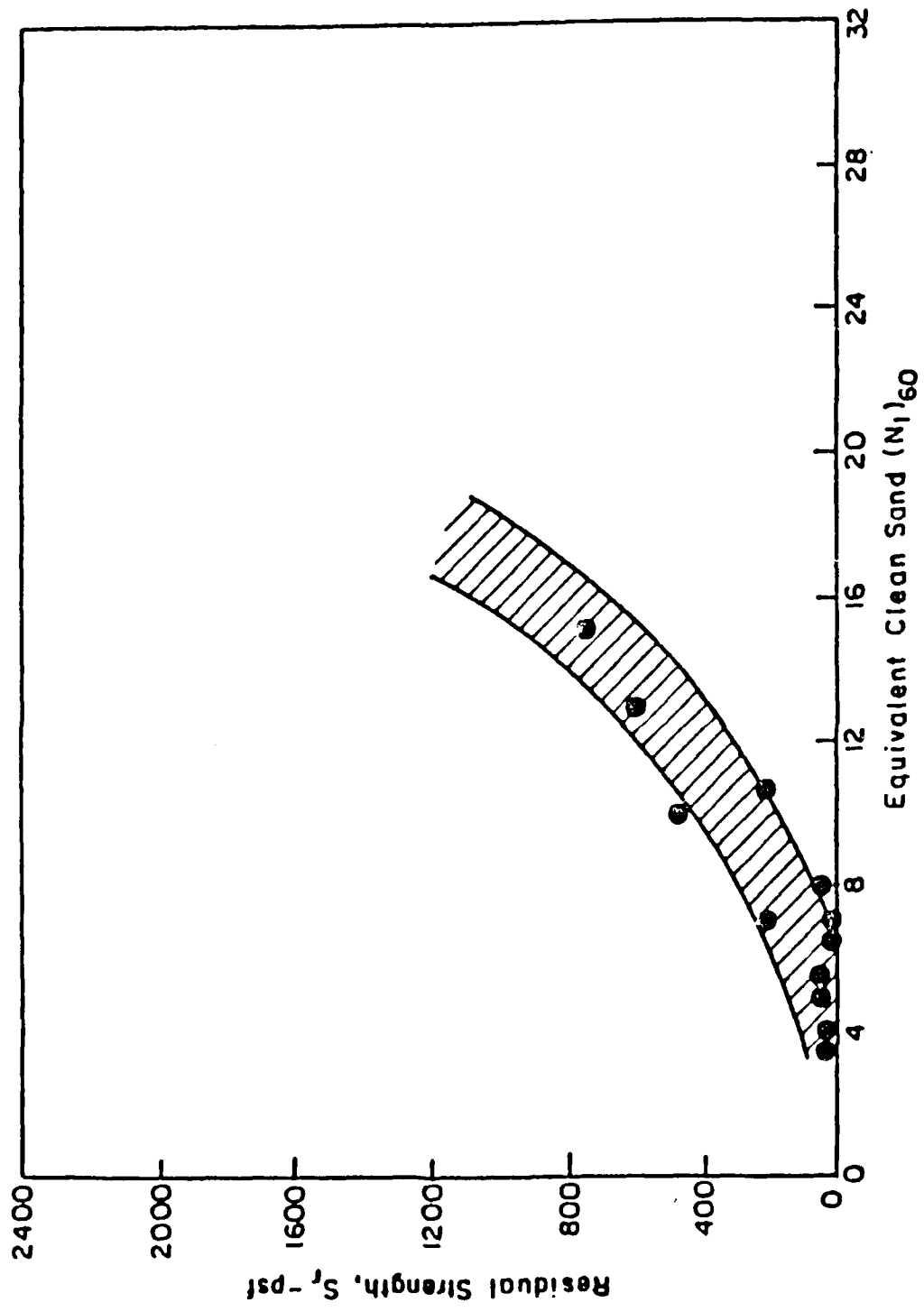


Figure 34. Tentative relationship between residual strength and SPT N-values for sands (after Seed 1984)

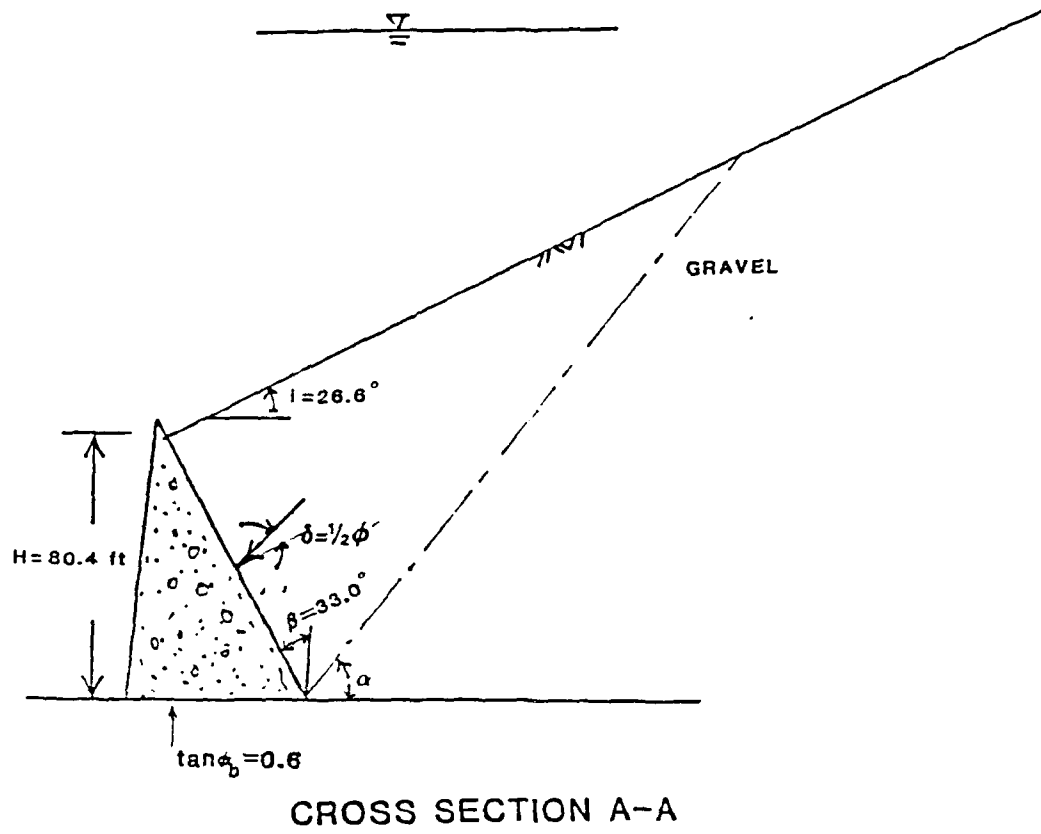


Figure 35. Idealized section of Retaining Wall B, Section A-A

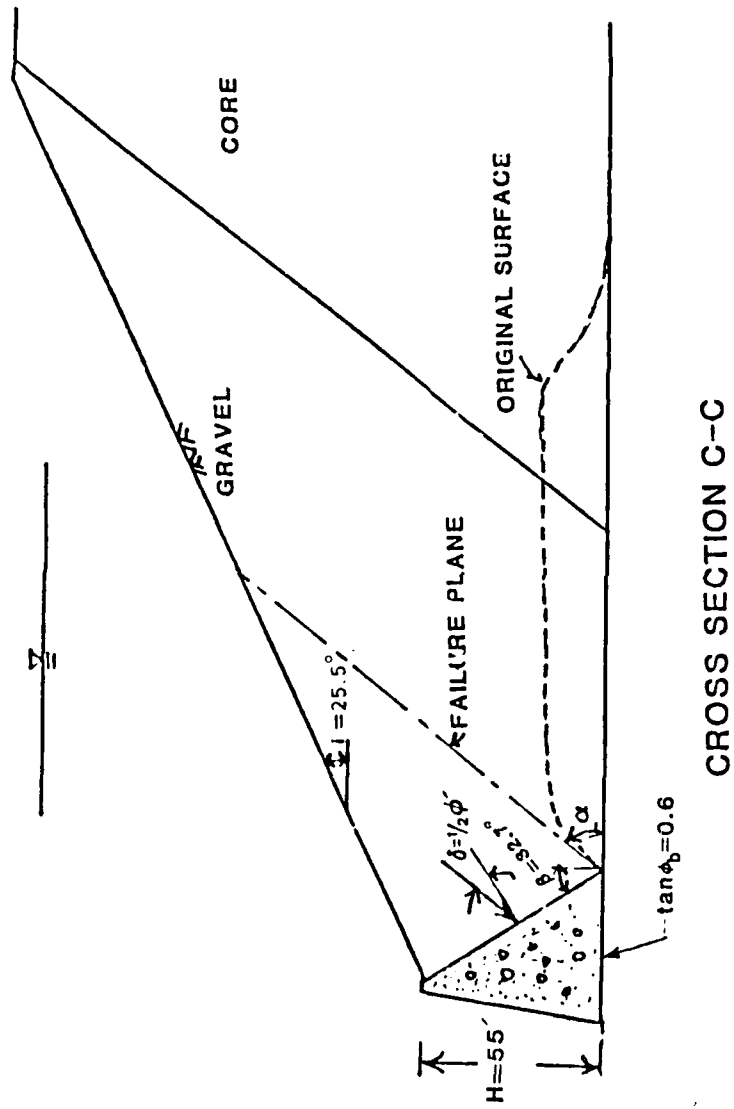


Figure 36. Idealized section of Retaining Wall B, Section C-C

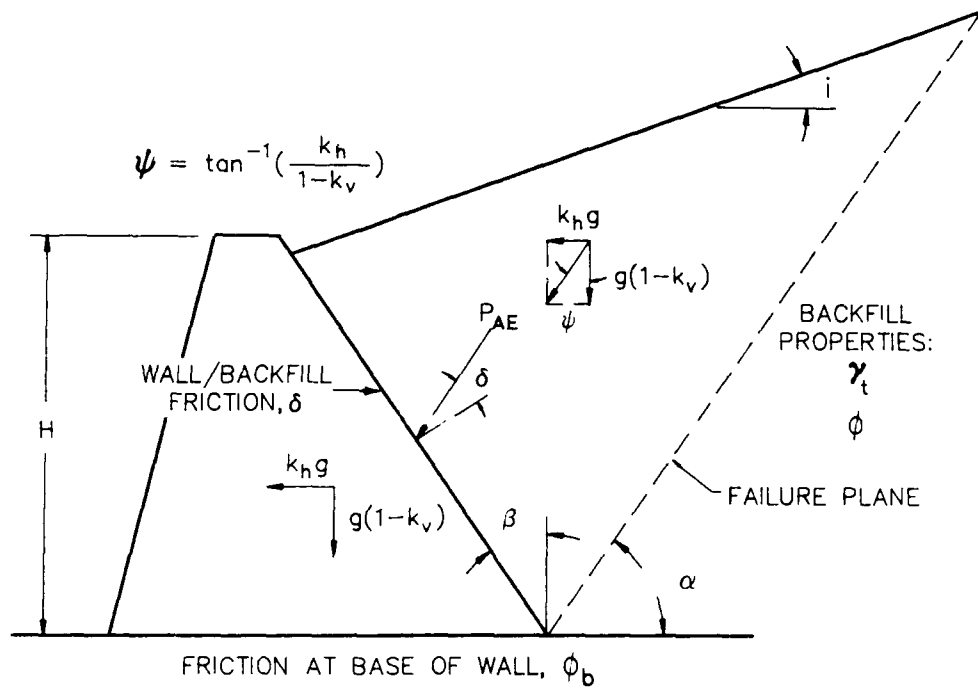


Figure 37. Definition of parameters for Mononobe-Okabe approach

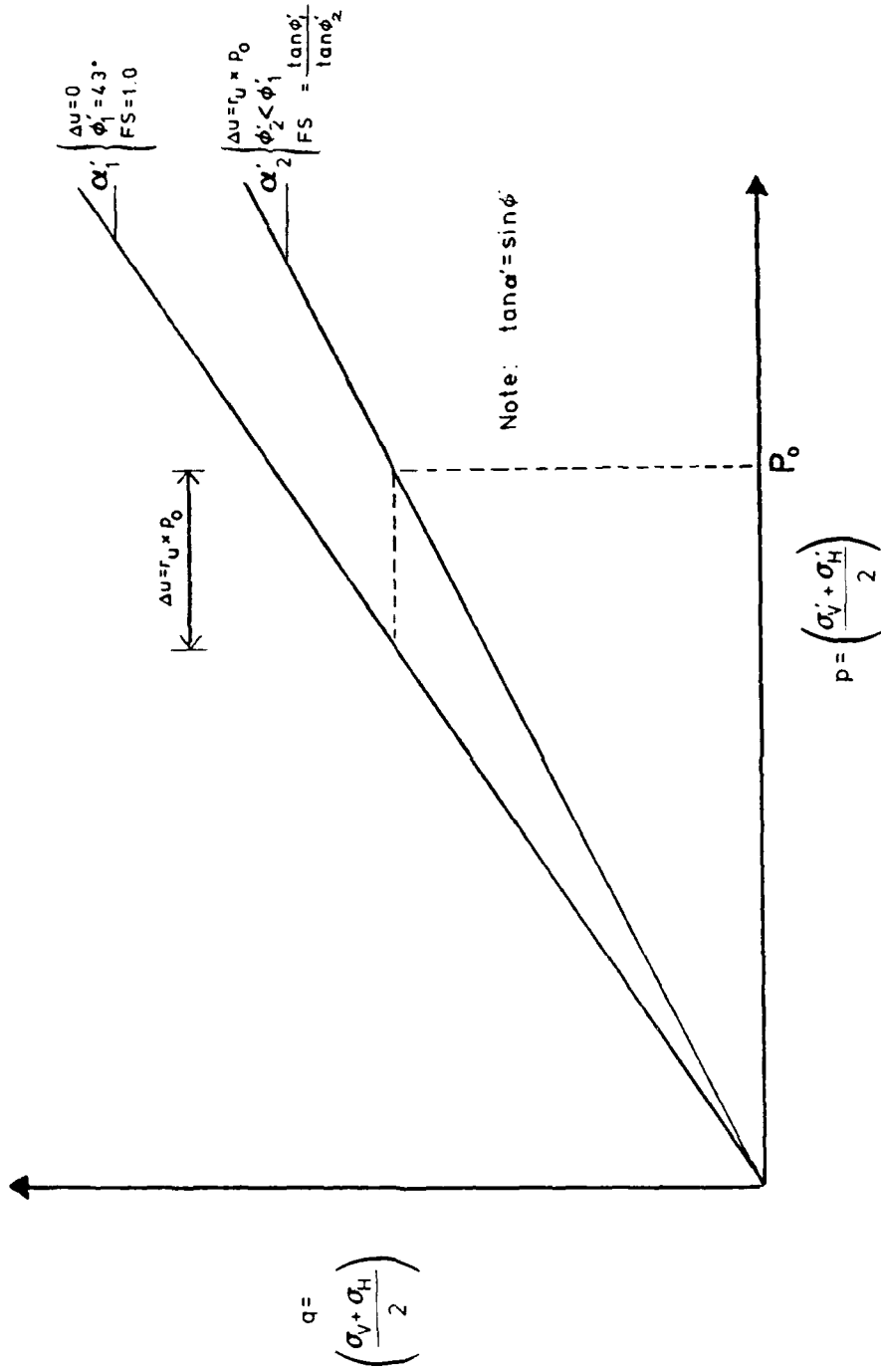


Figure 38. Procedure for estimating reduced friction angles corresponding to various levels of residual excess pore pressure

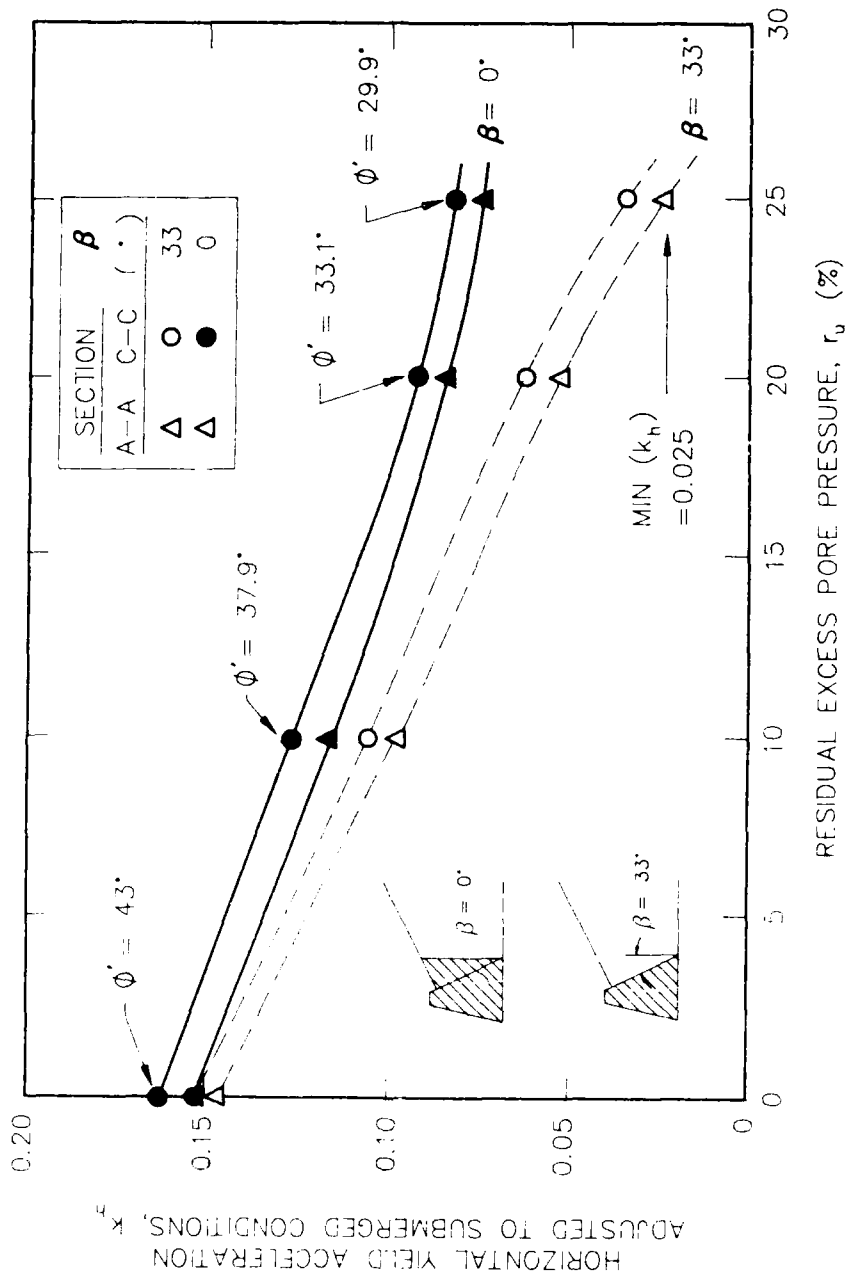
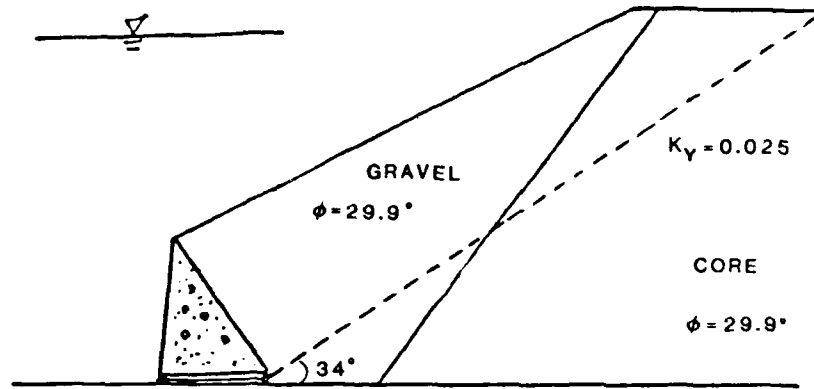


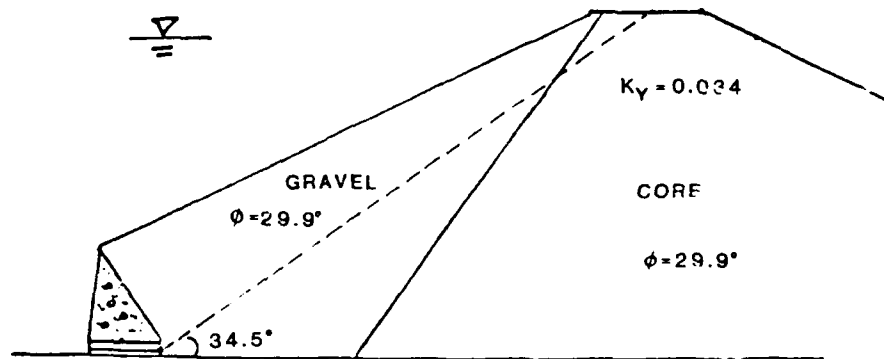
Figure 39. Yield acceleration, k_h , determined with Monobe-Okabe approach. The values plotted in this chart have already been modified by the factor 0.6, the ratio of the buoyant unit weight to the total unit weight

CROSS SECTION A-A



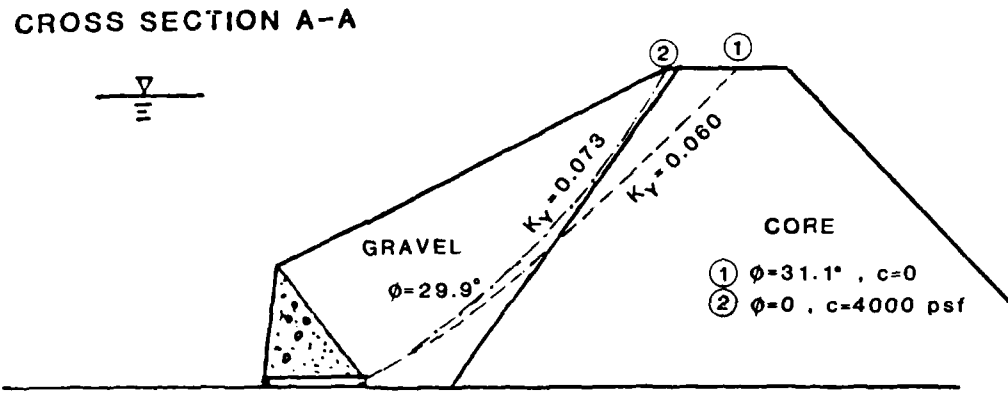
(a)

CROSS SECTION C-C

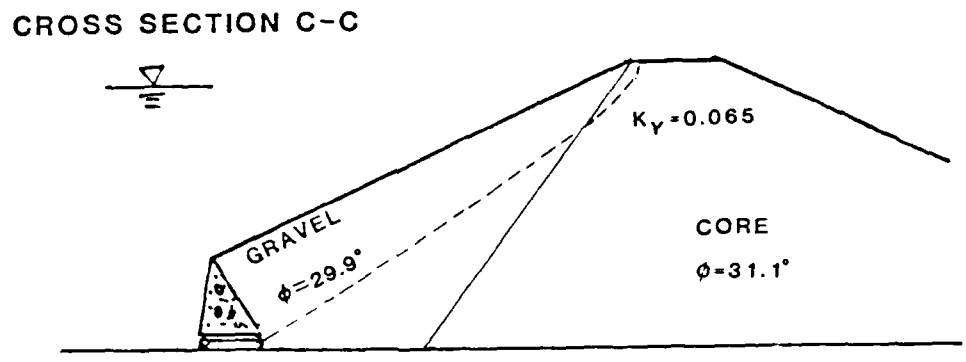


(b)

Figure 40. Locations of critical failure surfaces from Mononobe-Okabe calculations for Sections A-A and C-C with $r_u = 25$ percent



(a)



(b)

Figure 41. Locations of critical failure surfaces from UTEXAS2 calculations for Sections A-A and C-C with $r_u = 25$ percent in shell

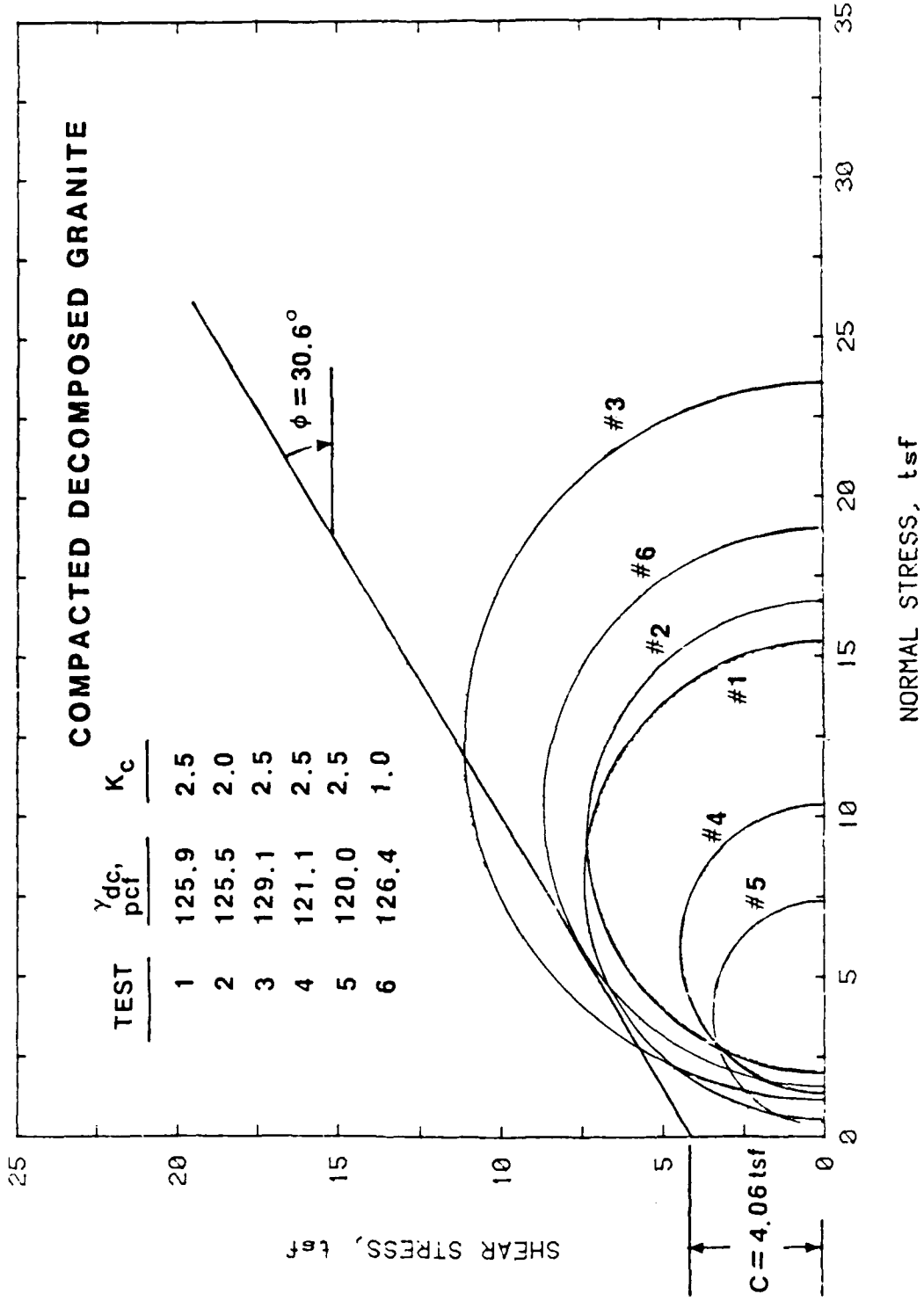
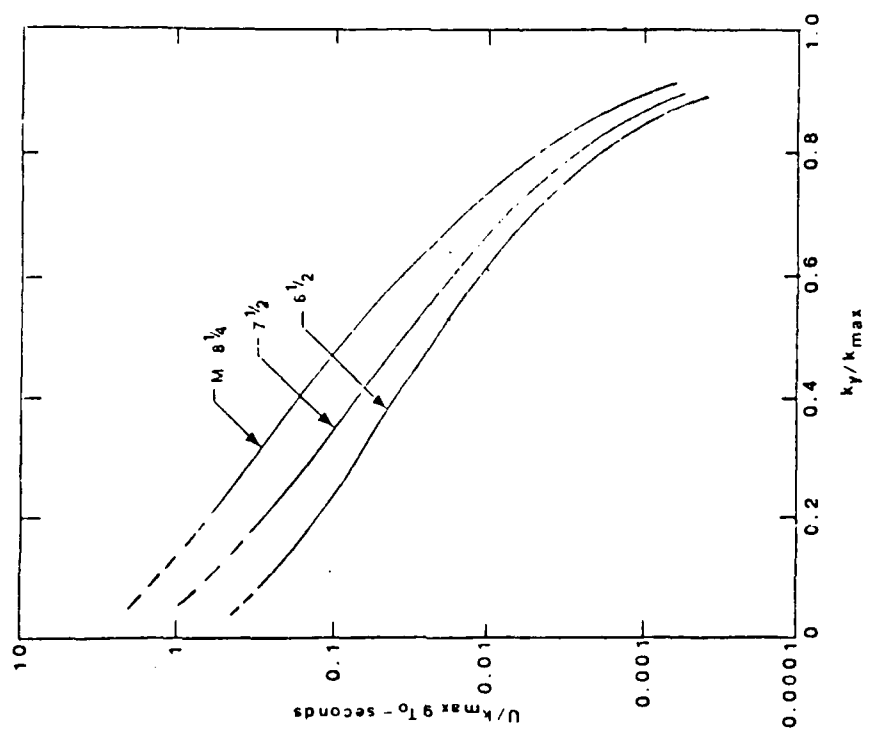
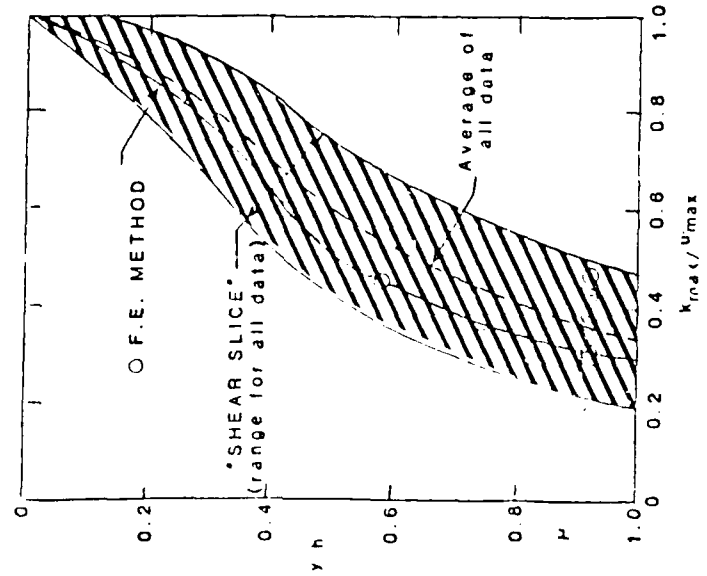


Figure 42. Total stress strength envelope from R tests on compacted decomposed granite

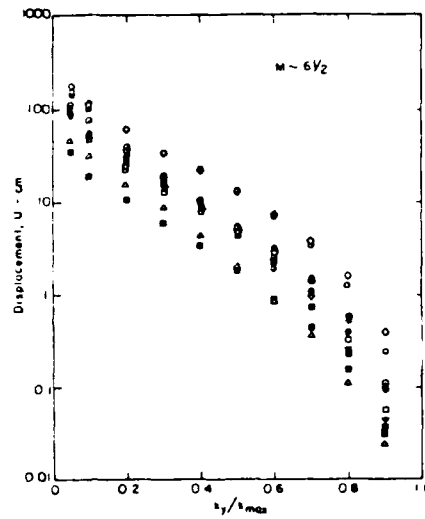


VARIATION OF AVERAGE NORMALIZED DISPLACEMENT WITH YIELD ACCELERATION
(AFTER MAKDISI-SEED, 1977)



VARIATION OF "MAXIMUM ACCELERATION RATIO" WITH DEPTH OF SLIDING MASS
(AFTER MAKDISI-SEED, 1977)

Figure 43. Normalized charts for computing permanent displacement using the Makdisi-Seed technique



VARIATION OF PERMANENT DISPLACEMENT WITH YIELD ACCELERATION - MAGNITUDE 6-1/2 EARTHQUAKE

Embankment Characteristics for Magnitude 6-1/2 Earthquake

Case #	Embankment Description	Height (ft.)	Base Acceleration (g)	T_0 (1)	$k_{max}^{(2)}$ (g)	Symbol
1	Example Case - slope = 2:1 - $k_{2max} = 60$	150	0.2 (Caltech record)	0.8	(a) 0.31 (b) 0.12	● ■
2	Example Case - slope = 2:1 - $k_{2max} = 60$	150	0.5 (Caltech record)	1.08	(a) 0.4 (b) 0.18	○ □
3	Example Case - slope = 2:1 - $k_{2max} = 80$	150	0.5 (Lake Hughes record)	0.84	(a) 0.33 (b) 0.16	○ △
4	Example Case - slope = 2-1/2:1 - $k_{2max} = 80$	150	0.5 (Caltech record)	0.95	(a) 0.49 (b) 0.22	○ ▽
5	Example Case - slope = 2:1 - $k_{2max} = 60$	75	0.5 (Caltech record)	0.6	(a) 0.86 (b) 0.26	● ■

(1) T_0 = Calculated first natural period of the embankment.

(2) k_{max} = Maximum value of time history of:

(a) crest acceleration

(b) average acceleration for sliding mass extending through full height of embankment.

Figure 44. Variation of permanent displacement with yield acceleration for Magnitude 6.5 earthquakes (from Makdisi and Seed 1977)

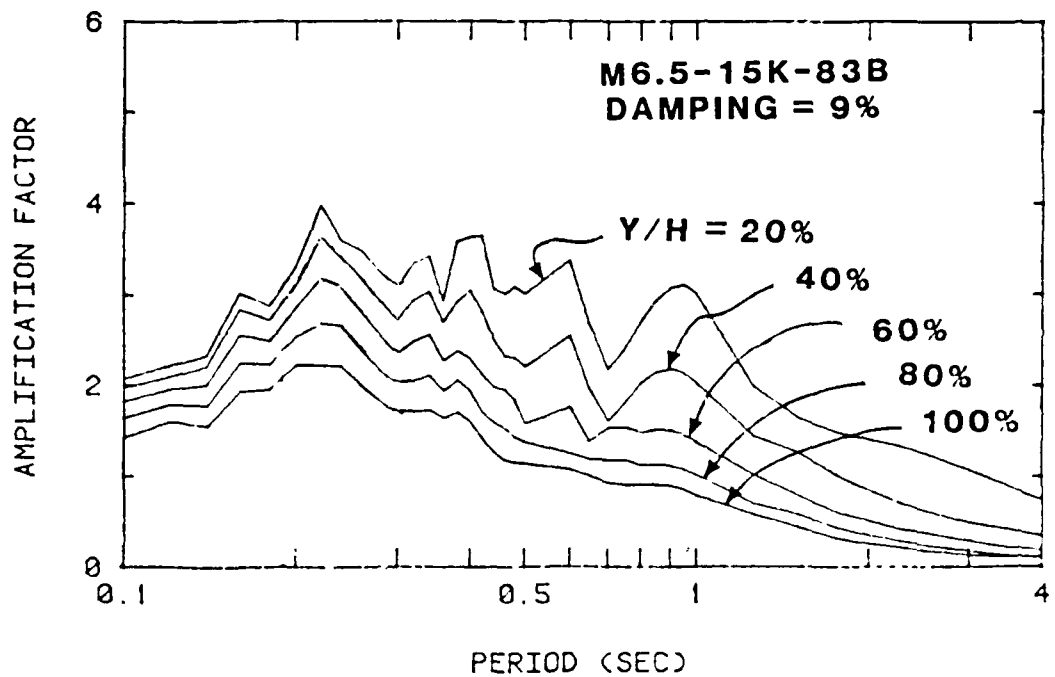
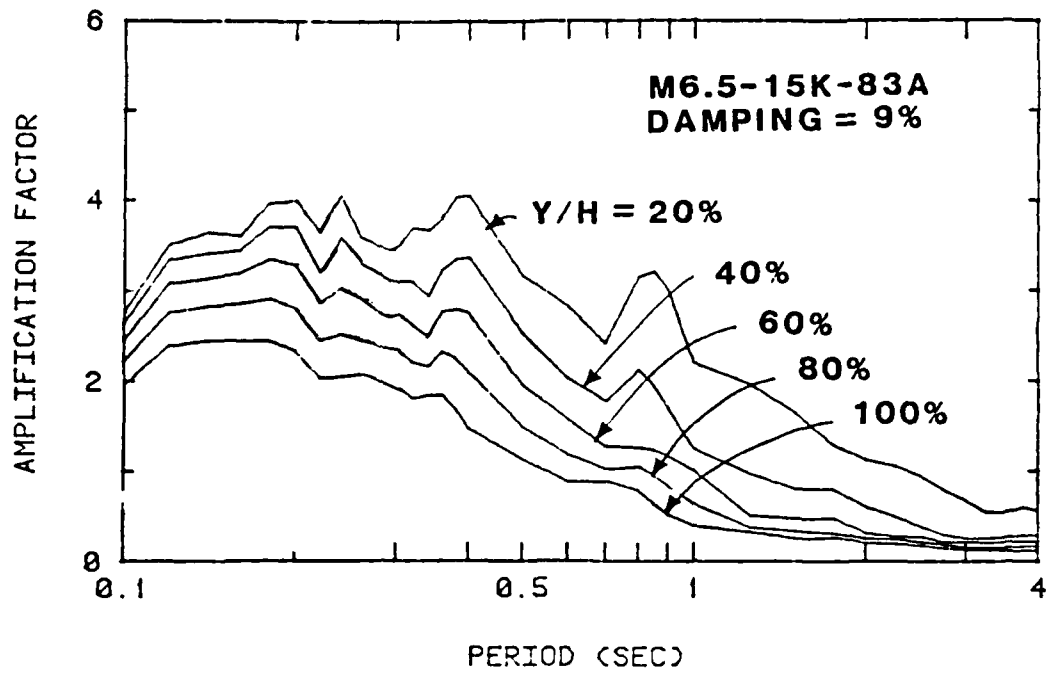


Figure 45. SEISCOE amplification factors from records A and B for embankments founded on rock

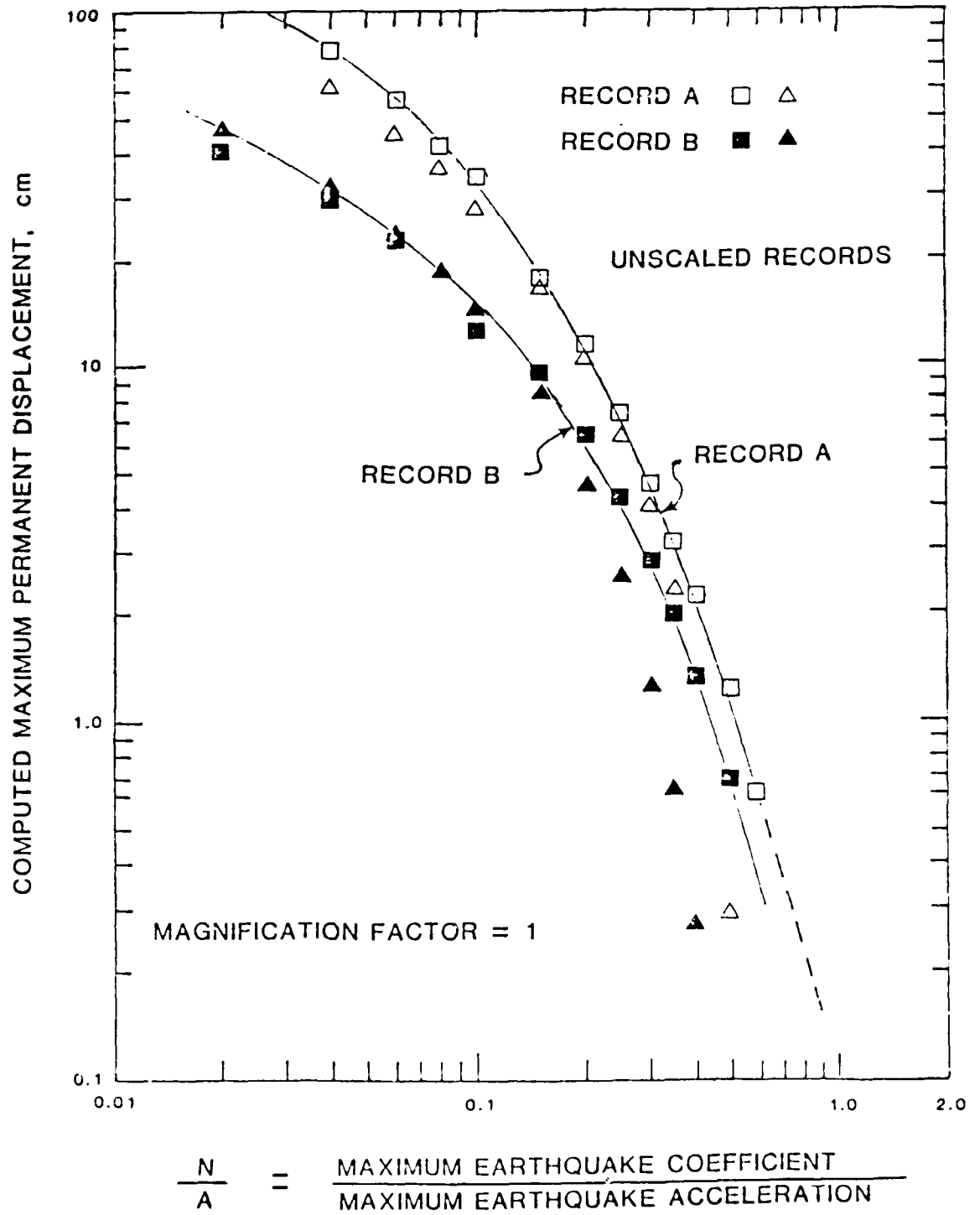


Figure 46. Sliding block analysis - computed permanent displacements for records A and B

APPENDIX A

COMPUTER PROGRAM LISTINGS AND OUTPUT FOR YIELD ACCELERATION
COMPUTATIONS WITH THE MONONOBE-OKABE PROCEDURE

```

MONONOBE - OKABE
EARTH PRESSURE DURING EARTHQUAKE
Retaining Wall B (Section A-A)
RD=3.1416/180! 'converts degrees to radians
FI=43*RD 'angle of internal friction
soilwtb=89.6 'buoyant unit weight of backfill
soilwtt=152 'total weight of backfill
H=80.4 'height of retaining wall
BETA=33*RD 'angle of inclination of back of wall to vertical
i=26.5*RD 'angle of inclination of backfill
delta=FI/2 'angle of friction between backfill and wall
Fib=30*RD 'friction angle between bottom of wall and ground
-----
input "to where (i.e. CON, LPT1, LPT2, PRN or DOS file name: ";IO.name$
if io.name$="" then
  io.name$="CON"
elseif io.name$="L" or io.name$="1" then
  io.name$="LPT2"
end if
OPEN IO.name$ FOR OUTPUT AS #2
PRINT #2, " Friction Angle (Degree) = ";FI/RD
PRINT #2, " Buoyant Weight of Backfill = ";soilwtb
PRINT #2, " Height of Retaining Wall = ";H
PRINT #2, " Beta (Degree) = ";BETA/RD
PRINT #2, " Inclination (Degree) = ";i/RD
PRINT #2, " Delta (Degree) = ";delta/RD
PRINT #2, " Fib (Degree) = ";Fib/RD
PRINT #2, ""

locate 12,35:print "working"
FOR kh= 0.0 TO 0.45 STEP .05

psy= ATN(kh)
alphamin= (FI-psy)/RD
IF 1/RD>alphamin THEN i=RD*(alphamin-.1) 'insures imax not violated
qlb= .5*H*H*soilwtb 'wedge weight buoyant
-----
Q2=COS(BETA)*COS(BETA) 'used to compute failure
Q3=COS(1-BETA)*COS(psy) 'angle, alpha, and the wedge
QLAST= -90000! 'weight at failure
FOR J= 0 TO 50 STEP .1
  ALP= alphamin+J
  RAP=ALP*FD
  X1=SIN(RAP-i)
  X2=COS(BETA-RAP)*SIN(RAP-FI+psy)
  X3=COS(BETA+delta+FI-RAP)
  Q4=X2/(X1*X3)
  Q=Qlb*Q3*Q4/Q2
-----
a1= fi-psy-beta 'constants used to compute
a2= psy+beta+delta 'Kae
a3= fi+delta
a4= 1-beta
a5= fi-psy-1
func1= 1+sqr( (sin(a1)*sin(a5)) / (cos(a4)*cos(a2)) )
func2= func1*func1
Kae= ( cos(a1)*cos(a1) ) / ( cos(psy)*cos(beta)*cos(beta)*cos(a2)*func2

WTb= 222900! 'bouyant weight of retaining wall/soil mass
AX= BETA+delta 'constant used to compute components of Pae
Paeb= qlb*kae
FS= ( (WTb+Paeb*SIN(AX)) *TAN(Fib) ) / ( WTb*kh+Paeb*COS(AX) )

IF Q < QLAST THEN
PRINT #2, USING "accel=+###.### Q(last) =+#####.## Angle=+###.## F
if io.name$<>"CON" then 'if sending output to
locate 12,35:print "accel=";kh 'a printer, lets the
locate 13,35:print "FS=";FS 'user know that the
end if 'program is functioning
exit for
end if
QLAST= Q
NEXT J
NEXT kh
END

```

Friction Angle (Degree) = 43
 Buoyant Weight of Backfill = 89.6
 Total Weight of Backfill = 152
 Height of Retaining Wall = 80.4
 Beta (Degree) = 33
 Inclination (Degree) = 26.5
 Delta (Degree) = 21.5
 Fib (Degree) = 30

accel	Q(last)	Angle	FS	Kae
+0.000	+247.6	+64.6	+1.705	+0.855
+0.050	+282.5	+59.8	+1.491	+0.978
+0.100	+326.4	+54.8	+1.327	+1.138
+0.150	+384.8	+49.3	+1.197	+1.359
+0.200	+469.8	+43.3	+1.092	+1.687
+0.250	+617.1	+36.7	+1.001	+2.264
+0.300	+1053.9	+27.8	+0.911	+3.967
+0.350	+1171.8	+25.1	+0.887	+4.542
+0.400	+1320.1	+22.5	+0.867	+5.288

Friction Angle (Degree) = 37.9
 Buoyant Weight of Backfill = 89.6
 Total Weight of Backfill = 152
 Height of Retaining Wall = 80.4
 Beta (Degree) = 33
 Inclination (Degree) = 26.5
 Delta (Degree) = 18.95
 Fib (Degree) = 30

accel	Q(last)	Angle	FS	Kae
+0.000	+287.1	+58.3	+1.465	+0.991
+0.050	+331.6	+52.7	+1.295	+1.148
+0.100	+393.4	+46.5	+1.158	+1.372
+0.150	+492.6	+39.4	+1.040	+1.739
+0.200	+797.2	+28.4	+0.910	+2.863
+0.250	+851.0	+25.7	+0.881	+3.122
+0.300	+916.7	+22.9	+0.854	+3.450
+0.350	+993.0	+20.2	+0.831	+3.849
+0.400	+1084.5	+17.6	+0.810	+4.344

Friction Angle (Degree) = 33.1
 Buoyant Weight of Backfill = 89.6
 Total Weight of Backfill = 152
 Height of Retaining Wall = 80.4
 Beta (Degree) = 33
 Inclination (Degree) = 26.5
 Delta (Degree) = 16.55
 Fib (Degree) = 30

accel	Q(last)	Angle	FS	Kae
+0.000	+338.8	+50.6	+1.263	+1.170
+0.050	+406.5	+43.3	+1.117	+1.407
+0.100	+543.6	+33.7	+0.977	+1.896
+0.150	+682.9	+26.7	+0.895	+2.411
+0.200	+719.8	+23.8	+0.863	+2.585
+0.250	+759.2	+21.0	+0.834	+2.785
+0.300	+802.3	+18.2	+0.809	+3.020
+0.350	+850.6	+15.5	+0.786	+3.297
+0.400	+906.6	+12.9	+0.766	+3.632

Friction Angle (Degree) = 29.9
 Buoyant Weight of Backfill = 89.6
 Total Weight of Backfill = 152
 Height of Retaining Wall = 80.4
 Beta (Degree) = 33
 Inclination (Degree) = 26.5
 Delta (Degree) = 14.95
 Fib (Degree) = 30

accel	Q(last)	Angle	FS	Kae
+0.000	+391.8	+43.5	+1.130	+1.353
+0.005	+400.2	+42.6	+1.116	+1.382
+0.010	+409.2	+41.7	+1.101	+1.413
+0.015	+419.0	+40.8	+1.086	+1.447
+0.020	+429.5	+39.9	+1.071	+1.484
+0.025	+441.1	+38.8	+1.056	+1.524
+0.030	+453.9	+37.7	+1.040	+1.569
+0.035	+468.4	+36.6	+1.024	+1.619
+0.040	+485.0	+35.3	+1.008	+1.677
+0.045	+504.7	+34.0	+0.991	+1.746
+0.050	+529.5	+32.4	+0.972	+1.833

Friction Angle (Degree) = 27
 Buoyant Weight of Backfill = 89.6
 Total Weight of Backfill = 152
 Height of Retaining Wall = 80.4
 Beta (Degree) = 33
 Inclination (Degree) = 26.5
 Delta (Degree) = 13.5
 Fib (Degree) = 30

accel=+0.000	Q(last) = +497.0	Angle= +32.6	FS= +0.985	Kae= +1.716
accel=+0.050	Q(last) = +567.7	Angle= +26.6	FS= +0.911	Kae= +1.965
accel=+0.100	Q(last) = +588.7	Angle= +23.7	FS= +0.875	Kae= +2.053
accel=+0.150	Q(last) = +609.4	Angle= +20.8	FS= +0.843	Kae= +2.152
accel=+0.200	Q(last) = +629.9	Angle= +17.9	FS= +0.813	Kae= +2.262
accel=+0.250	Q(last) = +650.7	Angle= +15.1	FS= +0.787	Kae= +2.387
accel=+0.300	Q(last) = +672.3	Angle= +12.3	FS= +0.762	Kae= +2.531
accel=+0.350	Q(last) = +695.6	Angle= +9.6	FS= +0.740	Kae= +2.696
accel=+0.400	Q(last) = +721.5	Angle= +7.0	FS= +0.720	Kae= +2.890

Friction Angle (Degree) = 27.8
 Buoyant Weight of Backfill = 89.6
 Total Weight of Backfill = 152
 Height of Retaining Wall = 80.4
 Beta (Degree) = 33
 Inclination (Degree) = 26.5
 Delta (Degree) = 13.9
 Fib (Degree) = 30

accel=+0.000	Q(last) = +452.6	Angle= +36.7	FS= +1.033	Kae= +1.563
accel=+0.005	Q(last) = +468.4	Angle= +35.3	FS= +1.015	Kae= +1.618
accel=+0.010	Q(last) = +487.5	Angle= +33.8	FS= +0.997	Kae= +1.684
accel=+0.015	Q(last) = +512.0	Angle= +32.1	FS= +0.975	Kae= +1.760
accel=+0.020	Q(last) = +549.7	Angle= +29.8	FS= +0.948	Kae= +1.899
accel=+0.025	Q(last) = +562.7	Angle= +28.9	FS= +0.938	Kae= +1.944
accel=+0.030	Q(last) = +565.0	Angle= +28.6	FS= +0.934	Kae= +1.953
accel=+0.035	Q(last) = +567.3	Angle= +28.3	FS= +0.930	Kae= +1.961
accel=+0.040	Q(last) = +569.5	Angle= +28.0	FS= +0.926	Kae= +1.970
accel=+0.045	Q(last) = +571.8	Angle= +27.7	FS= +0.922	Kae= +1.979
accel=+0.050	Q(last) = +574.1	Angle= +27.4	FS= +0.918	Kae= +1.987

```

MONONOBE - OKABE
EARTH PRESSURE DURING EARTHQUAKE
Retaining Wall B (Section A-A)
RD=3.1416/180! 'converts degrees to radians
FI=43*RD 'angle of internal friction
soilwtb=89.6 'buoyant unit weight of backfill
soilwtt=152 'total weight of backfill
H=80.4 'height of retaining wall
BETA=0*RD 'angle of inclination of back of wall to vertical
i=26.5*RD 'angle of inclination of backfill
delta=FI/2 'angle of friction between backfill and wall
Fib=30*RD 'friction angle between bottom of wall and ground
-----
input "to where (i.e. CON, LPT1, LPT2, PRN or DOS file name: ";IO.name$
if io.name$="" then
  io.name$="CON"
elseif io.name$="L" or io.name$="1" then
  io.name$="LPT2"
end if
OPEN IO.name$ FOR OUTPUT AS #2
PRINT #2, " Friction Angle (Degree) = ";FI/RD
PRINT #2, " Buoyant Weight of Backfill = ";soilwtb
PRINT #2, " Height of Retaining Wall = ";H
PRINT #2, " Beta (Degree) = ";BETA/RD
PRINT #2, " Inclination (Degree) = ";i/RD
PRINT #2, " Delta (Degree) = ";delta/RD
PRINT #2, " Fib (Degree) = ";Fib/RD
PRINT #2, ""

locate 12,35:print "working"
FOR kh= 0.0 TO 0.45 STEP .05

psy= ATN(kh)
alphamin= (FI-psy)/RD
IF 1/RD>alphamin THEN i=RD*(alphamin+.1) 'insures imax not violated
qlb= .5*H*H*soilwtb 'wedge weight buoyant
-----
Q2=CCS(BETA)*COS(BETA) 'used to compute failure
Q3=CCS(1-BETA)*COS(psy) 'angle, alpha, and the wedge
QLAST= -90000! 'weight at failure
FOR J= 0 TO 50 STEP .1
  ALP= alphamin+J
  RAP=ALP*RD
  X1=SIN(RAP-i)
  X2=COS(BETA-RAP)*SIN(RAP-FI+psy)
  X3=COS(BETA+delta+FI-RAP)
  Q4=X2/(X1*X3)
  Q=Q1b*Q3*Q4/Q2
-----

a1= fi-psy-beta 'constants used to compute
a2= psy+beta+delta 'Kae
a3= fi+delta
a4= i-beta
a5= fi-psy-i
func1= 1+sqrt( (sin(a3)*sin(a5)) / (cos(a4)*cos(a2)) )
func2= func1*func1
Kae= ( cos(a1)*cos(a1) ) / ( cos(psy)*cos(beta)*cos(beta)*cos(a2)*func2

WTb= 222900! 'buoyant weight of retaining wall/soil mass
AX= BETA+delta 'constant used to compute components of Pae
Paeb= qlb*kae
FS= ( (WTb+Paeb*SIN(AX)) *TAN(F. ) ) / ( W1b*kh+Paeb*COS(AX) )

IF Q < QLAST THEN
PRINT #2, USING "accel=##### Q(last) =##### Angle=##### F
if io.name$<>"CON" then 'if sending output to
locate 12,35:print "accel=";kh 'a printer, lets the
locate 13,35:print "FS=";FS 'user know that the
end if 'program is functioning
exit for
end if
QLAST= Q
NEXT J
NEXT kh
END

```

Friction Angle (Degree) = 43
 Buoyant Weight of Backfill = 89.6
 Height of Retaining Wall = 80.4
 Beta (Degree) = 0
 Inclination (Degree) = 26.5
 Delta (Degree) = 21.5
 Fib (Degree) = 30

accel=+0.000	Q(last) = +68.9	Angle= +59.8	FS= +4.362	Kae= +0.238
accel=+0.050	Q(last) = +81.3	Angle= +56.7	FS= +2.857	Kae= +0.281
accel=+0.100	Q(last) = +96.1	Angle= +53.2	FS= +2.096	Kae= +0.335
accel=+0.150	Q(last) = +114.4	Angle= +49.2	FS= +1.630	Kae= +0.404
accel=+0.200	Q(last) = +138.4	Angle= +44.5	FS= +1.309	Kae= +0.497
accel=+0.250	Q(last) = +174.5	Angle= +38.5	FS= +1.059	Kae= +0.640
accel=+0.300	Q(last) = +228.6	Angle= +28.5	FS= +0.811	Kae= +0.971
accel=+0.350	Q(last) = +275.7	Angle= +25.9	FS= +0.737	Kae= +1.069
accel=+0.400	Q(last) = +292.3	Angle= +23.3	FS= +0.675	Kae= +1.171

Friction Angle (Degree) = 37.9
 Buoyant Weight of Backfill = 89.6
 Height of Retaining Wall = 80.4
 Beta (Degree) = 0
 Inclination (Degree) = 26.5
 Delta (Degree) = 18.95
 Fib (Degree) = 30

accel=+0.000	Q(last) = +91.7	Angle= +54.9	FS= +3.254	Kae= +0.317
accel=+0.050	Q(last) = +108.6	Angle= +50.8	FS= +2.266	Kae= +0.376
accel=+0.100	Q(last) = +130.4	Angle= +46.2	FS= +1.699	Kae= +0.455
accel=+0.150	Q(last) = +162.1	Angle= +40.2	FS= +1.312	Kae= +0.572
accel=+0.200	Q(last) = +212.5	Angle= +32.8	FS= +0.945	Kae= +0.871
accel=+0.250	Q(last) = +257.2	Angle= +26.2	FS= +0.847	Kae= +0.944
accel=+0.300	Q(last) = +272.3	Angle= +21.5	FS= +0.766	Kae= +1.025
accel=+0.350	Q(last) = +286.6	Angle= +20.9	FS= +0.700	Kae= +1.111
accel=+0.400	Q(last) = +300.2	Angle= +18.4	FS= +0.644	Kae= +1.202

Friction Angle (Degree) = 33.1
 Buoyant Weight of Backfill = 89.6
 Height of Retaining Wall = 80.4
 Beta (Degree) = 0
 Inclination (Degree) = 26.5
 Delta (Degree) = 16.55
 Fib (Degree) = 30

accel=+0.000	Q(last) = +121.8	Angle= +48.6	FS= +2.441	Kae= +0.420
accel=+0.050	Q(last) = +148.2	Angle= +43.0	FS= +1.742	Kae= +0.513
accel=+0.100	Q(last) = +175.0	Angle= +38.4	FS= +1.263	Kae= +0.683
accel=+0.150	Q(last) = +211.7	Angle= +32.1	FS= +0.939	Kae= +0.853
accel=+0.200	Q(last) = +253.0	Angle= +24.3	FS= +0.800	Kae= +0.915
accel=+0.250	Q(last) = +269.3	Angle= +21.6	FS= +0.802	Kae= +0.988
accel=+0.300	Q(last) = +271.6	Angle= +18.9	FS= +0.730	Kae= +1.061
accel=+0.350	Q(last) = +283.4	Angle= +16.3	FS= +0.670	Kae= +1.137
accel=+0.400	Q(last) = +303.9	Angle= +13.8	FS= +0.619	Kae= +1.217

Friction Angle (Degree) = 29.9
 Buoyant Weight of Backfill = 89.6
 Height of Retaining Wall = 80.4
 Beta (Degree) = 0
 Inclination (Degree) = 26.5
 Delta (Degree) = 14.95
 Fib (Degree) = 30

accel=+0.000	Q(last) = +151.4	Angle= +42.8	FS= +1.966	Kae= +0.523
accel=+0.050	Q(last) = +180.6	Angle= +37.8	FS= +1.342	Kae= +0.705
accel=+0.100	Q(last) = +217.2	Angle= +32.9	FS= +1.002	Kae= +0.830
accel=+0.150	Q(last) = +251.3	Angle= +28.1	FS= +0.956	Kae= +0.887
accel=+0.200	Q(last) = +264.0	Angle= +21.3	FS= +0.856	Kae= +0.948
accel=+0.250	Q(last) = +275.7	Angle= +18.6	FS= +0.776	Kae= +1.012
accel=+0.300	Q(last) = +286.4	Angle= +15.9	FS= +0.709	Kae= +1.078
accel=+0.350	Q(last) = +295.9	Angle= +13.2	FS= +0.653	Kae= +1.147
accel=+0.400	Q(last) = +304.5	Angle= +10.7	FS= +0.605	Kae= +1.220

Friction Angle (Degree) = 27.8
 Buoyant Weight of Backfill = 89.6
 Height of Retaining Wall = 80.4
 Beta (Degree) = 0
 Inclination (Degree) = 26.5
 Delta (Degree) = 13.9
 Fib (Degree) = 30

accel=+0.000	Q(last) = +182.2	Angle= +36.8	FS= +1.640	Kae= +0.629
accel=+0.050	Q(last) = +231.2	Angle= +27.7	FS= +1.198	Kae= +0.800
accel=+0.100	Q(last) = +244.5	Angle= +24.9	FS= +1.047	Kae= +0.853
accel=+0.150	Q(last) = +257.0	Angle= +22.1	FS= +0.930	Kae= +0.907
accel=+0.200	Q(last) = +268.6	Angle= +19.3	FS= +0.837	Kae= +0.965
accel=+0.250	Q(last) = +279.1	Angle= +16.6	FS= +0.760	Kae= +1.024
accel=+0.300	Q(last) = +288.5	Angle= +13.9	FS= +0.697	Kae= +1.086
accel=+0.350	Q(last) = +296.8	Angle= +11.2	FS= +0.643	Kae= +1.151
accel=+0.400	Q(last) = +304.0	Angle= +8.7	FS= +0.597	Kae= +1.218

Friction Angle (Degree) = 27
 Buoyant Weight of Backfill = 89.6
 Height of Retaining Wall = 80.4
 Beta (Degree) = 0
 Inclination (Degree) = 26.5
 Delta (Degree) = 13.5
 Fib (Degree) = 30

accel=+0.000	Q(last) = +202.4	Angle= +32.9	FS= +1.484	Kae= +0.699
accel=+0.050	Q(last) = +233.9	Angle= +26.9	FS= +1.181	Kae= +0.810
accel=+0.100	Q(last) = +246.9	Angle= +24.1	FS= +1.035	Kae= +0.861
accel=+0.150	Q(last) = +259.0	Angle= +21.3	FS= +0.921	Kae= +0.915
accel=+0.200	Q(last) = +270.2	Angle= +18.5	FS= +0.830	Kae= +0.970
accel=+0.250	Q(last) = +280.2	Angle= +15.8	FS= +0.755	Kae= +1.028
accel=+0.300	Q(last) = +289.2	Angle= +13.1	FS= +0.692	Kae= +1.088
accel=+0.350	Q(last) = +297.0	Angle= +10.5	FS= +0.639	Kae= +1.151
accel=+0.400	Q(last) = +303.7	Angle= +8.0	FS= +0.594	Kae= +1.216

```

MONONOBE - OKABE
EARTH PRESSURE DURING EARTHQUAKE
Retaining Wall B (Section C-C)
RD=3.1416/180! 'converts degrees to radians
FI=43*RD 'angle of internal friction
soilwtb=89.6 'buoyant unit weight of backfill
soilwtt=152 'total weight of backfill
H=55 'height of retaining wall
BETA=33*RD 'angle of inclination of back of wall to vertical
i=25.5*RD 'angle of inclination of backfill
delta=FI/2 'angle of friction between backfill and wall
Fib=30*RD 'friction angle between bottom of wall and ground
-----
input "to where (i.e. CON, LPT1, LPT2, PRN or DOS file name:");IO.name$
if IO.name$="" then
  IO.name$="CON"
else if IO.name$="L" or IO.name$="1" then
  IO.name$="LPT2"
end if
OPEN IO.name$ FOR OUTPUT AS #2
PRINT #2, " Friction Angle (Degree) = ";FI/RD
PRINT #2, " Buoyant Weight of Backfill = ";soilwtb
PRINT #2, " Height of Retaining Wall = ";H
PRINT #2, " Beta (Degree) = ";BETA/RD
PRINT #2, " Inclination (Degree) = ";i/RD
PRINT #2, " Delta (Degree) = ";delta/RD
PRINT #2, " Fib (Degree) = ";Fib/RD
PRINT #2, ""

locate 12,35:print "working"
FOR kh= 0.0 TO 0.45 STEP .05

psy= ATN(kh)
alphamin= (FI-psy)/RD
IF 1/RD>alphamin THEN i=RD*(alphamin-.1) 'insures imax not violated
q1b= .5*H*H*soilwtb 'wedge weight buoyant
-----
Q2=COS(BETA)*COS(BETA) 'used to compute failure
Q3=COS(1-BETA)*COS(psy) 'angle, alpha, and the wedge
QLAST= -900001 'weight at failure
FOR J= 0 TO 50 STEP .1
  ALP= alphamin+J
  RAP=ALP*RD
  X1=SIN(RAP-i)
  X2=COS(BETA-RAP)*SIN(RAP-FI+psy)
  X3=COS(BETA+delta+FI-RAP)
  Q4=X2/(X1*X3)
  Q=Q1b*Q3*Q4/Q2
-----

a1= fi-psy-beta 'constants used to compute
a2= psy+beta+delta 'Kae
a3= fi+delta
a4= i-beta
a5= fi-psy-i
func1= 1+sqrt( (sin(a3)*sin(a5)) / (cos(a4)*cos(a2)) )
func2= func1*func1
Kae= ( cos(a1)*cos(a1) ) / ( cos(psy)*cos(beta)*cos(beta)*cos(a2)*func2

WTb= 219100! 'bouyant weight of retaining wall/soil mass
AX= BETA+delta 'constant used to compute components of Pae
Paeb= q1b*kae

FS= ( WTb+Paeb*SIN(AX) ) *TAN(Fib) / ( WTb*kh+Paeb*COS(AX)\ )

IF Q < QLAST THEN
PRINT #2, USING "accel=###.### Q(last) =#####.## Angle=###.## F
if IO.name$<>"CON" then 'if sending output to
locate 12,35:print "accel=";kh 'a printer, lets the
locate 13,35:print "FS=";FS 'user know that the
end if 'program is functioning
exit for
end if
QLAST= Q
NEXT J
NEXT kh
END

```

Friction Angle (Degree) = 43
 Buoyant Weight of Backfill = 89.6
 Height of Retaining Wall = 55
 Beta (Degree) = 33
 Inclination (Degree) = 25.5
 Delta (Degree) = 21.5
 Fib (Degree) = 30

accel=+0.000	Q(last) = +133.1	Angle= +65.1	FS= +1.737	Kae= +0.835
accel=+0.050	Q(last) = +128.5	Angle= +60.5	FS= +1.516	Kae= +0.951
accel=+0.100	Q(last) = +147.7	Angle= +55.5	FS= +1.348	Kae= +1.101
accel=+0.150	Q(last) = +172.7	Angle= +50.2	FS= +1.216	Kae= +1.303
accel=+0.200	Q(last) = +207.7	Angle= +44.4	FS= +1.109	Kae= +1.594
accel=+0.250	Q(last) = +264.0	Angle= +38.1	FS= +1.018	Kae= +2.069
accel=+0.300	Q(last) = +393.1	Angle= +30.5	FS= +0.935	Kae= +3.162
accel=+0.350	Q(last) = +548.4	Angle= +25.1	FS= +0.888	Kae= +4.542
accel=+0.400	Q(last) = +617.7	Angle= +22.5	FS= +0.868	Kae= +5.788

Friction Angle (Degree) = 37.9
 Buoyant Weight of Backfill = 89.6
 Height of Retaining Wall = 55
 Beta (Degree) = 33
 Inclination (Degree) = 25.5
 Delta (Degree) = 18.95
 Fib (Degree) = 30

accel=+0.000	Q(last) = +130.4	Angle= +59.0	FS= +1.495	Kae= +0.963
accel=+0.050	Q(last) = +149.7	Angle= +53.6	FS= +1.321	Kae= +1.107
accel=+0.100	Q(last) = +175.5	Angle= +47.7	FS= +1.181	Kae= +1.308
accel=+0.150	Q(last) = +214.5	Angle= +40.9	FS= +1.064	Kae= +1.618
accel=+0.200	Q(last) = +293.3	Angle= +32.5	FS= +0.954	Kae= +2.251
accel=+0.250	Q(last) = +398.2	Angle= +25.7	FS= +0.882	Kae= +3.122
accel=+0.300	Q(last) = +429.0	Angle= +22.9	FS= +0.855	Kae= +3.450
accel=+0.350	Q(last) = +464.7	Angle= +20.2	FS= +0.832	Kae= +3.849
accel=+0.400	Q(last) = +507.5	Angle= +17.6	FS= +0.811	Kae= +4.344

Friction Angle (Degree) = 33.1
 Buoyant Weight of Backfill = 89.6
 Height of Retaining Wall = 55
 Beta (Degree) = 33
 Inclination (Degree) = 25.5
 Delta (Degree) = 16.55
 Fib (Degree) = 30

accel=+0.000	Q(last) = +152.4	Angle= +51.8	FS= +1.293	Kae= +1.125
accel=+0.050	Q(last) = +179.9	Angle= +44.9	FS= +1.146	Kae= +1.331
accel=+0.100	Q(last) = +227.3	Angle= +36.6	FS= +1.014	Kae= +1.654
accel=+0.150	Q(last) = +319.6	Angle= +26.7	FS= +0.898	Kae= +2.411
accel=+0.200	Q(last) = +336.9	Angle= +23.8	FS= +0.865	Kae= +2.585
accel=+0.250	Q(last) = +355.3	Angle= +21.0	FS= +0.836	Kae= +2.785
accel=+0.300	Q(last) = +375.4	Angle= +18.2	FS= +0.810	Kae= +3.020
accel=+0.350	Q(last) = +398.1	Angle= +15.5	FS= +0.787	Kae= +3.297
accel=+0.400	Q(last) = +424.3	Angle= +12.9	FS= +0.767	Kae= +3.632

Friction Angle (Degree) = 29.9
 Buoyant Weight of Backfill = 89.6
 Height of Retaining Wall = 55
 Beta (Degree) = 33
 Inclination (Degree) = 25.5
 Delta (Degree) = 14.95
 Fib (Degree) = 30

accel=+0.000	Q(last) = +173.6	Angle= +45.4	FS= +1.164	Kae= +1.281
accel=+0.050	Q(last) = +218.7	Angle= +36.0	FS= +1.018	Kae= +1.617
accel=+0.100	Q(last) = +288.8	Angle= +26.5	FS= +0.903	Kae= +2.153
accel=+0.150	Q(last) = +301.6	Angle= +23.6	FS= +0.868	Kae= +2.275
accel=+0.200	Q(last) = +314.6	Angle= +20.7	FS= +0.837	Kae= +2.414
accel=+0.250	Q(last) = +328.1	Angle= +17.9	FS= +0.810	Kae= +2.573
accel=+0.300	Q(last) = +342.6	Angle= +15.1	FS= +0.784	Kae= +2.756
accel=+0.350	Q(last) = +358.5	Angle= +12.4	FS= +0.762	Kae= +2.970
accel=+0.400	Q(last) = +376.6	Angle= +9.8	FS= +0.741	Kae= +3.223

Friction Angle (Degree) = 27.8
 Buoyant Weight of Backfill = 89.6
 Height of Retaining Wall = 55
 Beta (Degree) = 33
 Inclination (Degree) = 25.5
 Delta (Degree) = 13.9
 Fib (Degree) = 30

accel=+0.000	Q(last) = +194.7	Angle= +39.6	FS= +1.075	Kae= +1.437
accel=+0.005	Q(last) = +199.6	Angle= +38.5	FS= +1.059	Kae= +1.473
accel=+0.010	Q(last) = +205.1	Angle= +37.4	FS= +1.044	Kae= +1.513
accel=+0.015	Q(last) = +211.2	Angle= +36.2	FS= +1.028	Kae= +1.559
accel=+0.020	Q(last) = +218.2	Angle= +35.0	FS= +1.011	Kae= +1.611
accel=+0.025	Q(last) = +226.4	Angle= +33.6	FS= +0.994	Kae= +1.672
accel=+0.030	Q(last) = +236.6	Angle= +32.0	FS= +0.974	Kae= +1.748
accel=+0.035	Q(last) = +250.6	Angle= +30.0	FS= +0.952	Kae= +1.852
accel=+0.040	Q(last) = +282.2	Angle= +26.3	FS= +0.912	Kae= +2.086
accel=+0.045	Q(last) = +267.6	Angle= +27.7	FS= +0.925	Kae= +1.979
accel=+0.050	Q(last) = +268.7	Angle= +27.4	FS= +0.922	Kae= +1.987
accel=+0.055	Q(last) = +269.7	Angle= +27.2	FS= +0.918	Kae= +1.996
accel=+0.060	Q(last) = +270.8	Angle= +26.8	FS= +0.914	Kae= +2.005
accel=+0.065	Q(last) = +271.8	Angle= +26.5	FS= +0.910	Kae= +2.014
accel=+0.070	Q(last) = +272.9	Angle= +26.2	FS= +0.906	Kae= +2.024
accel=+0.075	Q(last) = +274.0	Angle= +25.9	FS= +0.903	Kae= +2.033
accel=+0.080	Q(last) = +275.0	Angle= +25.6	FS= +0.899	Kae= +2.042
accel=+0.085	Q(last) = +276.1	Angle= +25.3	FS= +0.895	Kae= +2.052
accel=+0.090	Q(last) = +277.1	Angle= +25.1	FS= +0.892	Kae= +2.061
accel=+0.095	Q(last) = +278.2	Angle= +24.8	FS= +0.888	Kae= +2.071

```

MONONOBE - OKABE
EARTH PRESSURE DURING EARTHQUAKE
Retaining Wall B (Section C-C)
RD=3.1416/180! 'converts degrees to radians
FI=43*RD 'angle of internal friction
soilwtb=89.6 'buoyant unit weight of backfill
soilwtt=152 'total weight of backfill
H=55 'height of retaining wall
BETA=0*RD 'angle of inclination of back of wall to vertical
i=25.5*RD 'angle of inclination of backfill
delta=FI/2 'angle of friction between backfill and wall
Fib=30*RD 'friction angle between bottom of wall and ground
-----
input "to where (i.e. CON, LPT1, LPT2, PRN or DOS file name;";IO.name$
if io.name$="" then
  io.name$="CON"
elseif io.name$="L" or io.name$="1" then
  io.name$="LPT2"
end if
OPEN IO.name$ FOR OUTPUT AS #2
PRINT #2, " Friction Angle (Degree) = ";FI/RD
PRINT #2, " Buoyant Weight of Backfill = ";soilwtb
PRINT #2, " Height of Retaining Wall = ";H
PRINT #2, " Beta (Degree) = ";BETA/RD
PRINT #2, " Inclination (Degree) = ";i/RD
PRINT #2, " Delta (Degree) = ";delta/RD
PRINT #2, " Fib (Degree) = ";Fib/RD
PRINT #2, ""

locate 12,35:print "working"
FOR kh= 0.0 TO 0.45 STEP .05

psy= ATN(kh)
alphamin= (FI-psy)/RD
IF 1/RD>alphamin THEN i=RD*(alphamin-.1) 'insures imax not violated
qlb= .5*H*H*soilwtb 'wedge weight buoyant
-----
Q2=COS(BETA)*COS(BETA) 'used to compute failure
Q3=COS(i-BETA)*COS(psy) 'angle, alpha, and the wedge
QLAST= -90000! 'weight at failure
FOR J= 0 TO 50 STEP .1
  ALP= alphamin+J
  RAP=ALP*RD
  X1=SIN(RAP-i)
  X2=COS(BETA-RAP)*SIN(PAP-FI+psy)
  X3=COS(BETA+delta+FI-RAP)
  Q4=X2/(X1*X3)
  Q=Q1b*Q3*Q4/Q2
-----

a1= fi-psy-beta 'constants used to compute
a2= psy+beta+delta 'Kae
a3= fi+delta
a4= i-beta
a5= fi-psy-i
func1= 1+sqr( (sin(a3)*sin(a5)) / (cos(a4)*cos(a2)) )
func2= func1*func1
Kae= ( cos(a1)*cos(a1) ) / ( cos(psy)*cos(beta)*cos(beta)*cos(a2)*func2)

WTb= 219100! 'bouyant weight of retaining wall/soil mass
AX= BETA+delta 'constant used to compute components of Pae
Paeb= qlb*kae

FS= ( (WTb+Paeb*SIN(AX)) *TAN(Fib) ) / ( WTb*kh+Paeb*COS(AX) )

IF Q < QLAST THEN
PRINT #2, USING "accel="+#.### Q(last) =+####.# Angle=+###.# F
if io.name$<>"CON" then 'if sending output to
locate 12,35:print "accel=";kh 'a printer, lets the
locate 13,35:print "FS=";FS 'user know that the
end if 'program is functioning
exit for
end if
QLAST= Q
NEXT J
NEXT kh
END

```

Friction Angle (Degree)	=	43			
Buoyant Weight of Backfill	=	89.6			
Height of Retaining Wall	=	55			
Beta (Degree)	=	0			
Inclination (Degree)	=	25.5			
Delta (Degree)	=	21.5			
Fib (Degree)	=	30			
accel=+0.000	Q(last) =	+31.7	Angle= +60.1	FS= +4.521	Kae= +0.234
accel=+0.050	Q(last) =	+37.3	Angle= +57.0	FS= +2.941	Kae= +0.276
accel=+0.100	Q(last) =	+43.9	Angle= +53.7	FS= +2.152	Kae= +0.327
accel=+0.150	Q(last) =	+51.9	Angle= +49.9	FS= +1.675	Kae= +0.391
accel=+0.200	Q(last) =	+62.1	Angle= +45.4	FS= +1.349	Kae= +0.476
accel=+0.250	Q(last) =	+76.4	Angle= +40.0	FS= +1.103	Kae= +0.599
accel=+0.300	Q(last) =	+103.3	Angle= +32.1	FS= +0.882	Kae= +0.831
accel=+0.350	Q(last) =	+129.0	Angle= +25.9	FS= +0.743	Kae= +1.069
accel=+0.400	Q(last) =	+136.8	Angle= +23.3	FS= +0.680	Kae= +1.171

Friction Angle (Degree)	=	37.9			
Buoyant Weight of Backfill	=	89.6			
Height of Retaining Wall	=	55			
Beta (Degree)	=	0			
Inclination (Degree)	=	25.5			
Delta (Degree)	=	18.95			
Fib (Degree)	=	30			
accel=+0.000	Q(last) =	+41.9	Angle= +55.2	FS= +3.389	Kae= +0.309
accel=+0.050	Q(last) =	+49.4	Angle= +51.5	FS= +2.350	Kae= +0.365
accel=+0.100	Q(last) =	+58.8	Angle= +47.1	FS= +1.763	Kae= +0.438
accel=+0.150	Q(last) =	+71.6	Angle= +41.7	FS= +1.373	Kae= +0.540
accel=+0.200	Q(last) =	+94.2	Angle= +33.8	FS= +1.062	Kae= +0.723
accel=+0.250	Q(last) =	+120.4	Angle= +26.2	FS= +0.856	Kae= +0.944
accel=+0.300	Q(last) =	+127.4	Angle= +23.5	FS= +0.774	Kae= +1.025
accel=+0.350	Q(last) =	+134.1	Angle= +20.9	FS= +0.706	Kae= +1.111
accel=+0.400	Q(last) =	+140.5	Angle= +18.4	FS= +0.650	Kae= +1.202

Friction Angle (Degree)	=	33.1			
Buoyant Weight of Backfill	=	89.6			
Height of Retaining Wall	=	55			
Beta (Degree)	=	0			
Inclination (Degree)	=	25.5			
Delta (Degree)	=	16.55			
Fib (Degree)	=	30			
accel=+0.000	Q(last) =	+55.1	Angle= +49.4	FS= +2.565	Kae= +0.407
accel=+0.050	Q(last) =	+66.2	Angle= +44.3	FS= +1.842	Kae= +0.490
accel=+0.100	Q(last) =	+83.4	Angle= +37.2	FS= +1.367	Kae= +0.622
accel=+0.150	Q(last) =	+113.1	Angle= +27.1	FS= +1.012	Kae= +0.853
accel=+0.200	Q(last) =	+119.8	Angle= +24.3	FS= +0.901	Kae= +0.919
accel=+0.250	Q(last) =	+126.0	Angle= +21.6	FS= +0.811	Kae= +0.988
accel=+0.300	Q(last) =	+131.9	Angle= +18.9	FS= +0.738	Kae= +1.061
accel=+0.350	Q(last) =	+137.3	Angle= +16.3	FS= +0.677	Kae= +1.137
accel=+0.400	Q(last) =	+142.2	Angle= +13.8	FS= +0.625	Kae= +1.217

Friction Angle (Degree)	=	29.9			
Buoyant Weight of Backfill	=	89.6			
Height of Retaining Wall	=	55			
Beta (Degree)	=	0			
Inclination (Degree)	=	25.5			
Delta (Degree)	=	14.95			
Fib (Degree)	=	30			
accel=+0.000	Q(last) =	+67.6	Angle= +44.2	FS= +2.092	Kae= +0.499
accel=+0.050	Q(last) =	+85.5	Angle= +36.4	FS= +1.485	Kae= +0.633
accel=+0.100	Q(last) =	+111.3	Angle= +26.9	FS= +1.097	Kae= +0.830
accel=+0.150	Q(last) =	+117.6	Angle= +24.1	FS= +0.969	Kae= +0.887
accel=+0.200	Q(last) =	+123.5	Angle= +21.3	FS= +0.867	Kae= +0.948
accel=+0.250	Q(last) =	+129.0	Angle= +18.6	FS= +0.785	Kae= +1.012
accel=+0.300	Q(last) =	+134.0	Angle= +15.9	FS= +0.717	Kae= +1.078
accel=+0.350	Q(last) =	+138.5	Angle= +13.2	FS= +0.660	Kae= +1.147
accel=+0.400	Q(last) =	+142.5	Angle= +10.7	FS= +0.611	Kae= +1.220

Friction Angle (Degree)	=	27.8
Buoyant Weight of Backfill	=	89.6
Height of Retaining Wall	=	55
Beta (Degree)	=	0
Inclination (Degree)	=	25.5
Delta (Degree)	=	13.9
Fib (Degree)	=	30

accel=+0.000	Q(last) =	+79.2	Angle=	+39.3	FS=	+1.789	Kae=	+0.584
accel=+0.050	Q(last) =	+108.2	Angle=	+27.7	FS=	+1.218	Kae=	+0.800
accel=+0.100	Q(last) =	+114.4	Angle=	+24.9	FS=	+1.063	Kae=	+0.853
accel=+0.150	Q(last) =	+120.3	Angle=	+22.1	FS=	+0.943	Kae=	+0.907
accel=+0.200	Q(last) =	+125.7	Angle=	+19.3	FS=	+0.847	Kae=	+0.965
accel=+0.250	Q(last) =	+130.6	Angle=	+16.6	FS=	+0.769	Kae=	+1.024
accel=+0.300	Q(last) =	+135.0	Angle=	+13.9	FS=	+0.704	Kae=	+1.086
accel=+0.350	Q(last) =	+138.9	Angle=	+11.2	FS=	+0.650	Kae=	+1.151
accel=+0.400	Q(last) =	+142.3	Angle=	+8.7	FS=	+0.603	Kae=	+1.218